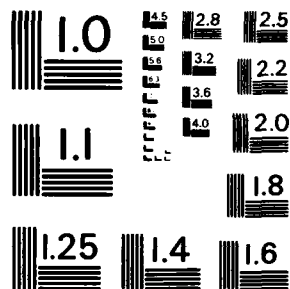


AD-A124 666    DESIGNING WAVEGUIDE COUPLERS FOR MICROWAVE EXCITATION  
OF LASER BASES(U) AIR FORCE INST OF TECH  
WRIGHT-PATTERSON AFB OH SCHOOL OF ENGINEERING  
UNCLASSIFIED    L C SHELTON 1982 AFIT/GE0/PH/820-13

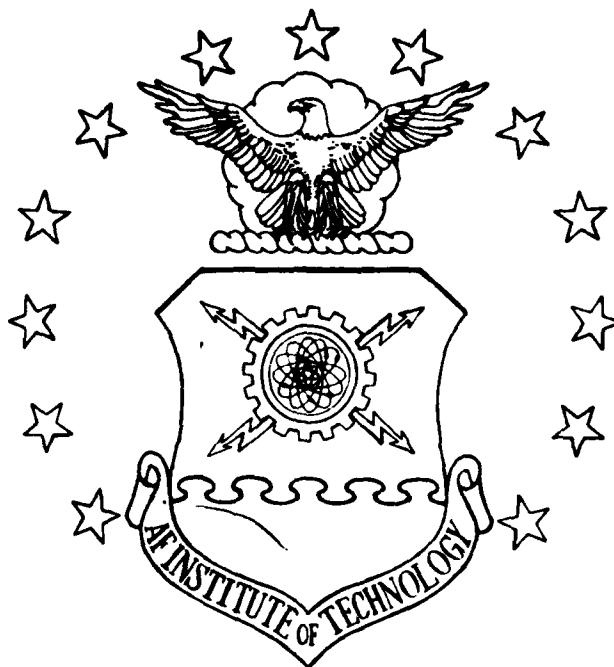
F/G 20/8

1/2  
NL



MICROCOPY RESOLUTION TEST CHART  
NATIONAL BUREAU OF STANDARDS - 1963 - A

ADA 124666



DESIGNING WAVEGUIDE COUPLERS  
FOR MICROWAVE EXCITATION  
OF LASER GASES

Leonard C. Shelton Jr.

1982

DTIC  
ELECTE  
S

DEPARTMENT OF THE AIR FORCE  
AIR UNIVERSITY (ATC)

**AIR FORCE INSTITUTE OF TECHNOLOGY**

Approved for public release; distribution unlimited.  
Wright-Patterson Air Force Base, Ohio

JTC FILE COPY

... 25

AFIT/GEO/PH/82D-13

DESIGNING WAVEGUIDE COUPLERS  
FOR MICROWAVE EXCITATION  
OF LASER CASES

Leonard C. Shelton Jr.

1982

OTIC  
TE

Approved for public release; distribution unlimited.

AFIT/GEO/PH/82D-13

# DESIGNING WAVEGUIDE COUPLERS FOR MICROWAVE EXCITATION OF LASER GASES

## THESIS

Presented to the Faculty of the School of Engineering  
at the Air Force Institute of Technology  
Air University  
in Partial Fulfillment of the  
Requirements for the Degree of  
Master of Science

by  
Leonard C. Shelton Jr.  
2 Lt. USAF  
Graduate Electro-Optics  
1982

**Reliability Index**

**Final Score**

**A**



Approved for public release; distribution unlimited.

## Preface

The purpose of this study was to develop an analytical model for designing a microwave waveguide coupler. The immediate need for this model is to design a coupler to excite laser gases, but the approach should be valid for other applications.

The final model was used to build a coupler which was tested against couplers designed by other means. Tests were run on each of these couplers in order to determine which coupler had the best overall performance. The design model used in building this "best" coupler was then chosen to be the superior method.

Extensive CW testing was performed on all of the coupler designs. However, a breakdown of the power supply for the pulsed microwave unit curtailed pulsed experiments except at the most rudimentary level. Although this limited testing makes the test results inconclusive, the design model that is presented here does seem to give promising results.

I hope that this work will be continued, since I feel it has a great potential and could be of significant value as a reliable laser excitation source.

In performing the research, experimentation, and writing of this thesis I have had a great deal of help from others.

I am deeply indebted to my faculty advisor Capt. T. W. Johnson for his continuing patience and assistance in times of need. I also wish to thank Joe Brandelik, Dr. W. K. Schuebel, and the remainder of the personnel at the Avionics Lab for their assistance and cooperation during the experimental stages of the thesis. A word of thanks is also owed to Ron Ruley and Carl Shortt of the Fabrication Shop for their cooperation in building the necessary hardware. I also wish to thank my wife Kim for her understanding and concern on those many nights when I was tied to my desk with work.

## List of Figures

<u>Figure</u>	<u>Page</u>
1 Microwave Excitation Methods - - - - -	3
2 Attenuation and Phase Constants Vs. Frequency for a Typical Plasma - - - - -	11
3 Plasma Frequency Vs. Electron Number Density - - - - -	18
4 Cross Section of Waveguide Containing Perturbing Medium - - - - -	22
5 System for Measuring VSWR of the Coupler - - - - -	53
6 System for Pulsed Inputs Using Cross-guide Couplers -	54
7 DX-453 Magnetron Powered by Cober Model 605 - - - - -	56
8 System for CW Inputs Using Cross-guide Couplers - - -	57
9 VSWR Measurements Vs. Frequency for an Empty Secondary Waveguide - - - - -	60
10 Transmitted Power Vs. Input Power for Various Mediums in the Waveguide - - - - -	61
11 Reflected Power Vs. Input Power for Various Mediums in the Waveguide - - - - -	63
12 % of 8 mm Tube Sustaining a Plasma Vs. Pressure of Ar at 500 W - - - - -	64
13 Transmitted Power Vs. Pressure of Ar at 500 W Input and 8 mm Tube - - - - -	65
14 Reflected Power Vs. Pressure of Ar at 500 W Input and 8 mm Tube - - - - -	66
15 % of 8 mm Tube Sustaining a Plasma Vs. Pressure of Ar at 600 W - - - - -	68
16 % of 1.5 mm Tube Sustaining a Plasma Vs. Pressure of Ar at 500 W - - - - -	69
17 Transmitted Power Vs. Pressure of Ar at 500 W Input and 1.5 mm Tube - - - - -	70



<u>Figure</u>		<u>Page</u>
18	% of 8 mm Tube Sustaining a Plasma Vs. Pressure of He at 500 W - - - - -	71
19	Transmitted Power Vs. Pressure of He at 500 W Input and 8 mm Tube - - - - -	72
20	8 Slot Sidewall Coupler Section - - - - -	96
21	Coupler Made from 6 Cascaded 8 Slot Sections - - - - -	97
22	Overall View of Separable Coupler - - - - -	100
23	Separable Coupler (Primary Waveguide Part) - - - - -	101
24	Separable Coupler (Secondary Waveguide Part) - - - - -	102
25	Separable Coupler (Plate with Coupling Holes) - - - - -	103
26	Reflected Power Vs. Pressure of He at 500 W Input and 8 mm Tube - - - - -	105
27	% of 8 mm Tube Sustaining a Plasma Vs. Pressure of N <sub>2</sub> at 500 W - - - - -	106
28	Transmitted Power Vs. Pressure of N <sub>2</sub> at 500 W Input and 8 mm Tube - - - - -	107
29	Reflected Power Vs. Pressure of N <sub>2</sub> at 500 W Input and 8 mm Tube - - - - -	108
30	% of 8 mm Tube Sustaining a Plasma Vs. Pressure of CO <sub>2</sub> at 500 W - - - - -	109
31	Transmitted Power Vs. Pressure of CO <sub>2</sub> at 500 W Input and 8 mm Tube - - - - -	110
32	Reflected Power Vs. Pressure of CO <sub>2</sub> at 500 W Input and 8 mm Tube - - - - -	111
33	Transmitted Power Vs. Pressure of Ar at 600 W Input and 8 mm Tube - - - - -	112
34	Reflected Power Vs. Pressure of Ar at 600 W Input and 8 mm Tube - - - - -	113
35	% of 8 mm Tube Sustaining a Plasma Vs. Pressure of He at 600 W - - - - -	114
36	Transmitted Power Vs. Pressure of He at 600 W Input and 8 mm Tube - - - - -	115

<u>Figure</u>		<u>Page</u>
37	Reflected Power Vs. Pressure of He at 600 W Input and 8 mm Tube - - - - -	116
38	% of 8 mm Tube Sustaining a Plasma Vs. Pressure of N <sub>2</sub> at 600 W - - - - -	117
39	Transmitted Power Vs. Pressure of N <sub>2</sub> at 600 W Input and 8 mm Tube - - - - -	118
40	Reflected Power Vs. Pressure of N <sub>2</sub> at 600 W Input and 8 mm Tube - - - - -	119
41	% of 8 mm Tube Sustaining a Plasma Vs. Pressure of CO <sub>2</sub> at 600 W - - - - -	120
42	Transmitted Power Vs. Pressure of CO <sub>2</sub> at 600 W Input and 8 mm Tube - - - - -	121
43	Reflected Power Vs. Pressure of CO <sub>2</sub> at 600 W Input and 8 mm Tube - - - - -	122
44	Reflected Power Vs. Pressure of Ar at 500 W Input and 1.5 mm Tube - - - - -	123
45	% of 1.5 mm Tube Sustaining a Plasma Vs. Pressure of He at 500 W - - - - -	124
46	Transmitted Power Vs. Pressure of He at 500 W Input and 1.5 mm Tube - - - - -	125
47	Reflected Power Vs. Pressure of He at 500 W Input and 1.5 mm Tube - - - - -	126
48	% of 1.5 mm Tube Sustaining a Plasma Vs. Pressure of N <sub>2</sub> at 500 W - - - - -	127
49	Transmitted Power Vs. Pressure of N <sub>2</sub> at 500 W Input and 1.5 mm Tube - - - - -	128
50	Reflected Power Vs. Pressure of N <sub>2</sub> at 500 W Input and 1.5 mm Tube - - - - -	129
51	% of 1.5 mm Tube Sustaining a Plasma Vs. Pressure of CO <sub>2</sub> at 500 W - - - - -	130
52	Transmitted Power Vs. Pressure of CO <sub>2</sub> at 500 W Input and 1.5 mm Tube - - - - -	131
53	Reflected Power Vs. Pressure of CO <sub>2</sub> at 500 W Input and 1.5 mm Tube - - - - -	132

## List of Symbols

### Roman Letter Symbols

- $A_i$  - The amplitude of the electric field for mode  $i$
- $A_{i0}$  - The amplitude of the incident field for mode  $i$
- $a$  - The broad dimension of the waveguide being used
- $b$  - The narrow dimension of the waveguide being used
- $C$  - An  $n \times n$  matrix of complex coupling coefficients
- $C_{ij}$  - A single element of the coupling coefficient matrix
- $E$  - The complex electric field
- $E_0$  - The unperturbed electric field of a waveguide
- $E_m$  - The real maximum magnitude of the electric field
- $E_{INT}$  - The electric field inside the perturbing dielectric
- $e$  - The charge of an electron
- $f$  - The cyclic frequency of incident microwave energy
- $f_c$  - The cutoff frequency for a waveguide
- $K$  - The complex coupling coefficient between guides
- $K_{ME}$  - A constant used in finding the T matrix
- $K_{MO}$  - A constant similar to the above
- $k_i$  - An arbitrary constant used in equations
- $m$  - The mass of an electron
- $n$  - The electron number density of a plasma
- $P_M$  - A constant proportional to the coupling of a hole
- $R_M$  - A constant used in evaluating the T matrix

- P - The power at a specific point along the waveguide
- r - The radius of each coupling hole
- S - The cross sectional area of a waveguide
- $\Delta S$  - The cross sectional area of a perturbation
- s - The spacing between two consecutive holes
- T - A matrix relating coupling to incident power
- $T_{ij}$  - An element of the T matrix
- Z - The ion charge of an element
- z - Axial Distance along the waveguide
- kT - The plasma temperature in electron-volts

#### Greek Letter Symbols

- $\alpha$  - The attenuation constant of a medium
- $\beta$  - The phase constant of a medium
- $\beta_i$  - A combination of coupling and propagation constants
- $\gamma$  - The propagation constant for a medium
- $\gamma^H$  - A constant used in evaluating the T matrix
- $\Delta?$  - Signifies a change in the ? value
- $\epsilon$  - The complex permittivity of a medium
- $\epsilon_r$  - The real part of the permittivity
- $\epsilon_i$  - The imaginary part of the permittivity
- $\epsilon_0$  - The permittivity of free space
- $\kappa$  - The complex relative dielectric constant
- $\kappa_r$  - The real part of the relative dielectric constant
- $\kappa_i$  - The imaginary part of the relative dielectric constant

- $\lambda$  - The free space wavelength of the microwaves
- $\lambda_g$  - The waveguide wavelength of the microwaves
- $\Lambda$  - A constant used to evaluate the collision frequency
- $\mu$  - The complex permeability of a medium
- $\mu_0$  - The permeability of free space
- $\nu$  - The collision frequency of the plasma
- $\omega$  - The radian frequency of microwaves
- $\omega_c$  - The cutoff frequency of a waveguide
- $\omega_p$  - The plasma frequency

#### Notational Symbols

- $\underline{?}$  - Signifies ? is a matrix
- $?^*$  - Signifies an excited state of the ? gas, or  
Signifies the complex conjugate of ?

Abstract

The goal of this thesis is to develop an analytical model from which a waveguide coupler can be designed. The specific application considered here is to use a waveguide coupler to excite a plasma tube inside a waveguide. This application is desirable for use in laser systems.

The approach taken is to model the plasma as an equivalent dielectric centered in the secondary waveguide. Standard waveguide analysis techniques are used to find a perturbed propagation constant in that waveguide. Successive approximations are made to the coupled wave equations until a piece-wise linear solution is obtained. This solution gives the field distribution resulting from any arbitrarily chosen coupling geometry. Thus, the distribution for any desired coupling characteristics can be determined in an iterative manner, essentially by trial and error.

Preliminary tests were made on couplers designed using the model; initial results are promising but inconclusive. It is believed that this design method will provide the tool for designing couplers to obtain a desired field distribution in the secondary waveguide.

## Contents

	<u>Page</u>
Preface	ii
List of Figures	iv
List of Symbols	vi
Abstract	ix
I. INTRODUCTION AND BACKGROUND	1
Reasons for Interest	1
Background	1
Goals of Research	4
Scope	5
Assumptions	6
General Approach	7
II. THE PLASMA MODEL	9
Plasma Definition and Properties	9
Existing Plasma Model	11
Simplified Model	16
Numerical Values for the Complex Dielectric Constant	17
III. PERTURBATION OF THE WAVEGUIDE	20
Deriving the Perturbation Equations	21
Numerical Evaluation of Parameters	28
IV. SOLUTION TO THE COUPLED WAVE EQUATIONS	31
Generalizing the Coupled Wave Equations	32
Parameter Evaluation	36
Piece-wise Linear Approximation	42
Computer Algorithm	45
V. EXPERIMENT AND RESULTS	50
Performing the Experiment	50
Experimental Results	58
VI. CONCLUSIONS AND RECOMMENDATIONS	73
Conclusions	73
Recommendations	76

	<u>Page</u>
BIBLIOGRAPHY	79
APPENDIX A: UNSUCCESSFUL APPROXIMATIONS TO THE COUPLED WAVE EQUATIONS	80
APPENDIX B: SOLVING FOR THE ELEMENTS OF THE T MATRIX	82
APPENDIX C: COMPUTER ALGORITHM FOR SOLVING THE COUPLED WAVE EQUATIONS	87
APPENDIX D: DISCRETE COUPLER DESIGN	95
APPENDIX E: SEPARABLE COUPLER DESIGN	98
APPENDIX F: SUPPLEMENTARY DATA	104
Vita	133



## I. INTRODUCTION AND BACKGROUND

### Reasons for Interest

The Air Force has a continuing interest in low-power lasers. Applications such as target designation and ranging do not require a high-power laser. These applications require only a low-power laser that is (1) relatively cheap, (2) easy to maintain, and (3) reliable. Current Air Force research is directed toward improving performance in these areas.

One line of research involves finding alternate excitation sources for gas lasers. An example of one of these alternate sources would be a microwave magnetron such as is used in RADAR applications. It is hoped that one of these previously unexplored means of exciting a laser medium will improve the laser's reliability, lifetime, and maintainability.

### Background

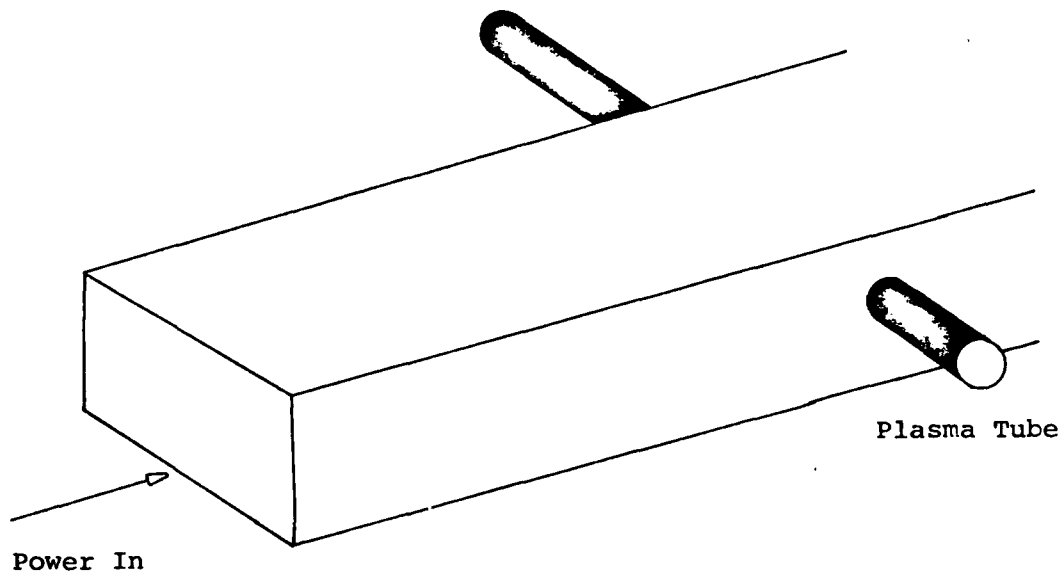
There has not been extensive research into the area of laser excitation by microwaves. Most of the work that has been done deals with a laser tube mounted transverse to the axis of the waveguide as shown in Figure 1(a). However, recent work by Mendelsohn, Normandin, Harris, and Young (Ref 1) involves a new design with the laser tube mounted along

the axis of the waveguide. Mendelsohn, et al., constructed a directional coupler to transfer energy from a primary waveguide to a secondary waveguide containing a plasma tube. The coupler consisted of a series of Riblet Tee slots arranged over a 40 cm section of the common wall between the two waveguides. Figure 1(b) on page 3 is a sketch of the longitudinal coupler of Mendelsohn, et al.

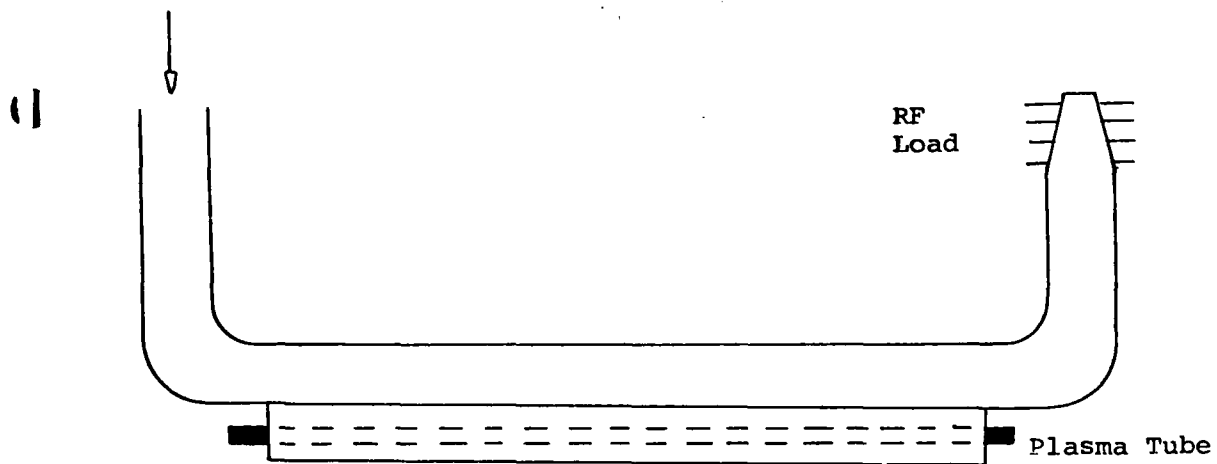
Using this system, powered by a 600 KW magnetron (peak power) delivering a 2  $\mu$ s pulse at 9.375 GHz, laser pulses as long as 100 ns were produced. This is an order of magnitude improvement in pulse length over the avalanche-discharge excitation method. The laser gas in both cases was XeCl\*.

As mentioned earlier, the coupler consisted of a series of Riblet Tee slots arranged to give a uniform energy transfer to the guide containing the plasma tube. The quartz plasma tube was centered in the secondary waveguide and had a 3mm internal diameter. The system coupled from 80 to 90% of the energy in the primary guide into a variety of rare-gas-halogen mixtures in the plasma tube. The gas pressures ranged from 1 to 3 atm. and had a power deposition of from 100 to 200 KW/cm<sup>3</sup>.

A follow on article by Young, Harris, Wisoff, and Mendelsohn (Ref 2) includes a section describing the behavior of a plasma discharge excited by microwaves. This section includes equations for calculating the electron number density and collision frequency.



( a ) - Transverse excitation



( b ) - Longitudinal excitation

Figure 1 - Microwave Excitation Methods

Although much of the first article was repeated, new work by Young, et al., was also included. This new research was performed using a higher power magnetron (1.4 MW peak power) and a modified secondary waveguide. The new secondary waveguide tapers down to an inner height equal to the plasma tube's outer diameter. The coupling structure was also changed. The new coupler consisted of a combination of Riblet Tee slots and a completely open common wall between the waveguides.

With this structure, microwave absorption was 50% or greater over the duration of the microwave pulse. The laser pulse width was increased to approximately 200 ns, but overall laser output power declined. By increasing laser gas pressures to 5 atm., nonuniform excitation of the plasma became noticeable. A conclusion was reached that electron number density increases faster than collision frequency and thereby limits microwave absorption by the plasma.

#### Goals of Research

The goal of this thesis was to reproduce and extend the work of Mendelsohn, et al., and Young, et al., using E-band (2.625 GHz) equipment. This involved developing an analytical model to describe the coupling of power from one waveguide to the other using existing microwave circuit theory. This model was then tested by designing and building a coupler which underwent testing in the laboratory.

### Scope

The matter of primary interest in this thesis was to develop a model for building a waveguide coupler. Although the reason for building this coupler was to excite a laser gas, it was the coupler design and testing that was of primary importance. Therefore, the laboratory testing was conducted to verify the coupler design and did not incorporate extensive testing of the laser output produced by the microwave excited system.

The rare-gas-halides were not used as the plasma gases in the testing since, in general, they are expensive. The gases used as substitutes included Helium, Argon, Nitrogen, and Carbon Dioxide. These gases cover a wide range of electro-negativity, and since it is the generation of a plasma and not laser lines that is important in designing a coupler, these gases should suffice.

Many experimental constraints were set by equipment limitations or unavailability. The lowest pressure attainable for the plasma gases was limited by the vacuum pump to a few Torr. Similarly, the maximum pressure attainable was limited by the maximum pressure reading on the pressure guages of 3 atm. The lack of suitable glass tubing forced the plasma tube to be made with an inner diameter of either 8 mm using thin-wall quartz or 3 mm using heavy-wall pyrex instead of the 5 mm used in the design work.

Finally, the type of microwave excitation had to be changed from pulsed to CW due to a failure in the power supply for the pulsed unit. This became critical when the microwave absorbers, which were adequate for pulsed work, became overheated under CW conditions. Also, if any pulsed laser is to be built using this system, a pulsed microwave supply will be essential.

#### Assumptions

One of the most difficult problems encountered in the development of an analytical model to describe the coupling of power between the two waveguides was the development of a model for the plasma in the laser tube. A full analytical model of a plasma is far beyond the scope of this thesis, so several approximations were made in order to work with more tractable mathematics.

The first of these approximations was to assume that the plasma is homogeneous over the length of the discharge tube. This assumption can be made because it is the overall effect of the plasma, and not local variations, that is the important factor influencing the system. The variations referred to here are variations in the plasma flow and temperature, and not variations in the degree with which the plasma is excited.

The next assumption is to accept a Lorentz plasma as an adequate description of the laser plasma. This assumption

takes into account only electron-electron interactions, neglecting collisions and thermal effects. It is a gross over simplification, especially at higher gas pressures, but more accurate models are far too complicated to deal with in a report of this nature.

One further assumption is to limit the electron number density to variations between  $10^{13}$  and  $10^{14}$ . This range of densities was obtained from earlier experiments dealing with the rare-gas-halides, and especially  $\text{XeCl}^*$ . Any deviation between these values and actual values can be corrected by varying the laser gas's pressure and mixture.

#### General Approach

The overall approach to the problem was broken into three parts. First, a model was developed for the plasma which yielded its complex permittivities. Second, these complex permittivities, which describe a lossy dielectric, were used to perturb the propagation constant of the waveguide containing the plasma tube. Finally, standard microwave circuit techniques were used to model the coupling of energy in one waveguide to another waveguide containing the "lossy dielectric."

Chapter II deals with the modeling of the plasma. The simplified equations of Young, et al., are used to calculate the collision frequency of the plasma. This value is then used to calculate the complex permittivities of the plasma.

This allows the plasma to be replaced by an equivalent dielectric.

Chapter III uses the equivalent dielectric idea of Chapter II along with standard perturbation techniques to find a modified propagation constant for the waveguide containing the plasma tube. The resulting propagation constant treats this waveguide as a uniform but lossy structure.

Chapter IV then uses the propagation constant of the lossy waveguide to develop a model for the coupling between waveguides. This model is based on standard coupled wave equations and the equivalent polarization currents for holes (Bethe-holes), following the approach of Sporleder (Ref 11: 36,55). This model can be solved to obtain the required size and distribution of holes in the waveguide wall in order to meet system requirements.

Chapters V and VI give the results and conclusions respectively for the testing performed on couplers designed using the model developed in Chapter IV. Chapter VI also gives recommendations for future research in the same area.



## II. THE PLASMA MODEL

In order to build any kind of waveguide coupler for microwaves, the manner in which power is propagated in both waveguides must be understood. This is not possible unless the effects (on the propagation of power) of all objects contained within the waveguides are adequately modeled. In the present case, this involves modeling the effects due to the plasma contained within the secondary waveguide. Therefore, this chapter is devoted to modeling this plasma in such a way as to describe its effects on the propagation of power in that waveguide.

To assist the reader, an extensive amount of background material is given on the subject of plasmas and plasma excitation by microwaves. Covered material includes the definition of a plasma, some of its properties, and the accepted theoretical model of a plasma excited by microwaves. This model is extremely complex, and difficult to use, so a much simpler model is introduced. It is this simplified model upon which subsequent results are based. Finally, the plasma is likened to a dielectric and described by its complex permittivities.

### Plasma Definition and Properties

Heald and Wharton (Ref 3:1) describe a plasma as a

medium for propagating electromagnetic waves that is "refractive, lossy, dispersive, resonant, anisotropic, nonreciprocal, nonlinear, and inhomogeneous." A more simplified description given by Golant, et al., (Ref 4:2) defines a plasma as a collection of highly ionized gas particles. From the diversity of these descriptions, it is obvious that a plasma is an extremely complicated phenomenon.

One of the most interesting properties of a plasma is the variation of its propagation constant with the frequency of microwaves passing through it (Ref 3:7-10). Let the propagation constant  $\gamma$  be defined as

$$\gamma = \alpha + j\beta \quad (1)$$

where  $\alpha$  is the attenuation constant and  $\beta$  is the phase constant. Figure 2 shows the dependence of  $\alpha$  and  $\beta$  on frequency for a typical plasma. As can be seen, the propagation constant varies greatly in the vicinity of  $\omega_p$  and much more slowly elsewhere.

A property of plasmas that is important to remember is that a plasma is essentially a conductor. The electrical properties of a typical plasma are similar to room temperature copper (Ref 3:8). Thus, if a plasma exists within an electric field, the reaction of the field will be as if a conducting medium were present.

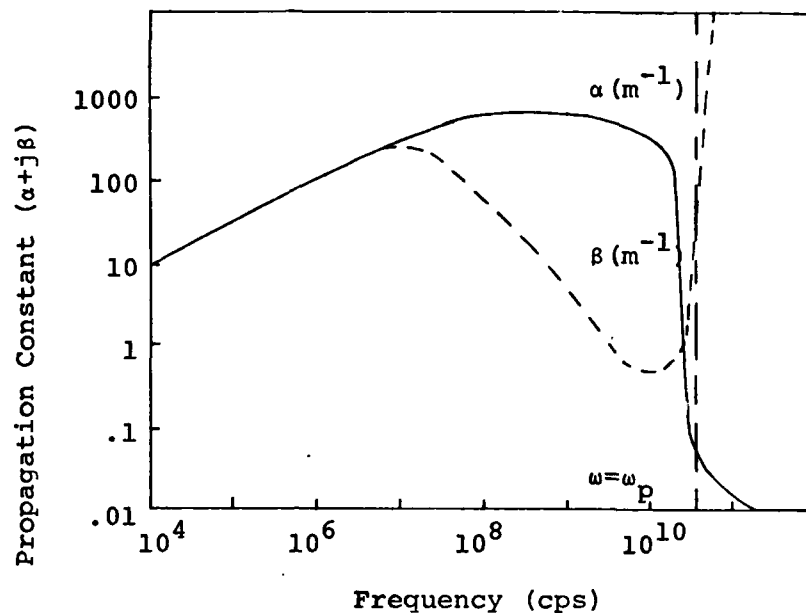


Figure 2 - Attenuation and Phase Constants Versus Frequency for a Typical Plasma

#### Existing Plasma Model

The currently accepted model for a plasma under microwave excitation is extremely complex. Entire books have been written on the subject (Ref 4;5;6), so it is far beyond the scope of this thesis to explain the model in detail. However, enough of the model will be presented to understand the effects of microwaves on a plasma, and conversely, the

effects of a plasma on a microwave waveguide. Points to be covered include defining the plasma frequency, the collision frequency, shielding, and the Lorentz dielectric constants.

Plasma frequency. In its most simple form, a definition for plasma frequency is the frequency at which electrons oscillate about their equilibrium positions after removal of a perturbing force. This force can be an electric field, (DC or alternating) or a magnetic field. Independent of the means of perturbing the plasma, the plasma frequency is the same. This is due to the fact that this resonant frequency is linked to parameters of the plasma gas and not to the excitation source. This parameter dependence of the plasma frequency  $\omega_p$  is defined in the following equation (Ref 3:3).

$$\omega_p = [(ne^2)/(\epsilon_0 m)]^{1/2} \quad (2)$$

where

$n$  = the electron number density ( $\text{cm}^{-3}$ )

$e$  = the electron charge

$\epsilon_0$  = the permittivity of free space

$m$  = the mass of an electron

If the electron number density is given in units of  $\text{cm}^{-3}$ , the Eq 2 reduces to

$$\omega_p = 56417(n)^{1/2} \quad (3)$$

The plasma frequency is one of the most essential parameters used to describe a plasma. Since the only unknown in this equation is the electron number density, it is relatively easy to evaluate. None of the other parameters used to describe a plasma are as easily obtained.

Collision Frequency. The collision frequency  $\nu$  is another one of the basic parameters used to describe a plasma. In essence, this parameter describes a damping force exerted on oscillating electrons which is proportional to their velocity (Ref 3:57). The equations necessary to evaluate the collision frequency are quite complicated. Even after reducing and combining these equations as much as possible, the two resulting equations are still complicated. Also, even though the collision frequency is the parameter of interest, only its effective value is described as follows.

$$\langle \nu \rangle = 2.9 \times 10^{-6} [Zn \ln(\Lambda) / (kT)^{3/2}] \quad (4)$$

where

$Z$  = the charge of the ions in the plasma

$n$  = the electron number density in  $\text{cm}^{-3}$

$kT$  = the electron temperature in electron volts

$\Lambda$  = the Debye length divided by the mean impact parameter for a  $90^\circ$  electron-ion collision

The value for  $\Lambda$  is found using (Ref 3:67)

$$\Lambda = 3.88 \times 10^9 [(kT)^{3/2} / Z(n)^{1/2}] \quad (5)$$

Using these equations, the effective collision frequency (in Hertz) can be calculated. Although these equations are theoretically correct, both are extremely hard to evaluate. There are three unknowns in each of these equations, and only two of them ( $Z$  and  $n$ ) can be determined with any degree of accuracy. The third quantity,  $kT$ , is only a theoretical concept. It cannot be found by simply measuring the temperature of the plasma gas. Therefore, a theoretical value for the collision frequency is difficult to obtain.

Shielding. Shielding is a property of plasmas that are excited by microwave frequencies approaching the plasma frequency. The significance of shielding is that beyond a certain distance, a local excess of charge does not effect the remainder of the plasma. The distance at which this occurs is known as the Debye shielding length  $\lambda_D$  (Ref 3:76-79) and is given by

$$\lambda_D = [\epsilon_0 kT / ne^2]^{1/2} \quad (6)$$

This length is extremely important for microwave excitation, since it gives the maximum plasma thickness through

which microwave excitation takes place. In the present case of a tube inside the microwave waveguide. The shielding length is the maximum radius for a gas column in the tube. As before, this distance is difficult to calculate since it contains the value for electron temperature.

Lorentz dielectric constant. Assuming the values for the collision frequency and the plasma frequency are known, the equation for the Lorentz dielectric constant is relatively simple. Remembering that this constant  $\kappa$  is, in general, a complex quantity given by (Ref 3:6)

$$\begin{aligned}\kappa &= \kappa_r - j\kappa_i \\ &= [1 - \omega_p^2 / (\omega^2 + \nu^2)] - j[(\omega_p^2 \nu / \omega) / (\omega^2 + \nu^2)] \quad (7)\end{aligned}$$

where

- $\kappa_r$  = the real part of  $\kappa$
- $\kappa_i$  = the imaginary part of  $\kappa$
- $\omega_p$  = the plasma frequency
- $\nu$  = the collision frequency
- $\omega$  = the input microwave frequency

Although this equation is simple to evaluate in itself, it does contain the collision frequency. If this value is not known, the equation is useless.

From the complex dielectric constant, the complex permit-

tivity is known. In fact, this value is called the relative dielectric constant by some authors (Ref 5). As such, the complex permittivity  $\epsilon$  is defined as

$$\epsilon = \epsilon_0 \kappa \quad ( 8 )$$

where  $\epsilon_0$  is the permittivity of free space.

#### Simplified Model

The greatest difficulty encountered in using the plasma model of the previous section is solving for the collision frequency. Therefore, a more simplified model for the collision frequency will be developed. Once this quantity is calculated, the remainder of the theory from the previous section will be used as stands.

The simplification used will be the same one used by Young, et al., (Ref 2:64) in their solution to the same modeling problem for the plasma. Young, et al., observed that for pressures above about 500 Torr, the plasma frequency equals the collision frequency. Therefore, if the plasma frequency can be calculated, then the collision frequency is known as well. At this point, the complex dielectric constant is calculated using Eq 7.

This simplified model depends solely on being able to calculate the plasma frequency. However, as is shown in Eq 3, the only parameter that must be known in order to calcu-



late the plasma frequency is the electron number density. In essence, knowing the electron number density is sufficient knowledge to calculate the complex dielectric constant of the plasma.

#### Numerical Values for the Complex Dielectric Constant

As stated at the end of the previous section, the electron number density must be known in order to obtain numerical values for the complex dielectric constant. The value used in this thesis is obtained from previous work with microwave excitation of plasmas. Since the specific laser gas of interest is  $\text{XeCl}^*$ , the number density for this gas was used. According to Dr. W. K. Schuebel (Ref 7), typical electron number densities for a  $\text{XeCl}^*$  plasma are in the range of  $10^{13}$  to  $10^{14} \text{ cm}^{-3}$ . Figure 3 is a plot of the plasma frequency (also the collision frequency) over this density range.

As can be seen, the plasma frequency increases quite rapidly at first then more slowly as the number density gets larger. Since the changes are less pronounced for higher densities, the value for the number density was chosen as

$$n = 8.0 \times 10^{13} \text{ cm}^{-3} \quad (9)$$

There is one more reason for choosing a high value for the number density. If the value chosen for the model is too

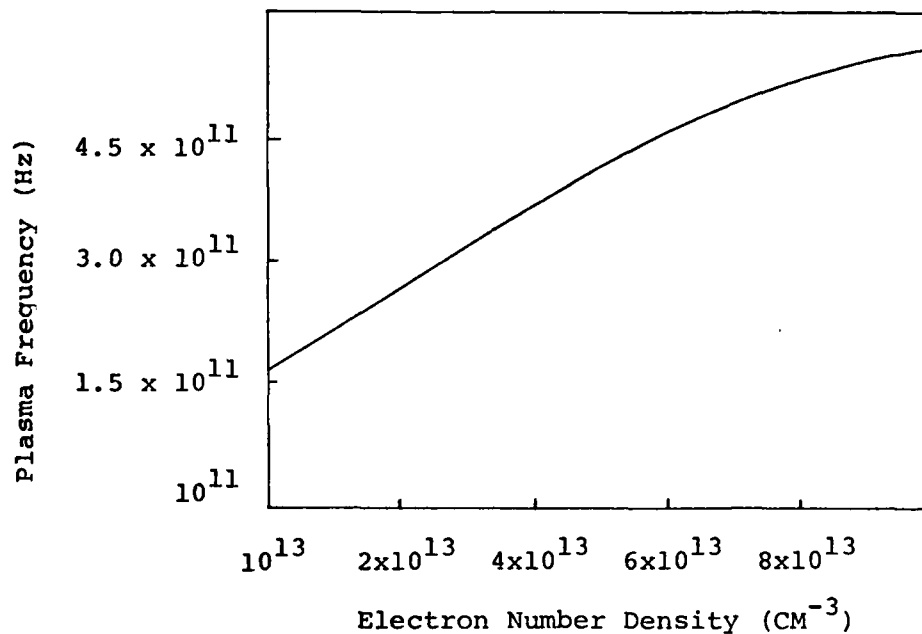


Figure 3 - Plasma Frequency versus Electron Number Density

high then less energy will be coupled into the plasma, but the plasma will never be shielded.

Substituting Eq 8 into Eq 3, with an input microwave frequency of 2.625 GHz, gives a plasma frequency of

$$\omega_p = 504.6 \text{ GHz} \quad (10)$$

Thus, the collision frequency is also 504.6 GHz. Substi-

tuting these two values into Eq 7 yields

$$\kappa = 0.00106 + j30.563 \quad ( 11 )$$

Thus, Eq 8 yields a complex permittivity of

$$\epsilon = \epsilon_0 (0.00106 + j30.563) \quad ( 12 )$$

With this knowledge, the plasma is now modeled as a lossy dielectric. Since the effects of dielectrics in waveguides is well understood, this knowledge allows a better understanding of the variations in the propagation constant of the waveguide containing the plasma tube.

### III. PERTURBATION OF THE WAVEGUIDE

Accepting the plasma model as correct, the next step toward designing a coupler for the system is to find the altered propagation constant in the secondary waveguide. Since this waveguide is now a composite structure of a plasma tube within a waveguide, its propagation constant will be markedly altered. A knowledge of the propagation constant in this guide is essential for building a coupler.

Chapter II developed a model for the plasma as a lossy dielectric. The plasma was modeled in such a manner so as to exploit standard perturbation techniques for finding the propagation constant of the combined structure. These techniques most often deal with cases where the perturbing medium is a dielectric. Therefore, the plasma was intentionally modeled to conform to the perturbation techniques.

Even if the model of the plasma as a dielectric is adequate, there is still one configuration which has not been modeled. All discussions to this point have assumed that the plasma was always present in the laser tube. This, of course, is not the case. For a short period of time, before the plasma forms, the secondary waveguide is essentially an empty waveguide. Coupling between this now "lossless" waveguide and the primary "lossless" waveguide has been studied extensively, and will not be considered here. Although this

initial coupling is important, since it initiates the plasma, it is the coupling of energy into the plasma itself that is of importance in this thesis.

The following sections will use the perturbation techniques for the case of the laser tube containing a plasma. First the equations are derived for the particular perturbation of interest (a longitudinally centered dielectric). Then, numerical solutions are found for the perturbed propagation constant.

#### Deriving the Perturbation Equations

There are several types of perturbation formulas. The ones used here cover the case of a perturbation within the waveguide. As shown in Figure 4, the perturbing medium of interest is a longitudinally centered "dielectric rod." This type of perturbing sample can be well modeled by the perturbational approach, since it has a small local effect on the electric field.

Since perturbation formulas depend on a knowledge of the properties of the empty structure, it is appropriate to define the propagation constant  $\gamma_0$  for that case.

$$\gamma_0 = \alpha_0 + j\beta_0 \quad (13)$$

where  $\alpha_0$  is the attenuation constant and  $\beta_0$  is the phase constant of the waveguide with no perturbing medium present.

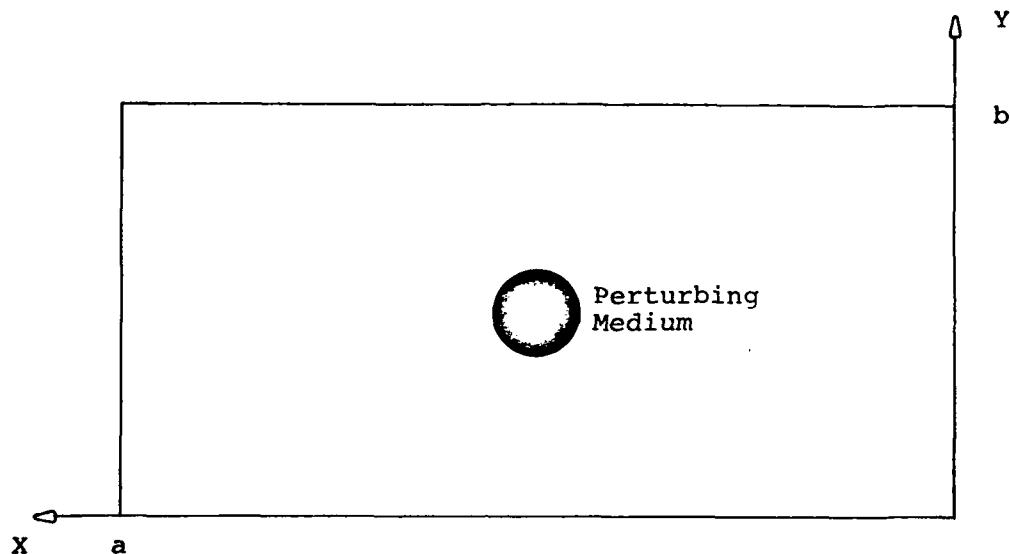


Figure 4 - Cross Section of Waveguide Containing Perturbing Medium

If it is assumed that the waveguide is lossless then  $\alpha_0$  becomes zero and Eq 12 simplifies to

$$\gamma_0 = j\beta_0 \quad (14)$$

A numerical value for  $\beta_0$  can be calculated by using the following equation (Ref 9:68).

$$\beta_o = 2\pi/\lambda [1 - (f_c/f)^2]^{1/2} \quad (15)$$

where

$\lambda$  = the free space wavelength of the microwaves

$f_c$  = the cutoff frequency for the principle mode  
of the waveguide in use

$f$  = the microwave frequency

The objective of using a perturbational method is to calculate the new propagation constant  $\gamma$ . This constant is defined as

$$\gamma = \alpha + j\beta \quad (16)$$

In general, both  $\alpha$  and  $\beta$  will be nonzero.

The derivation of the perturbation equations to be used begins with the accepted equations that follow (Ref 8:415; 9:329).

$$\beta - \beta_o = [\epsilon_o (\kappa_r - 1) \omega \int_{\Delta S} E_o^* \cdot E \, dA] / 4P \quad (17)$$

$$\alpha - \alpha_o = [\epsilon_o (\kappa_i) \omega \int_{\Delta S} E_o^* \cdot E \, dA] / 4P \quad (18)$$

where

$E_o$  = The unperturbed complex electric field

$E$  = The perturbed complex electric field

of the composite structure

$\Delta S$  = the cross sectional area of the perturbation

$\epsilon_0$  = the permittivity of free space

$\kappa_r$  = the real part of the complex dielectric  
constant

$\kappa_i$  = the imaginary part of the complex  
dielectric constant

$\omega$  = the input microwave radian frequency

$P$  = the power passing through the waveguide

These equations are quite general, and fit a variety of applications. At this point, however, these equations are modified to suit this particular problem.

The first step in evaluating Eqs 17 and 18 is to develop a functional form of  $E$  and  $E_0$ . This is also where the first customization of the two equations occur. The equation for  $E_0$  is straight forward (Ref 8:173).

$$E_0 = E_m \sin(\pi x/a) \exp(-\gamma_0 z) \quad (19)$$

where

$E_m$  = the maximum amplitude of the electric field

$x$  = the distance along the  $x$  axis

(see Figure 4)

$a$  = the width of the waveguide in the



x direction

$\gamma_0$  = the unperturbed propagation constant

If the variation of the permittivity or permeability is small, then the assumption can be made that the perturbed electric field is approximately the same as the unperturbed field (Ref 8:173). However, better results can be obtained if a quasi-static approximation is made. This approximation is based on the fact that, for a dielectric rod with the electric field normal to its axis, the internal field is related to the external field by (Ref 9:324)

$$E_{INT} = 2/(1 + \kappa_r) E_0 \quad (20)$$

where

$E_{INT}$  = the internal electric field  
 $E_0$  = the external electric field  
 $\kappa_r$  = the relative permittivity of the rod

To use the quasi-static approximation, the functional form for E in Eqs 17 and 18 becomes  $E_{INT}$  in the numerator and  $E_0$  in the denominator. Thus, in the numerator of Eqs 17 and 18, the functional form of E is

$$E = 2/(1 + \kappa_r) E_0 \quad (21)$$

while in the denominator the functional form is

$$E = E_0 \quad (22)$$

Thus,  $E=E_0$  over most of the cross-section of the waveguide, but it varies from that value near the perturbation.

Before substituting these functional forms into Eqs 17 and 18, the  $z$  dependence is removed. (The  $z$  direction is along the axis of the waveguide.) This is done because only cross-sectional variations of the electric field are important. Without the  $z$  dependency, Eqs 19, 21, and 22 become respectively.

$$E_0 = E_m \sin(\pi x/a) \quad (23)$$

$$E = [2E_m \sin(\pi x/a)]/(1 + \kappa_r) \quad (24)$$

for points inside the perturbation, and

$$E = E_m \sin(\pi x/a) \quad (25)$$

for points outside the perturbing medium. Once again, Eq 24 is used in the numerator of Eqs 17 and 18 while Eq 25 is used in the denominator.

Substituting Eqs 23 and 24 into the integral in the

numerator of Eqs 17 and 18 gives

$$\int_{\Delta S} E_O^* \cdot E \, dA = 2E_m^2 / (1 + \kappa_r) \int_{\Delta S} [\sin(\pi x/a)]^2 dA \quad (26)$$

This equation can be greatly simplified if an approximation is made that  $\Delta S$  is so small that  $x$  is essentially constant at its central value of  $a/2$ . With this approximation, Eq 26 becomes

$$\begin{aligned} \int_{\Delta S} E_O^* \cdot E \, dA &= 2E_m^2 [\sin(\pi a/2a)]^2 / (1 + \kappa_r) \int_{\Delta S} dA \\ &= (E_m^2 \pi d^2) / 2(1 + \kappa_r) \end{aligned} \quad (27)$$

where  $d$  is the diameter of the plasma tube.

In a similar manner, Eqs 23 and 25 are substituted into the denominator of Eqs 17 and 18 to evaluate  $P$ . This is done by using the following equation (Ref 8:174).

$$\begin{aligned} P &= 1/2 \epsilon_0 \int_S |E|^2 \, dA \\ &= E_m^2 \lambda_g ab / [4\lambda (\mu_0 / \epsilon_0)^{1/2}] \end{aligned} \quad (28)$$

where  $\lambda_g$  is the guide wavelength of the unperturbed system.

Substituting Eqs 27 and 28 into Eqs 17 and 18 yields respectively

$$\begin{aligned} \beta - \beta_0 &= [(\pi d)^2 (\kappa_r - 1)] \\ &\quad / [\lambda ab (\kappa_r + 1) (1 - (\omega_c/\omega)^2)^{1/2}] \end{aligned} \quad (29)$$

$$\alpha = [(\pi d)^2 \kappa_i] / [\lambda ab (\kappa_r + 1) (1 - (\omega_c/\omega)^2)^{1/2}] \quad (30)$$

where b is the narrow internal dimension of the waveguide in use.

One more perturbation equation is necessary in this particular instance. With a perturbing medium in the waveguide, the cutoff frequency changes. Therefore, if the input microwave frequency is near the unperturbed cutoff frequency, as it is in this case, a perturbed cutoff frequency should be used. The equation for this perturbation is (Ref 9:374)

$$\Delta\omega_c = \omega_c (\pi d^2 / 2ab) [(1 - \kappa_r) / (\kappa_r + 1)] \quad (31)$$

where  $\Delta\omega_c$  is the incremental change to be added to the unperturbed cutoff frequency in order to get the new perturbed cutoff frequency.

#### Numerical Evaluation of Parameters

The equations presented in the previous section were used to calculate the perturbed propagation constant of the secondary waveguide. The constants describing the system are as follows:

$$d = 0.50 \text{ cm} \quad \omega = 16.493361 \text{ G rad/sec}$$

$$\begin{aligned} a &= 7.214 \text{ cm} & \omega_c &= 13.055529 \text{ G rad/sec} \\ b &= 3.404 \text{ cm} & \lambda &= 11.4207 \text{ cm} \end{aligned}$$

This value for  $d$  was chosen as a typical bore size for a laser tube. Similarly, the value for  $\omega$  was chosen because it was near the mid point of the two frequency extremes to be used in testing. The other parameters which describe the waveguide were taken from a microwave handbook (Ref 10:350). The value of the dielectric constant is given in Eq 11.

Substituting and evaluating, gives

$$\Delta\omega_c = 208.338 \text{ M rad/sec} \quad ( 32 )$$

Thus, the new perturbed cutoff frequency  $\omega_c^1$  is

$$\omega_c^1 = 13.264 \text{ G rad/sec} \quad ( 33 )$$

The value for  $\beta_0$  as calculated using Eq 15 is

$$\beta_0 = 0.3362 \text{ rad/cm} \quad ( 34 )$$

Finally, substituting into Eqs 29 and 30 yields

$$\beta = 0.3214 \text{ rad/cm} \quad ( 35 )$$

$$\alpha = 0.4516 \text{ Np/cm} \quad ( 36 )$$

or substituting into Eq 16, the perturbed propagation constant is

$$\gamma = (0.4516 + j0.3214) / \text{cm}$$

( 37 )

Thus, the value for the propagation constant of the secondary waveguide is known. With this value, designing a coupler is now possible.

#### IV. SOLUTION TO THE COUPLED WAVE EQUATIONS

This chapter develops the model to be used in designing a microwave waveguide coupler. The starting point for this model is the coupled wave equations. These differential equations describe the variations of the electric fields occurring in both waveguides due to coupling between the waveguides and propagation along each waveguide. Thus, a model based on these equations includes all physical properties of the actual system.

The merit of the system was judged on a combination of two parameters. First, the distribution of energy in the secondary waveguide should remain nearly constant (to within a few percent) along its length. Second, as much energy as possible should be coupled out of the primary waveguide. Therefore, the "ideal" design would couple all of the energy out of the primary waveguide while maintaining a constant energy density in the secondary waveguide. As will be seen in the following sections, this "ideal" design is impossible to build.

The model was developed by, first, generalizing the coupled wave equations for the present situation. Then, a method was developed for evaluating the parameters in the equation. Next, a piece-wise linear approximation was used to solve these equations. Finally, a computer algorithm was

developed to iteratively solve these equations until the system performance was acceptable.

### Generalizing the Coupled Wave Equations

Before introducing the coupled wave equations, some notation must be defined. (this notation is consistent with that of Sporleder [Ref 11].) A subscript of 1 denotes a parameter describing the primary waveguide. Similarly, a subscript of 2 denotes a parameter describing the secondary waveguide. The appearance of minus signs in front of these subscripts denotes waves traveling toward the microwave source, while the absence of a sign denotes waves traveling away from the microwave source. This notation will prevail throughout the rest of the chapter.

Since a waveguide coupler is a four-port device, the coupled wave equations defined by Sporleder (Ref 11:27) are

$$d/dz \underline{A} = [-\underline{\gamma} + \underline{C}] \underline{A} \quad (38a)$$

or, in expanded form

$$d/dz \begin{bmatrix} A_1 \\ A_2 \\ A_{-1} \\ A_{-2} \end{bmatrix} = \begin{bmatrix} -\gamma_1 + C_{11} & C_{12} & C_{1-1} & C_{1-2} \\ C_{21} & -\gamma_2 + C_{22} & C_{2-1} & C_{2-2} \\ C_{-11} & C_{-12} & -\gamma_{-1} + C_{-1-1} & C_{-1-2} \\ C_{-21} & C_{-22} & C_{-2-1} & -\gamma_{-2} + C_{-2-2} \end{bmatrix} \begin{bmatrix} A_1 \\ A_2 \\ A_{-1} \\ A_{-2} \end{bmatrix} \quad (38b)$$



where, in accordance with the notation just defined

$A_1$  = The amplitude of a traveling wave in the primary waveguide

$A_2$  = The amplitude of a traveling wave in the secondary waveguide

$\gamma_1$  = The propagation constant in the primary waveguide

$\gamma_2$  = The propagation constant in the secondary waveguide

$C_{ij}$  = The coupling coefficient of wave  $j$  to wave  $i$

$z$  = the distance along the axis of the waveguide

These equations describe the changes in the wave amplitudes that occur due to a continuous coupling between modes. However, the coupler design being considered here consists of a series of small holes and therefore coupling occurs only at discrete points and not continuously. Eq 38a gives a continuous description of the effect of these holes that remains adequate as long as the separation between holes remains less than half the waveguide wavelength (Ref 11: 256). This stipulation must be made because holes separated by this length will strongly couple the forward and backward traveling waves of the two waveguides. Since Eq 38b does not allow this type of coupling, the hole spacing must be

restricted to less than one half the waveguide wavelength. With such a restriction, Eq 38b can be used to find an analytic model to be used in designing a coupler even though discrete holes are used.

Simplifications. The restriction on hole spacing of the last section is of great significance. Not only does it allow Eq 38b to be used, but it also allows that equation to be simplified. If the coupler is several guide wavelengths in length, then the restriction on hole spacing ensures that coupling between forward and backward traveling waves is minimal. This allows the assumption to be made that the coupling to backward traveling waves from forward traveling waves is negligible. Hence, all references to backward traveling waves in Eq 38b are ignored and the equation simplifies to

$$d/dz \begin{bmatrix} A_1 \\ A_2 \end{bmatrix} = \begin{bmatrix} -\gamma_1 + C_{11} & C_{12} \\ C_{21} & -\gamma_2 + C_{22} \end{bmatrix} \begin{bmatrix} A_1 \\ A_2 \end{bmatrix} \quad ( 39 )$$

To simplify notation, three new variables are introduced.

$$\beta_1 = -\gamma_1 + C_{11} \quad ( 40 )$$

$$\beta_2 = -\gamma_2 + C_{22} \quad ( 41 )$$

$$K = C_{12} = C_{21} \quad ( 42 )$$

Although it is not explicitly stated here, all three of

these parameters are implicitly dependent on  $z$ . This  $z$  dependence may be constant over the length of the coupler, but, it is most likely varying with distance along the waveguide. The most important point to be made here is that this dependence on  $z$  is not known. In fact, the functional dependence on  $z$  of the coupling coefficients is the information necessary to design a waveguide coupler.

After substituting these new parameters, Eq 39 becomes

$$d/dz \begin{bmatrix} A_1 \\ A_2 \end{bmatrix} = \begin{bmatrix} \beta_1 & K \\ K & \beta_2 \end{bmatrix} \begin{bmatrix} A_1 \\ A_2 \end{bmatrix} \quad ( 43 )$$

Although this equation looks deceptively simple, it does not have an analytic solution when the coupling coefficients have an arbitrary dependence on  $z$  (Ref 11:160). Therefore, in order to solve the equation, either some approximations must be made or the functional form for the coupling coefficients must be known. Since this functional form is the solution being sought, it obviously cannot be known. Thus, some kind of approximation must be made in the equation.

Several types of seemingly logical approximations were tried. These unsuccessful approximations are listed in Appendix A in order to prevent others from spending fruitless effort in deriving them. The approximation finally decided upon was to accept  $\beta_1$ ,  $\beta_2$ , and  $K$  as constant over a specified interval and solve Eq 43 accordingly. The same

process is repeated in adjacent intervals with the values of  $\beta_1$ ,  $\beta_2$ , and  $K$  taken to be new and possibly different constants. An inherent part of this process is, of course, being able to determine numerical values for  $\beta_1$ ,  $\beta_2$ , and  $K$ . Thus, the next section develops a method for calculating these parameters.

#### Parameter Evaluation

Much of following parallels the approach of Sporleder (Ref 11:52-55) where the coupling coefficients are calculated with respect to system parameters. The concept used models holes in the common wall of two waveguides as equivalent polarization currents. These currents are then used to calculate the coupling coefficients for the system. This section will present the essential parts of Sporleders approach, expand this approach for the present case of a lossy waveguide, and simplify the resulting equations as much as possible. These equations are used to evaluate the coupling coefficients which will be used in solving Eq 43.

Sporleder begins his development by replacing a hole in the common wall of the waveguide by its equivalent electric and magnetic dipoles (Ref 11:50). Then the amplitude with which these dipoles excite the modes in each waveguide is calculated in the following matrix equation (Ref 11:52).

$$\Delta \underline{A}(z) = \underline{T} \underline{A}(z) \quad (44)$$

where  $\Delta \underline{A}$  is the vector of the amplitudes of the excited modes in both waveguides, and  $\underline{A}$  is a vector of the amplitudes of the incident modes in both waveguides. This equation describes the discrete coupling between waveguides of a single coupling hold. A method of calculating the elements of the  $\underline{T}$  matrix follows.

The equations necessary to evaluate the matrix  $\underline{T}$  are many and complicated (Ref 11:36-52). In the present case of holes centered in the common narrow wall of two waveguides which support the  $TE_{10}$  mode, these equations can be combined (see Appendix B) to give the following simplified equation for each element of the  $\underline{T}$  matrix.

$$T_{mn} = P_M \pi^2 / [8(a/2)^3 b (\gamma_m \gamma_n)^{1/2}] \quad (45)$$

where

$P_M$  = a real constant related to hole size

$a$  = the broad dimension of the waveguide in use

$b$  = the narrow dimension of the waveguide in use

$\gamma_1$  = the propagation constant in the primary  
waveguide

$\gamma_2$  = the propagation constant in the secondary  
waveguide

The value for  $P_M$  is evaluated differently for  $n$  equal to  $m$  than for  $n$  different from  $m$ . In the case where  $n$  equals  $m$ ,  $P_M$  is given by (Ref 11:51)

$$P_M = 4/3 r^3 R_M K_{ME} \quad (46)$$

where  $r$  is the hole radius, and  $R_M$  and  $K_{ME}$  are positive real constants related to the hole size.

Similarly, for  $n$  not equal to  $m$ ,  $P_M$  is given by

$$P_M = 4/3 r^3 R_M K_{MO} \quad (47)$$

where, as before,  $K_{MO}$  is a real positive constant related to the hole size.

In both of the above equations, the values for  $R_M$ ,  $K_{ME}$ , and  $K_{MO}$  are calculated using the following equations (Ref 11:52).

$$R_M = 1/[1-0.4(kr)^2] \quad (48)$$

$$K_{ME} = 1 - [0.35+0.15(kr)^2][1-\exp(-2\gamma^H t)] \quad (49)$$

$$K_{MO} = \exp(-\gamma^H t([1-(0.1+(0.3+0.15(kr)^2)^2)(1-\exp(-2\gamma^H t))]) \quad (50)$$

where

$$\gamma^H = [(1.84/r)^2 - k^2]^{1/2} \quad (51)$$

It must be stressed that Eq 44 describes discrete coupling only. In order to use it in the continuous regime, the effects it predicts must be smeared out over some distance. Adopting the approach of Sporleder (Ref 11:53), this is done by considering the distance from  $z = z_1 - s/2$  to  $z = z_1 + s/2$  where  $s$  is the separation between holes. If, over this distance, the elements of the matrix in Eq 43 are constant, then the conversion from discrete to continuous coupling is accomplished in the following manner.

First, all mode coupling is neglected and the incident modes are propagated according to the following equation (Ref 11:53).

$$A_n(z) = A_n(z_1) \exp[-\gamma_n(z-z_1)] \quad (52)$$

Then, the coupled wave equation is integrated with the value for  $C_{mn}$  assumed negligible. The resulting equation is (Ref 11:53)

$$\Delta A_m(z_1) = \int_{z_1-s/2}^{z_1+s/2} A_n(z) C_{mn} \exp[-\gamma_m(z_1-z)] dz \quad (53)$$

Taking  $z = z_1$  as a reference point, this becomes

$$\Delta A_m(z) = A_n(z) s C_{mn} \frac{[\sinh((\gamma_m - \gamma_n)s/2)]}{[(\gamma_m - \gamma_n)s/2]} \quad (54)$$

Eqs 44 and 54 can be combined to solve for the coupling coefficient  $C_{mn}$ . The resulting equation is the link between the discrete coupling of Eq 44 and the continuous coupling of Eq 43. The results of combining and simplifying are

$$C_{mn} = T_{mn}/s [(\gamma_m - \gamma_n)s/2]/[\sinh((\gamma_m - \gamma_n)s/2)] \quad (55)$$

To simplify the forthcoming discussion, as many of the preceding equations as possible are evaluated using the known parameters of the system. The following equations give the results.

The values for the propagation constants in both waveguides have already been calculated. Since both waveguides have the same inner dimensions, the unperturbed propagation constant of the secondary waveguide is the propagation constant of the primary waveguide. The propagation constant of the secondary waveguide is the result of Chapter III, listed in Eq 37. To summarize, both propagation constants are listed below with the subscript notation.

$$\gamma_1 = 0 + j \, 0.3362 \text{ /cm} \quad (56)$$

$$\gamma_2 = 0.4516 + j \, 0.3214 \text{ /cm} \quad (57)$$

Next, Eq 45 is simplified. Although there are four elements of the matrix as it is defined, only three of them



are distinct. These values are listed below.

$$T_{11} = (0 - j 0.002297)P_M \quad ( 58 )$$

$$T_{22} = (0.01128 - j 0.007882)P_M \quad ( 59 )$$

where  $P_M$  is evaluated according to Eq 46. The off diagonal entries of the  $\underline{T}$  matrix are equal, and are given by

$$T_{12} = (-0.008218 + j 0.01577)P_M \quad ( 60 )$$

where  $P_M$  is evaluated according to Eq 47.

Using this information, Eq 55 can be simplified. For the case of  $n$  and  $m$  equal, Eq 55 simplifies to the following forms

$$C_{11} = (0 - j 0.002297)P_M s \quad ( 61 )$$

$$C_{22} = (0.001128 - j 0.007882)P_M/s \quad ( 62 )$$

where  $P_M$  is evaluated using Eq 46. The case for  $n$  and  $m$  not equal is much more complex, but it solves directly for the off-diagonal terms of the matrix in Eq 43. Thus, substituting Eq 42 for the left hand side of Eq 55, and simplifying the right hand side gives

$$K = (-0.008218 + j 0.01577)P_M/s$$

$$[(\gamma_1 - \gamma_2)s/2]/\sinh[(\gamma_1 - \gamma_2)s/2] \quad ( 63 )$$

where  $P_M$  is evaluated according to Eq 47.

Thus, by knowing the values for the hole spacing and radius the coupling coefficients for the system can be calculated. Once these values are known, they can be substituted into Eqs 40, 41, and 42 to define the parameters in Eq 43. Thus, for a one-hole coupler these parameters can be used to solve Eq 43. The next section expands this approach for the case of a multi-hole coupler with slowly varying coupling characteristics.

#### Piece-wise Linear Approximation

An approximation to Eq 43 which gives tractable mathematics is a piece-wise linear approximation. This approach approximates the values of  $\beta_1$ ,  $\beta_2$ , and  $K$  as constants over a short distance. This is the same type of approximation used in the previous section, so the results of that section are compatible with this approach. Thus, the parameters in Eq 43 can be evaluated as constants for a coupling section with a length comparable to the hole spacing. This allows Eq 43 to be solved as a system of differential equations with constant coefficients.

A solution to this system of equations is simple, as long as the initial conditions for the system are known. In this case, the initial conditions are the amplitudes of the waves incident on a coupling section. Thus, a solution to

Eq 43 gives the amplitudes of these waves at a point further down the waveguide.

The method chosen for solving Eq 43 was the eigenvalue approach. This method yields the following characteristic equation for the matrix in Eq 43.

$$0 = \lambda^2 - \lambda(\beta_1 + \beta_2) - K^2 + \beta_1 \beta_2 \quad (64)$$

Thus, the eigenvalues for this matrix are given by

$$\lambda_1 = (\beta_1 + \beta_2)/2 + [(\beta_1 + \beta_2)^2/4 - \beta_1 \beta_2 + K^2]^{1/2} \quad (65)$$

$$\lambda_2 = (\beta_1 + \beta_2)/2 - [(\beta_1 + \beta_2)^2/4 - \beta_1 \beta_2 + K^2]^{1/2} \quad (66)$$

where the values for  $\beta_1$ ,  $\beta_2$ , and  $K$  are constants (complex constants) as defined in the previous section. Using these eigenvalues, the functional forms of  $A_1$  and  $A_2$  can be written down immediately.

$$A_1 = k_1 \exp(\lambda_1 z) + k_2 \exp(\lambda_2 z) \quad (67)$$

$$A_2 = k_3 \exp(\lambda_1 z) + k_4 \exp(\lambda_2 z) \quad (68)$$

where  $k_1$ ,  $k_2$ ,  $k_3$ , and  $k_4$  are constants (perhaps complex) determined by the incident boundary conditions.

By substituting Eqs 67 and 68 into Eq 43, two of these

constants can be eliminated. Performing this substitution yields

$$A_2 = k_1 (\lambda_1 - \beta_1) / K \exp(\lambda_1 z) + k_2 (\lambda_2 - \beta_1) / K \exp(\lambda_2 z) \quad (69)$$

and Eq 67 remains unchanged. The values for  $k_1$  and  $k_2$  are obtained by setting  $z = 0$  in Eqs 67 and 69. Since the values for  $A_1$  and  $A_2$  must equal the values of the incident waves at the beginning of the section ( $z=0$ ), the values for  $k_1$  and  $k_2$  can be determined. In equation form, these values are given by

$$k_1 = [KA_{20} - A_{10}(\lambda_2 - \beta_1)] / [\lambda_1 - \lambda_2] \quad (70)$$

$$k_2 = A_{10} - k_1 \quad (71)$$

where  $A_{10}$  and  $A_{20}$  are the amplitudes of the incident waves in the primary and secondary waveguides respectively.

At this point, all the necessary equations have been developed. Their use in the piece-wise linear approximation will now be explained. For a given hole size and spacing, Eqs 61, 62, and 63 are evaluated. The resulting values, along with the values given in Eqs 56 and 57, are then substituted into Eqs 40, 41, and 42. These values are then substituted into Eqs 67 and 69. The two arbitrary constants in these equations are then removed by using Eqs 70 and 71.

The resulting equations give the functional form for the wave amplitudes that remains adequate as long as the approximations made are valid.

One way to ensure that the approximations remain valid is to limit the above equations to distances equal to the hole spacing. In this manner, the above process is performed for the first coupling hole and gives the wave amplitudes that reach the second coupling hole. At this point, these amplitudes become  $A_{10}$  and  $A_{20}$  as given in Eqs 70 and 71 since they are the incident wave amplitudes at this hole. This process is repeated until all coupling holes have been used. The values given at this stage are the terminal wave amplitudes in each waveguide.

The next section presents a computer algorithm to perform this cascading of wave amplitudes along the waveguide. This algorithm does not determine the correct hole size and spacing, but it does provide a means of determining the effects on the system for any hole configurations entered.

#### Computer Algorithm

The computer code included in Appendix C solves the coupled wave equations using the piece-wise linear approximations. The program logic sequence is as follows. First, the values for the coupling coefficients are computed based on a user supplied functional form. These values are then used to compute the parameters in the matrix of Eq 43.

Next, the eigenvalues are computed. These values are then used to calculate the arbitrary constants in Eqs 67 and 68. The values used for  $A_{10}$  and  $A_{20}$  in this calculation are the output wave amplitudes from the previous section (For the first coupling hole these values are preset at 100% and 0% respectively). Finally, the values for  $A_1$  and  $A_2$  are calculated and printed. The program then recycles until the end of the coupler is reached.

Before running the program, the user must enter a functional form for the hole radius on program line 1110. The program is currently set up for constant hole spacing which the user inputs during program execution; however, it would be a simple matter to have the hole separation and radius vary along the length of the coupler. Program outputs give the distance along the coupler and the hole radius, both in centimeters. Also included are the magnitudes of the complex values for  $A_1$  and  $A_2$ .

The computer code included in Appendix C is written in BASIC and is short enough to run on a home computer. All computer runs made with this code were run on an Atari model 800 personal computer with 32K of memory. Run times for the algorithm are on the order of a minute.

Using the algorithm. The algorithm was used to design a coupler by trying several types of coupling geometry. This was done iteratively, with the results being judged by the uniformity of the wave amplitudes for  $A_2$ . Listing 1 is a

typical run which shows that uniformity for  $A_2$  can easily be achieved. However, the algorithm predicts that only about 20% of the power in the primary waveguide is coupled out. Practical experience has shown that a more reasonable figure would be on the order of 80 or 90% for the power coupled out of the primary waveguide.

On this assumption, a modification was made in the algorithm which artificially forces the magnitude of  $A_1$  to decline linearly to 10% of the input power at the end of the coupler. The phase information as given by the algorithm was not altered, only the magnitude was changed. Listing 2 shows a typical run for this empirically altered algorithm. Once again, it is possible to maintain uniformity in  $A_2$ .

One coupler was fabricated using each of these printouts for the design specifications. In both cases, the hole spacing was kept to a minimal value since this would provide for a larger amount of coupling. This is necessary, since a sidewall coupler typically is less efficient than the broad-wall couplers used by Young, et al. (Ref 2).

A third design was built which used standard coupler elements in cascade. This design assumes that all power coupled into the secondary waveguide is immediately absorbed. This design procedure is given in Appendix D.

Testing was then performed on all three coupler designs to determine which gives the "best" performance.

Listing 1 - Program Execution

THE HOLE SPACING IS 3.4 cm.

$R = 0.25 * \exp(-4.4E-03 * Z) + 1.41 * \exp(8.4E-04 * Z)$

IF Z=0 THEN R=1.7

FUNCTIONAL FORM FOR HOLESIZE Vs. DISTANCE

Z	r	A(1)	A(2)
0	1.7	99.75	6.38
3.4	1.66	99.38	7.16
6.8	1.661	99	7.32
10.2	1.661	98.63	7.33
13.6	1.662	98.25	7.32
17	1.662	97.88	7.31
20.4	1.663	97.51	7.29
23.8	1.664	97.13	7.28
27.2	1.664	96.76	7.27
30.6	1.665	96.39	7.25
34	1.666	96.01	7.24
37.4	1.667	95.64	7.23
40.8	1.668	95.27	7.22
44.2	1.669	94.89	7.22
47.6	1.67	94.52	7.21
51	1.671	94.14	7.2
54.4	1.673	93.77	7.2
57.8	1.674	93.39	7.2
61.2	1.675	93.91	7.19
64.6	1.677	92.63	7.19
68	1.678	92.25	7.19
71.4	1.68	91.87	7.19
74.8	1.681	91.49	7.19
78.2	1.683	91.11	7.19
81.6	1.685	90.72	7.19
85	1.686	90.33	7.19
88.4	1.688	89.94	7.2
91.8	1.69	89.55	7.2
95.2	1.692	89.15	7.21
98.7	1.694	88.77	7.21
102	1.696	88.37	7.22
105.4	1.698	87.98	7.23
108.8	1.7	87.58	7.23
112.2	1.702	87.17	7.24



Listing 2 - Program Execution with Declining Power

THE HOLE SPACING IS 3.5 cm.

```
R=0.87*EXP(-3.8E-03*Z)+0.47*EXP(7.65E-03*Z)
IF Z=0 THEN R=1.42
IF Z>104 THEN R=1.638
IF Z>107 THEN R=1.665
IF Z>110 THEN R=1.702
```

z	r	A(1)	A(2)
0	1.42	99.94	2.91
3.5	1.341	99.93	2.92
7	1.343	98.52	2.9
10.5	1.345	97.09	2.87
14	1.348	95.64	2.85
17.5	1.351	94.17	2.84
21	1.355	92.67	2.82
24.5	1.36	91.15	2.81
28	1.364	89.6	2.8
31.5	1.37	88.02	2.8
35	1.376	86.42	2.79
38.5	1.383	84.78	2.79
42	1.39	83.11	2.8
45.5	1.398	81.41	2.8
49	1.406	79.67	2.81
52.5	1.415	77.89	2.82
56	1.425	76.08	2.83
59.5	1.435	74.21	2.84
63	1.446	72.3	2.86
66.5	1.457	70.34	2.87
70	1.47	68.32	3.89
73.5	1.483	66.23	2.9
77	1.496	64.09	2.92
80.5	1.511	61.86	2.93
84	1.526	59.56	2.95
87.5	1.542	57.16	2.96
91	1.558	54.65	2.96
94.5	1.576	52.03	2.96
98	1.594	49.27	2.95
101.5	1.613	46.34	2.93
105	1.638	43.22	2.92
108.5	1.665	39.85	2.9
112	1.702	36.17	2.9

## V. EXPERIMENT AND RESULTS

The purpose of any experimental testing on a new device should be to determine the reaction of the device under a diversity of conditions. With this in mind, the testing on the three coupling plates incorporated as many parameter variations as possible. These include the following

- (1) - Species of gas being excited
- (2) - Pressure of this gas
- (3) - Input microwave power
- (4) - Type of microwave input (pulsed Vs. CW)
- (5) - Bore size of the plasma tube

The sections that follow will describe the experiments that were performed, and the results obtained from them. The first section gives a detailed description of the experimental equipment and the configurations used during the experiment. The second section presents the data resulting from these experiments. The conclusions to be drawn from this data are presented in Chapter VI.

### Performing the Experiment

In performing the experiment, several configurations were employed. Each of these configurations was dictated by the particular combination of the variable parameters being tested. To facilitate replication of this experiment, in-

formation will be given on the equipment used in those configurations as well as the tests that were performed.

Equipment. The following equipment was used in the experiment. There is nothing special about any of this equipment, but a list is included for completeness.

- several sections of WR-284 waveguide
- a slotted line for WR-284 waveguide
- an E-H tuner for WR-284 waveguide
- a Hewlett-Packard SWR meter
- a four-port circulator (1-2-3-4-1)
- a 1 KW waveguide load
- several 10 W waveguides loads
- several pieces of Ecosorb MF-117 microwave absorbers
- an Amperex DX-453 magnetron
- a Cober model 605 high-voltage pulse generator
- two 30 dB cross-guide couplers (Moreno type)
- a stepdown transformer for the heater on the magnetron  
(5 KV stand-off capability)
- a Hewlett-Packard Network Analyzer
- a Boonton Electronics averaging power meter
- an Ailtech RF signal source
- a cavity type frequency meter
- a Voltronics DC power supply (4 KV @ 450 mA)
- assorted vacuum equipment  
(gauges, tubing, pump, flow meters, etc.)
- 3 waveguide to coaxial cable transitions  
( WR-284 to type N )
- a Tektronics model 555 oscilloscope
- a quartz tube (70 inches long with a 8 mm bore)
- a pyrex tube (70 inches long with a 1.5 mm tube bore)
- a DV-6 vacuum tube and meter
- a cylinder each of Ar, N<sub>2</sub>, CO<sub>2</sub>, and He gas

This is not an exhaustive list, but it gives the essential pieces of equipment that were used.

One piece of equipment not listed above is the coupler itself. In order to minimize "down time" when changing coupler designs, the coupler was designed to be dismantled

(see Appendix E). This approach lets the coupling geometry be placed on a plate that is sandwiched between the primary and secondary waveguides. Thus, when a new coupling scheme is desired, the coupler "sandwich" is taken apart, the new coupler plate replaces the old, and the waveguides are bolted back together. In short, a mechanical joint is used in joining the waveguides instead of an electrical joint, as is provided when the two waveguides are soldered together.

In order to simplify references to the three coupler designs, some notation will be introduced. All subsequent references to the coupler that uses standard coupling elements (slots) in cascade will be referred to as the "slotted coupler." Since two different coupling schemes were designed using the computer algorithm, they must be differentiated. The coupler based directly on the original algorithm will be referred to as the "direct design" coupler. Similarly, the coupler based on the magnitude of  $A_1$  declining will be referred to as the "decreasing magnitude" coupler.

Pulsed Input Configuration. For a pulsed microwave input, the system shown in Figure 5 was used. This system contains four Ecosorb MF-117 microwave absorbers in the end of the secondary waveguide furthest from the magnetron. This setup minimizes reflected waves from that waveguide.

Using this setup, VWSR measurements were made on the "slotted coupler." Since the Ailtech source has a tunable

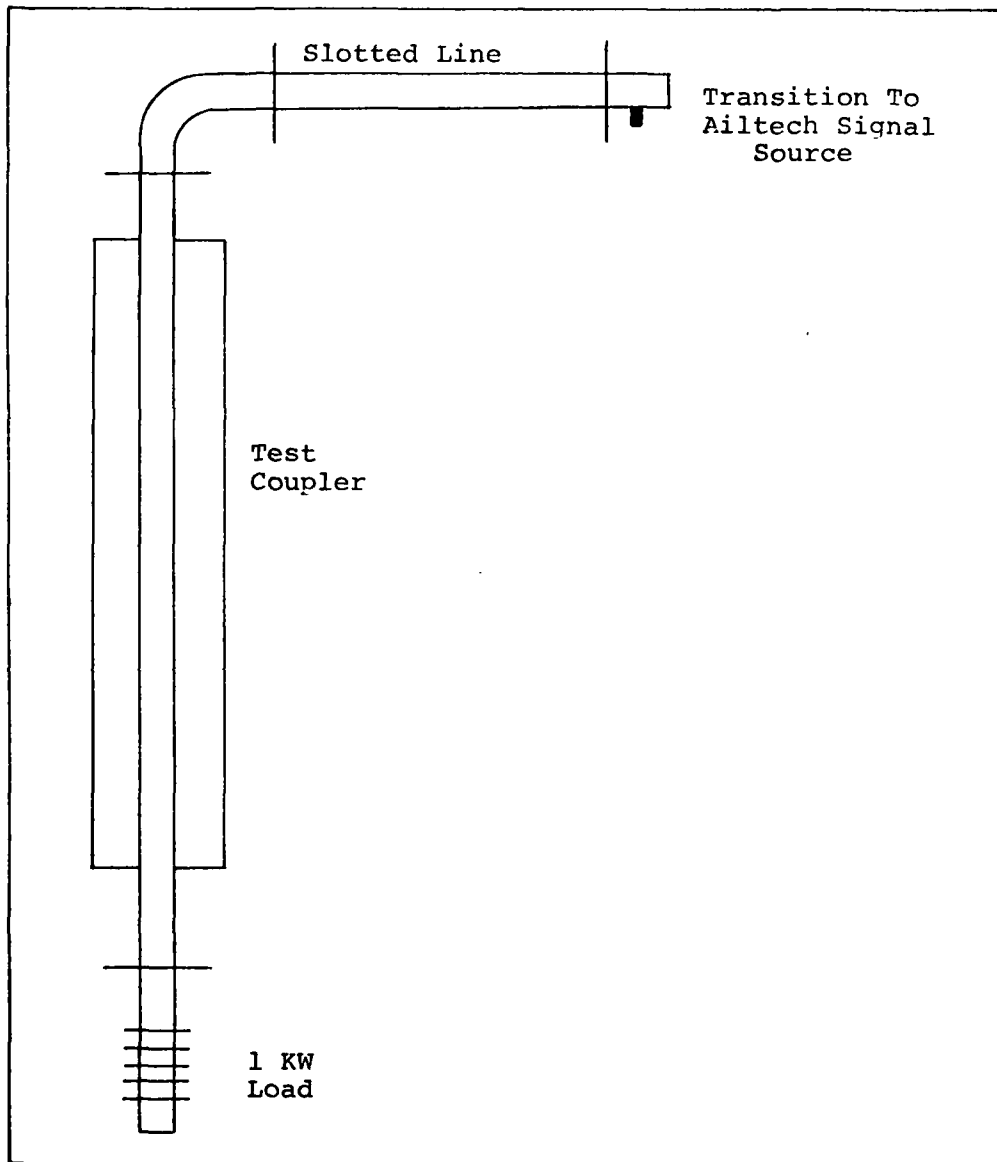


Figure 5 - System for Measuring VSWR  
of the Coupler

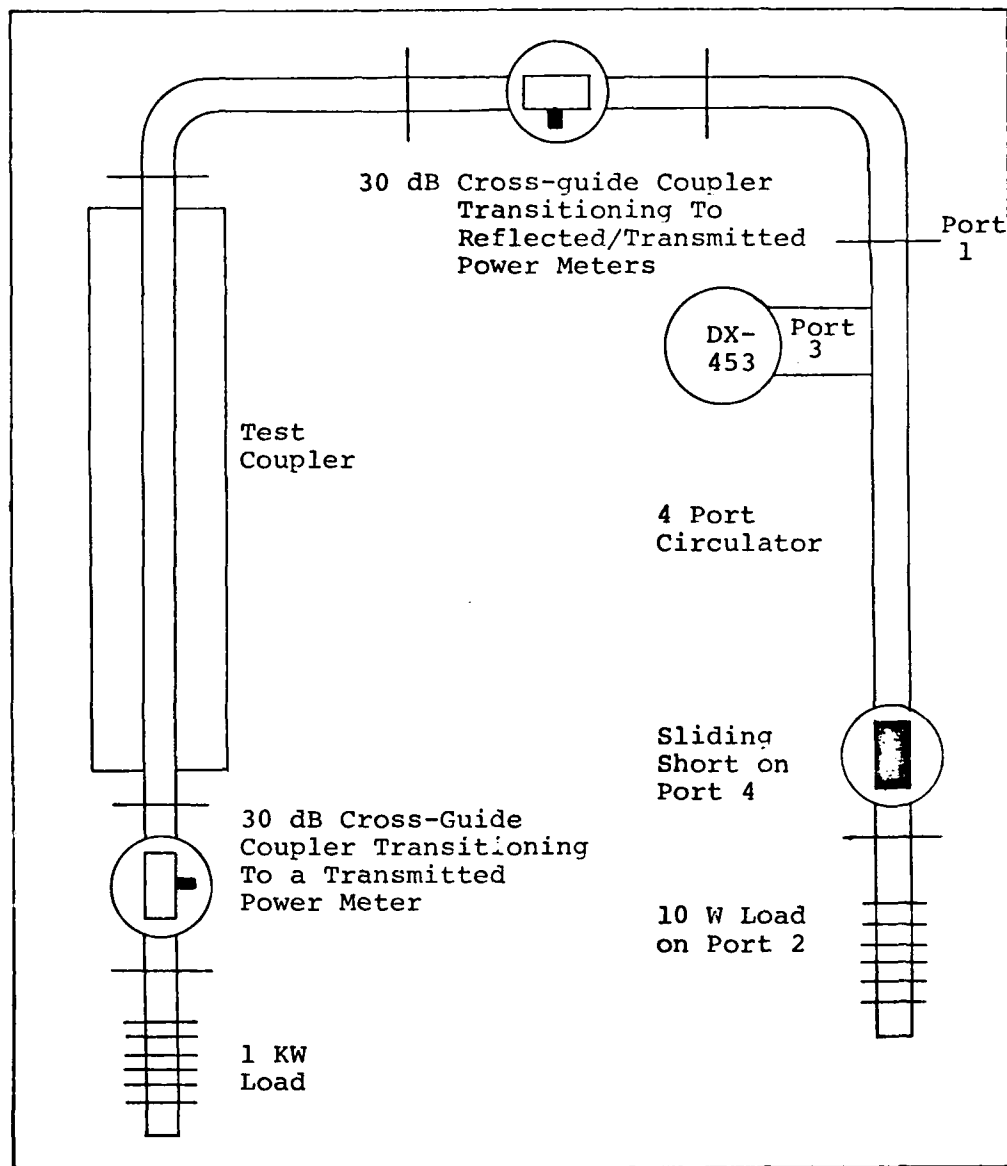


Figure 6 - System for Pulsed Inputs Using  
30 dB Cross-guide Couplers

frequency, these measurements were made over a range in frequency of 2.45 to 2.9 GHz. (These are the frequency extremes for the two proposed microwave sources.) VSWR measurements were also made with the coupler removed in order to see what effects the load itself has on VSWR.

Another pulsed input configuration is shown in Figure 6. In this setup, the slotted line is replaced by monitoring the transmitted and reflected power as measured at each arm of the 30 dB cross-guide coupler nearest the magnetron. The second coupler is used to monitor output power to give information on the power absorbed in the system. These couplers were normalized by using the network analyzer to determine the amount of coupling by each and then using attenuators to match outputs. In this manner, a 1 mW signal at the transmitted power arm of one coupler will give a 1 mW signal at the transmitted power arm of the other if no energy is lost in the waveguide that separates them. All measurements made using these couplers assume that there is perfect directivity, and hence will always give a worse measure of VSWR than actually exists.

Several types of measurements were made using this setup. Using the Cober model 605 to power the DX-453 magnetron (see Figure 7), measurements were made of the reflected, input, and transmitted power under various conditions. First, these measurements were made for the waveguide completely empty. Then the empty plasma tube was

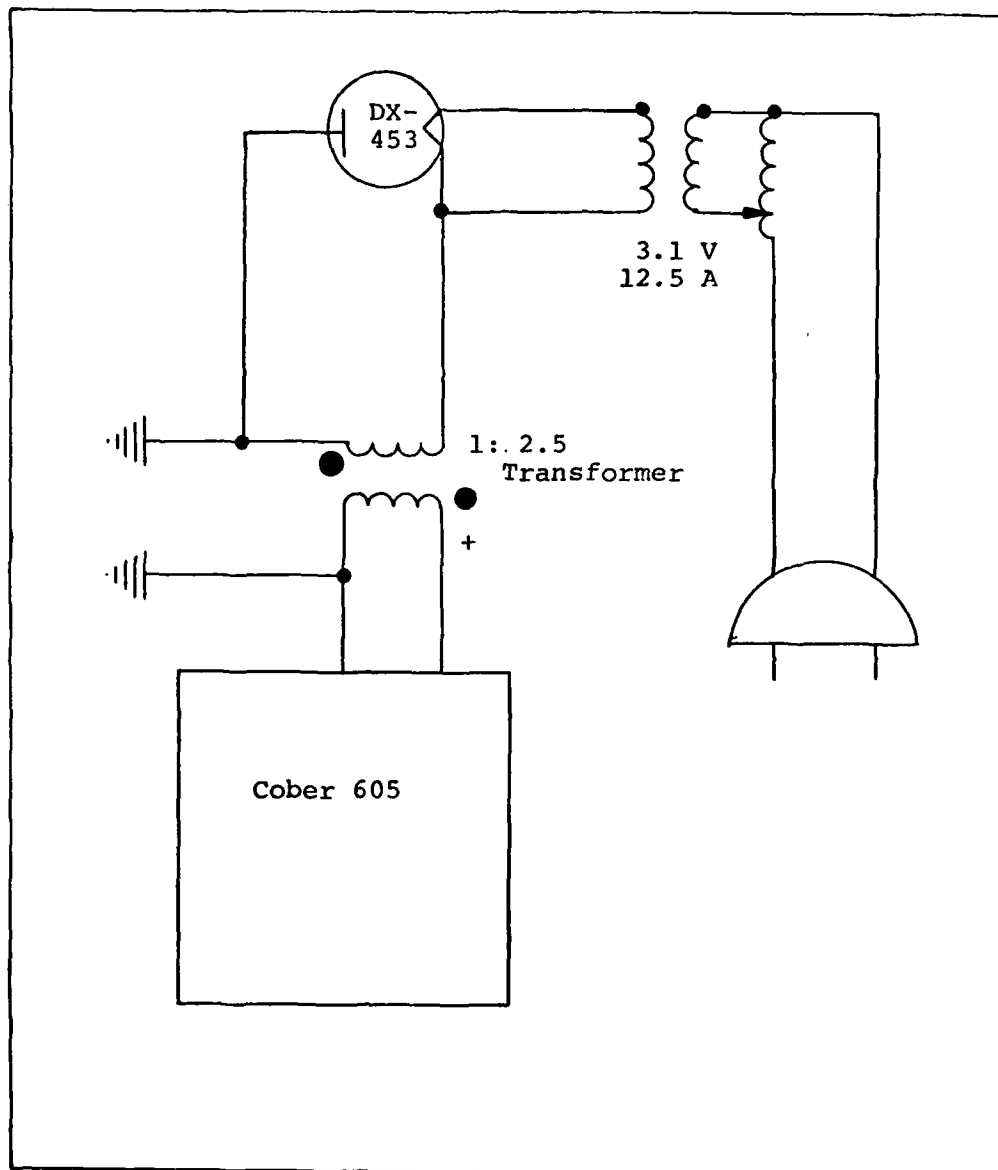


Figure 7 - DX-453 Magnetron Powered by  
Cober Model 605



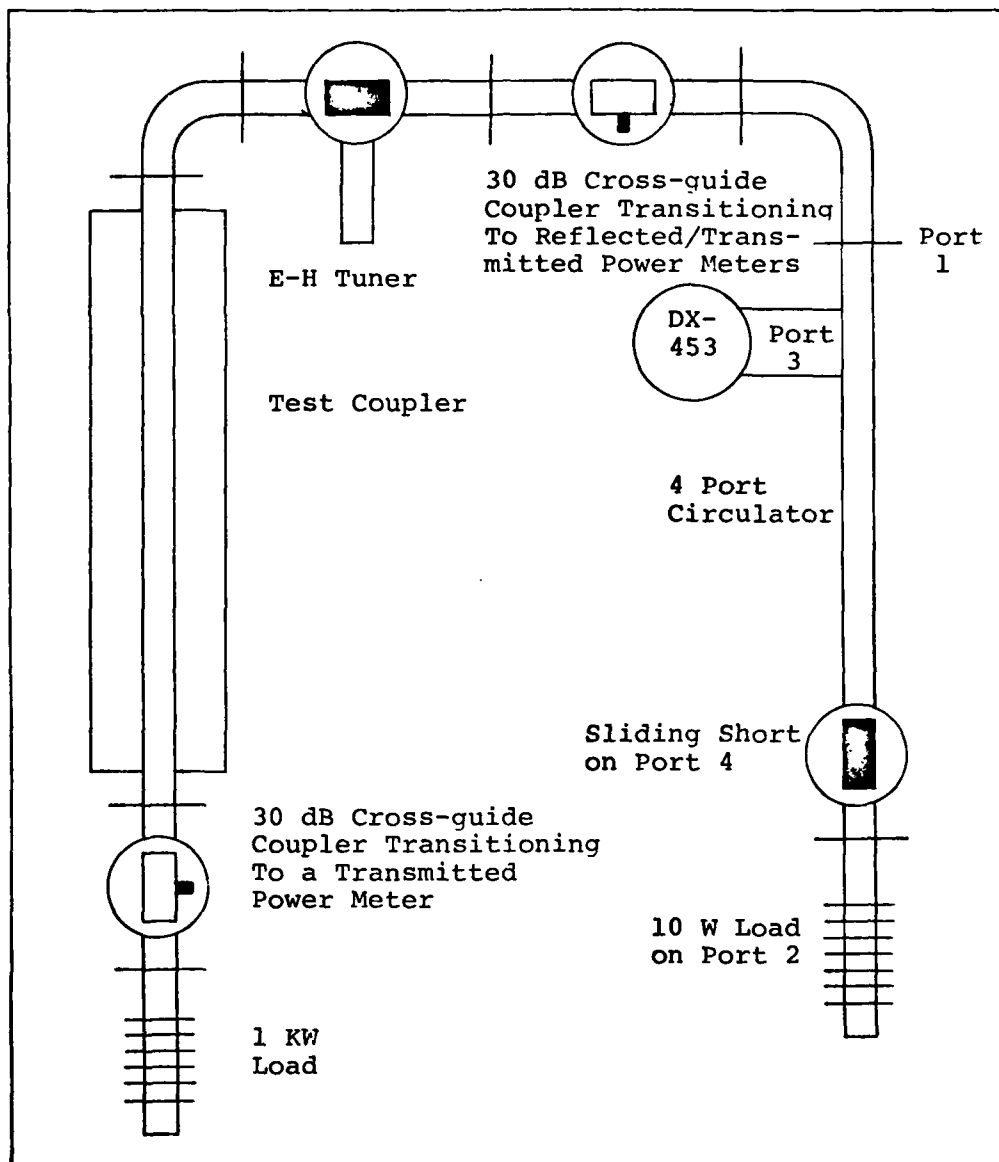


Figure 8 - System for CW Inputs Using  
30 dB Cross-guide Couplers

inserted into the waveguide and the measurements were repeated. Finally, the same measurements were made with a brass rod inside the plasma tube to simulate the effects of the plasma. (As noted in Chapter II, a plasma has the characteristics of a conductor.) The measurements made in each of these cases were taken for various pulse widths, repetition rates, and duty cycles. The input frequency was a constant (measured) 2.474 Ghz for all of these tests.

CW System Configuration. When the Voltronics DC power supply replaced the Cober pulsed supply, the system of Figure 6 was initially used for CW operation. However, the average power being absorbed by the loads inside the secondary waveguide was too great and they had to be removed. This caused entirely too much power to be reflected back to the source (more than 30% of the input), so an E-H tuner was inserted into the system as shown in Figure 8.

The experiments performed for the system in this configuration had two major variations. Either the input power was varied for a specific gas, or the gases were varied for a given input power. In both cases, the gas pressure was varied as much as possible. The measurements taken were, as before, the input, reflected, and output powers.

It was in this configuration that most of the testing occurred. All three coupling plates were tested in the manner described above. The results of this testing are included in the next section.

### Experimental Results

As in the previous section, the experimental results will be broken down into two sections. The first includes all the results of the pulsed testing. The second section includes only a representative sample of the testing in the CW configuration. The reason for this is that there is entirely too much data to list at one time. This data is given in Appendix F. Both sets of data are given in graphical forms instead of tabular listings. This is done to give a direct visual comparison of the coupler plates being tested.

#### Results of experiments in the pulsed configuration.

When in the pulsed configuration of Figure 5, direct VSWR measurements were made using a slotted line. These results are plotted in Figure 9 for the "slotted coupler" while the input frequency ranges from 2.4 to 2.9 GHz. This data was taken with the secondary waveguide completely empty since that configuration should give the worst VSWR readings. The values are typically between 1.05 and 1.15.

The next set of data curves (Figure 10) represents the transmitted power as measured by the system of Figure 6. With the Cober power supply delivering a 50 Hz pulse with a width of 80  $\mu$ s, and assuming the peak power of the magnetron is 600 W as given in the specifications, the average power entering the system is, at most, 2.4 W. Using this figure

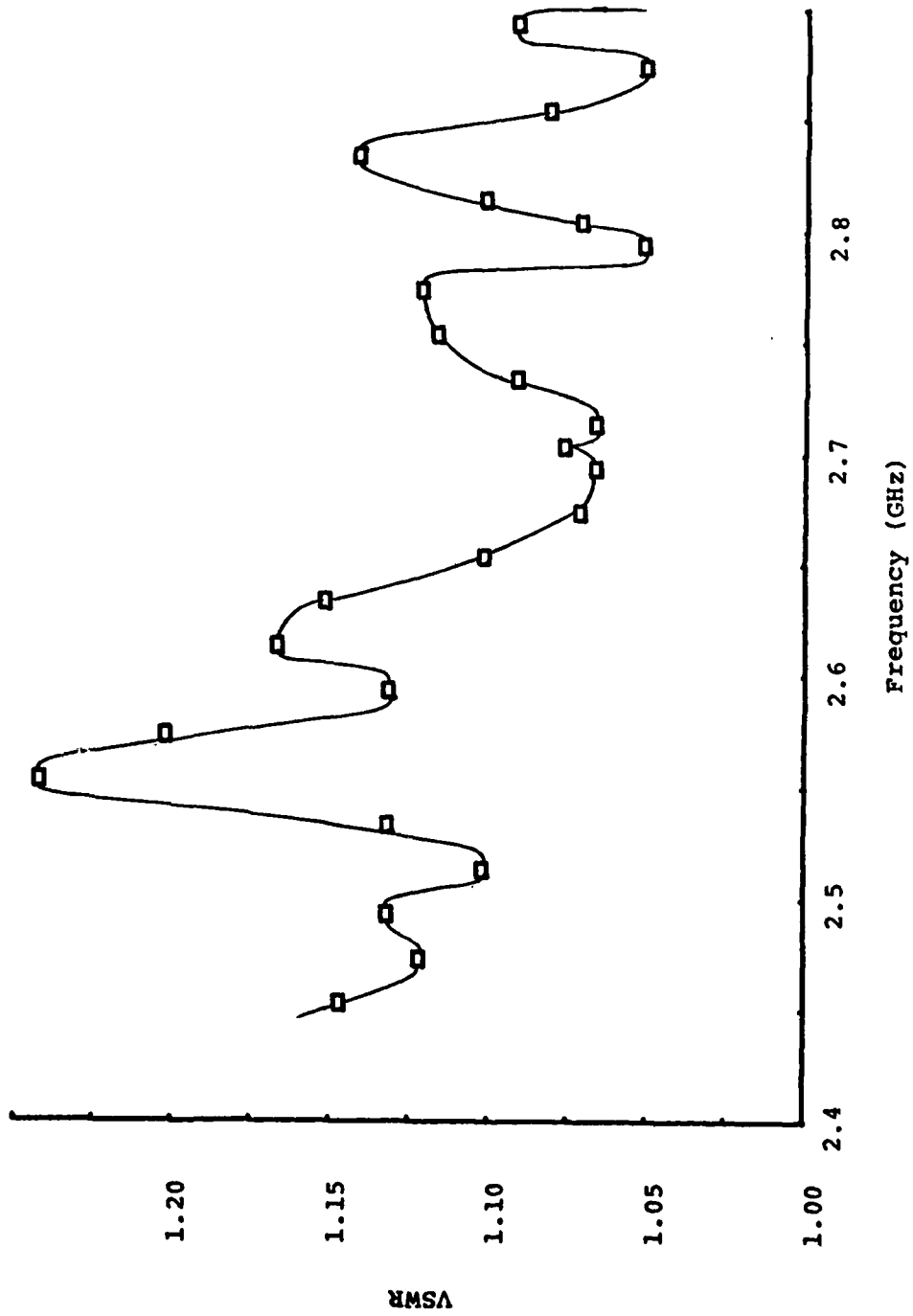


Figure 9 - VSWR Measurements Vs. Frequency for an Empty Secondary Waveguide

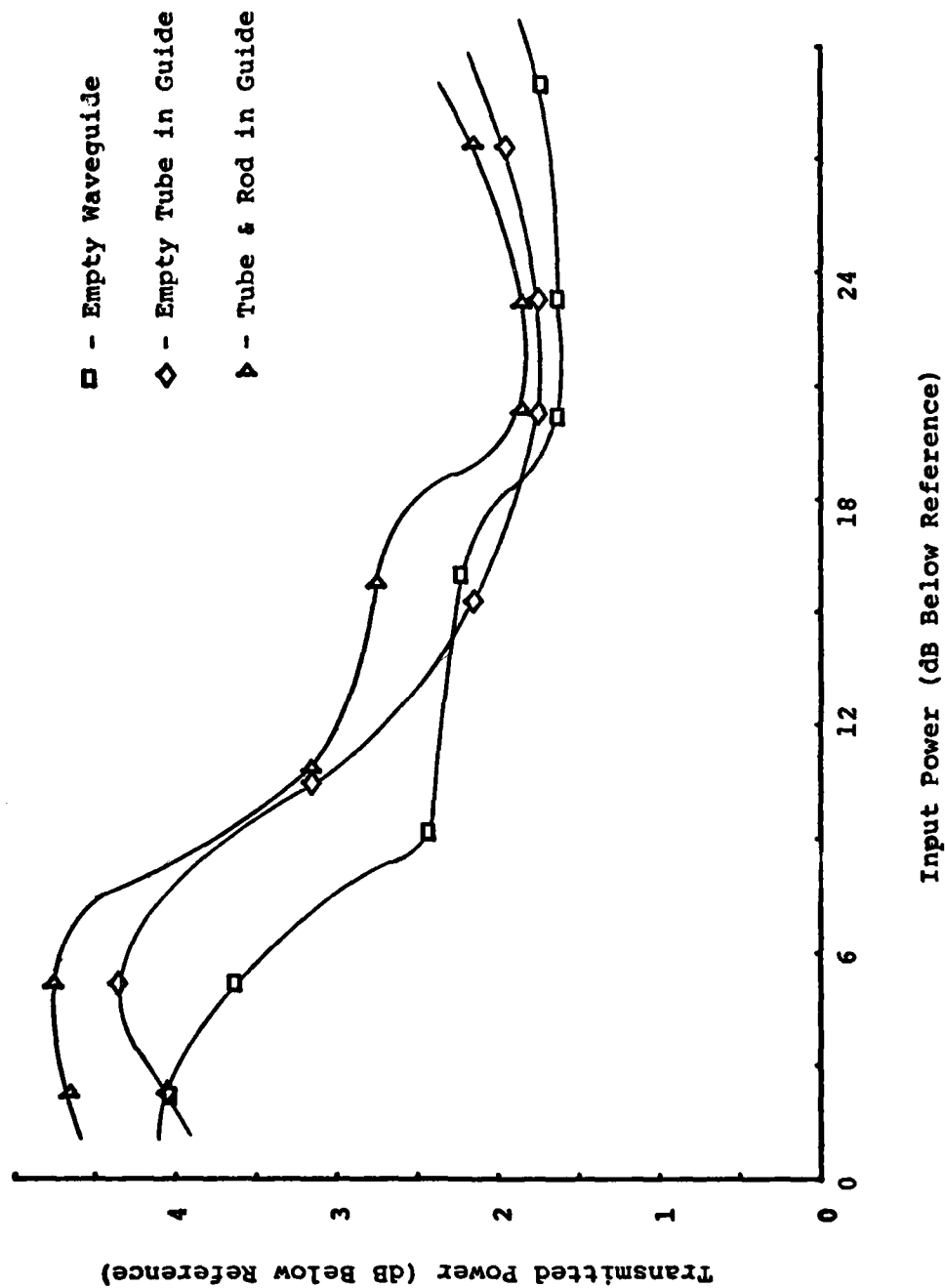


Figure 10 - Transmitted Power Vs. Input Power for Various Mediums in the Waveguide

as a reference, the transmitted power is plotted versus the input power. Both values are given in dB below the reference power given above. The three cases plotted are for the secondary waveguide completely empty, the empty plasma tube centered in the waveguide, and the plasma tube containing a brass rod centered in the waveguide. This last case is meant to simulate the effects on the waveguide of an internal plasma.

Figure 11 plots the reflected power under the same conditions as in the previous plot. Once again, the values are given in dB below the 2.4 W reference. The values plotted were obtained under the assumption that the cross-guide couplers are perfect; no effort was made to compensate for coupling of the incident wave to the detector measuring the reflected power.

Results of the experiments for the CW configuration.

The CW configuration of Figure 8 was used for the collection of all remaining data. All of this data involves variations of one or more of the parameters listed on page 50 with a constant input frequency of 2.474 GHz. Since there are many possible combinations of these parameters, only a small subset of the data taken is given here. A complete listing of the data taken is given in Appendix E.

One of the most important relationships measured was the effect of gas pressure on the plasma discharge. Figure 12 plots the percent of the plasma tube sustaining a discharge

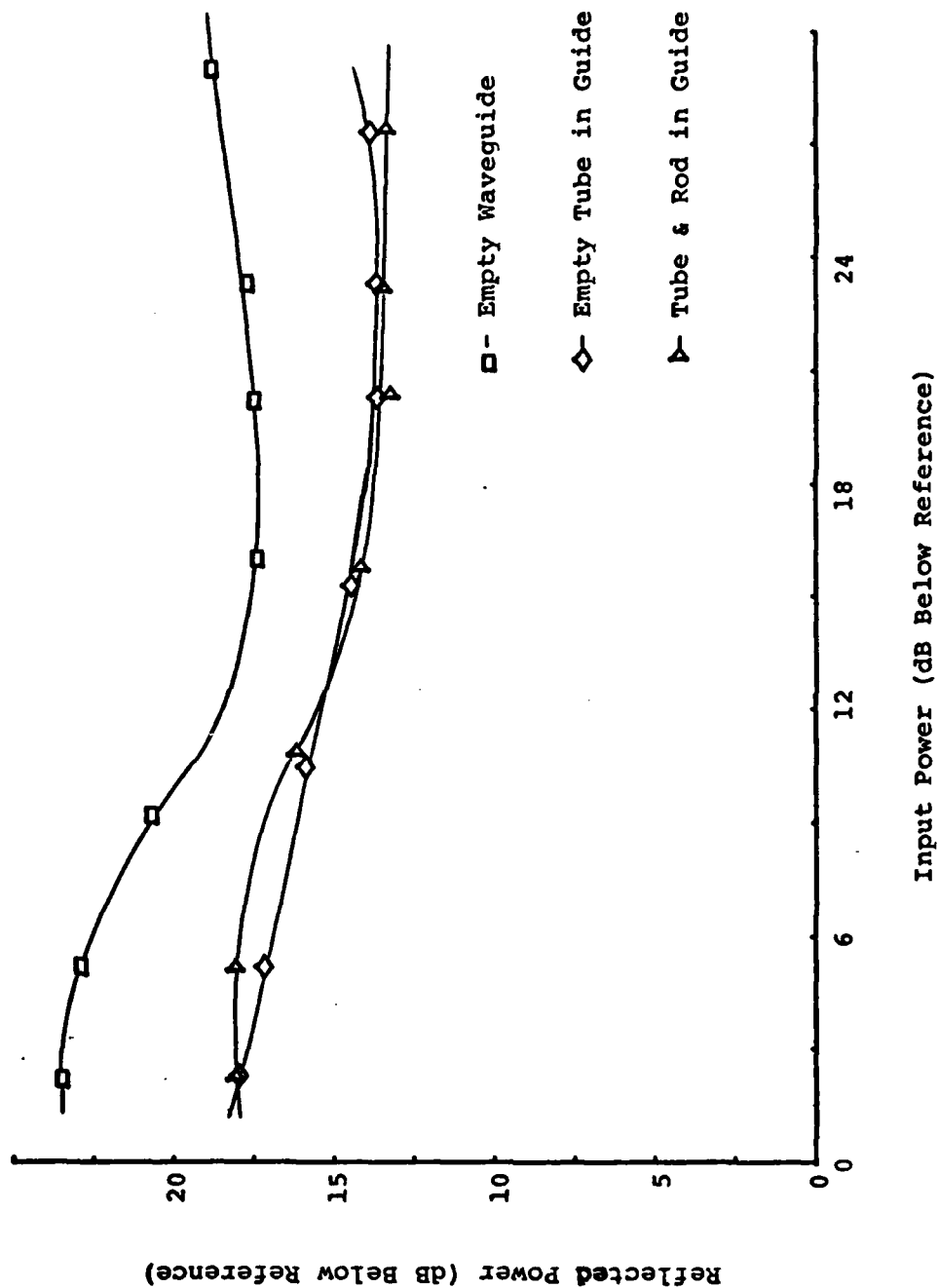


Figure 11 - Reflected Power Vs. Input Power for Various Mediums in the Waveguide

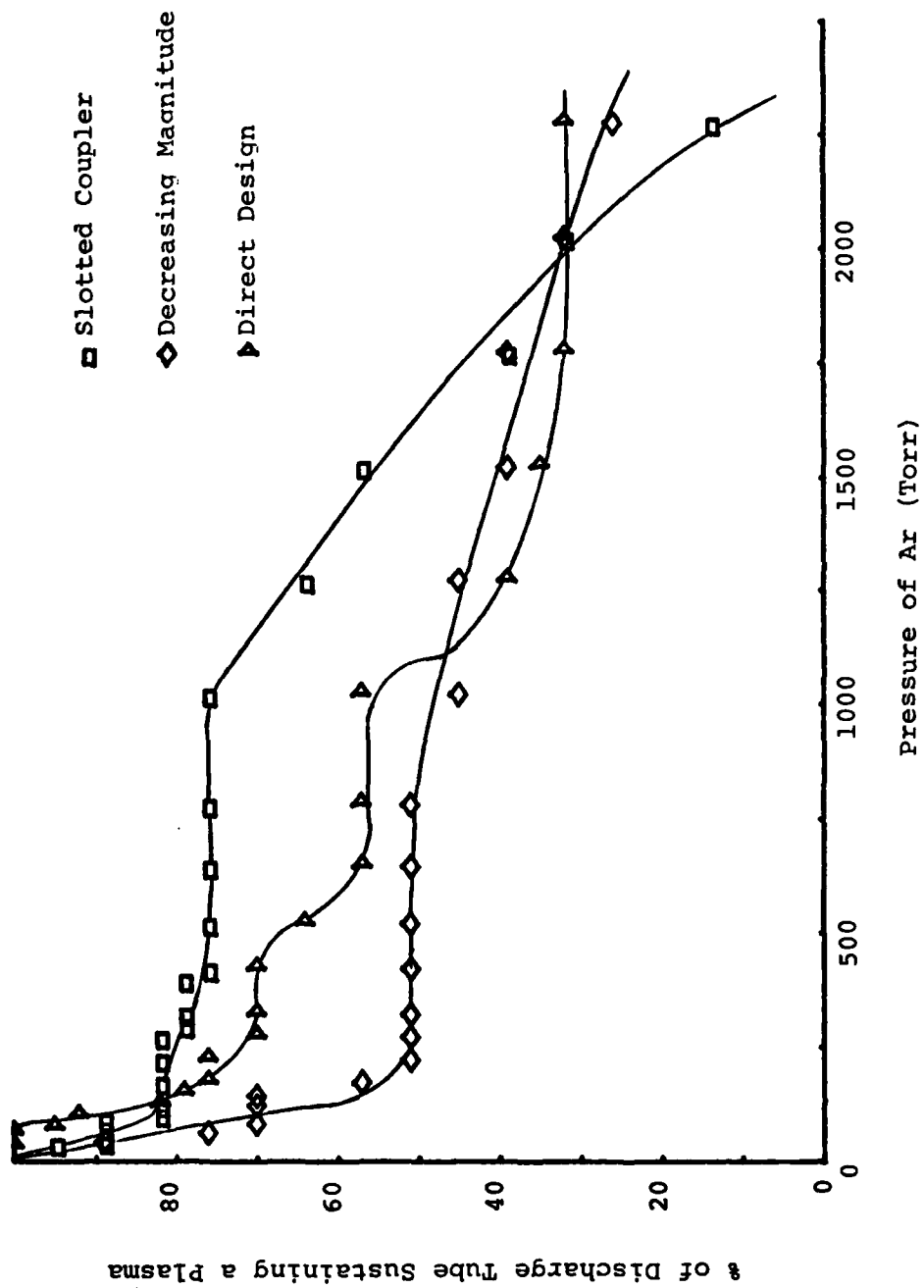


FIGURE 12 - % of 8 mm Tube Sustaining a Plasma Vs. Pressure of Ar at 500 W



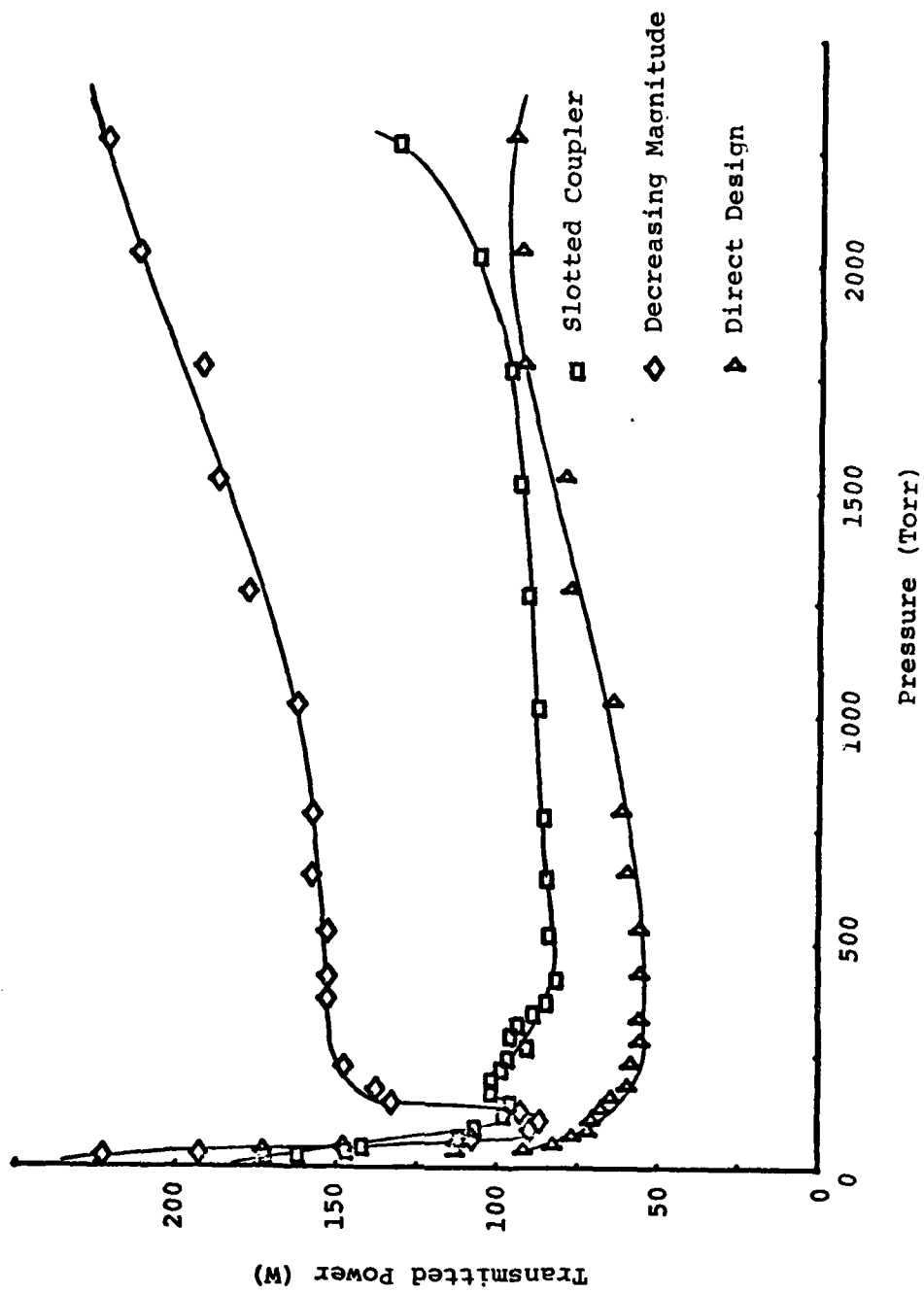


FIGURE 13 - Transmitted Power Vs. Pressure of Ar at 500 W Input and 8 mm Tube

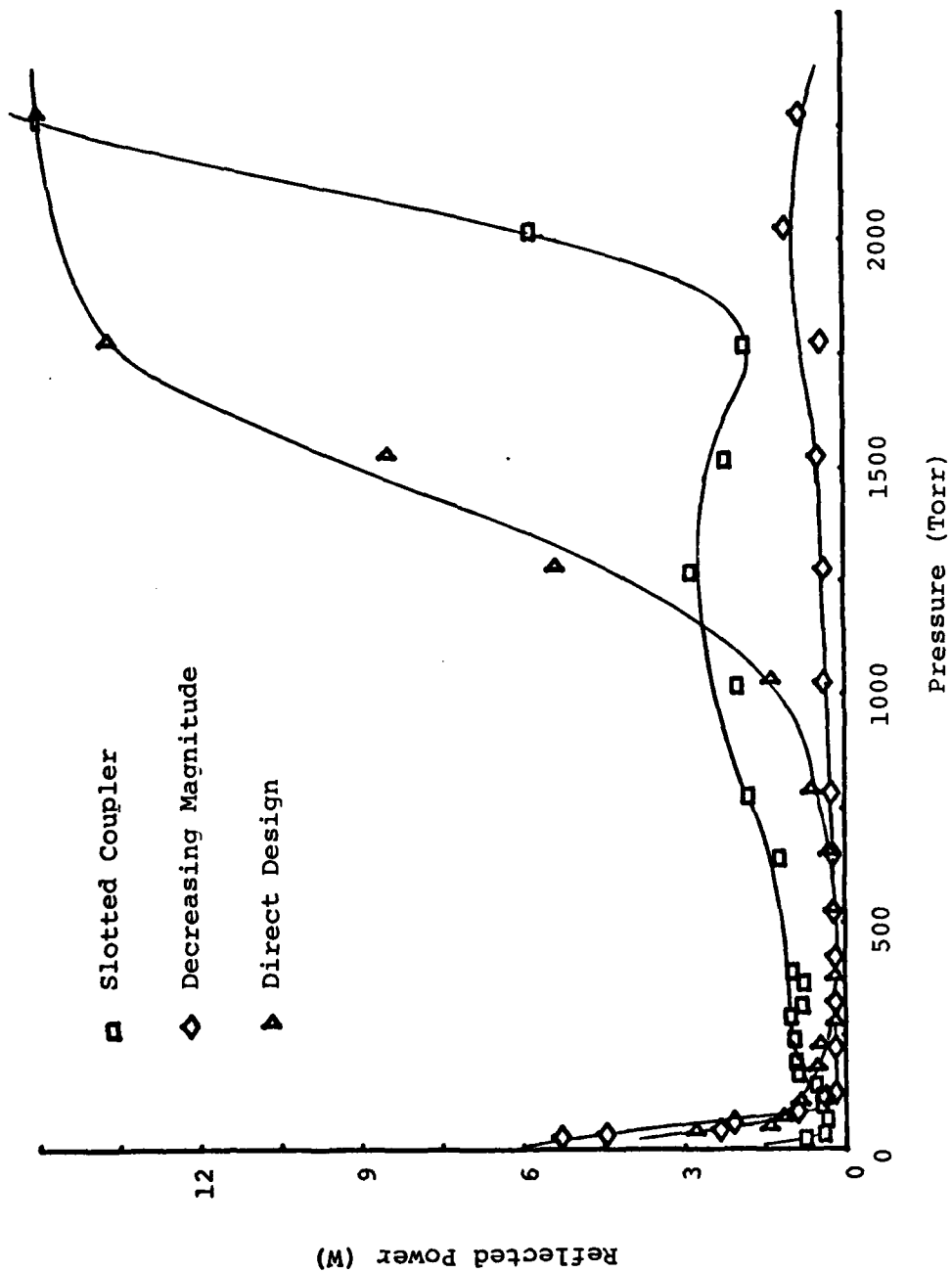


FIGURE 14 - Reflected Power Vs. Pressure of Ar at 500 W Input and 8 mm Tube

(as observed visually through holes in the side of the waveguide) for variations in the pressure of Ar gas for all three coupler plates. The bore of the plasma tube was 8 mm, and the microwave input was maintained at 500 W. Figure 13 plots the amount of transmitted power that was measured over the same pressure range. Figure 14 plots the amount of reflected power under the same conditions. The reflected power that was measured here was the minimum achievable reflected power using the E-H tuner.

To see what effect increasing the input power has, Figure 15 plots the percent of the discharge tube that sustains a discharge versus Ar gas pressure for two of the three coupling plates. The input power was raised to 600 W, but the 8 mm tube was still used. In contrast, Figure 15 plots the same effect while changing the tube bore to 1.5 mm with the input power returned to 500 W. Figure 17 plots the transmitted power under these same conditions.

Finally, to show the effect of filling the plasma tube with a different gas, Figures 18 and 19 plot the percent of tube sustaining a discharge and transmitted power respectively for He. The same conditions exist as in Figures 12 and 13, 500 W of input power with a 8 mm plasma tube.

Although other variations of parameters are possible, those given here are sufficient to determine the best coupling plate tested. This determination and other conclusions are given in the final chapter.

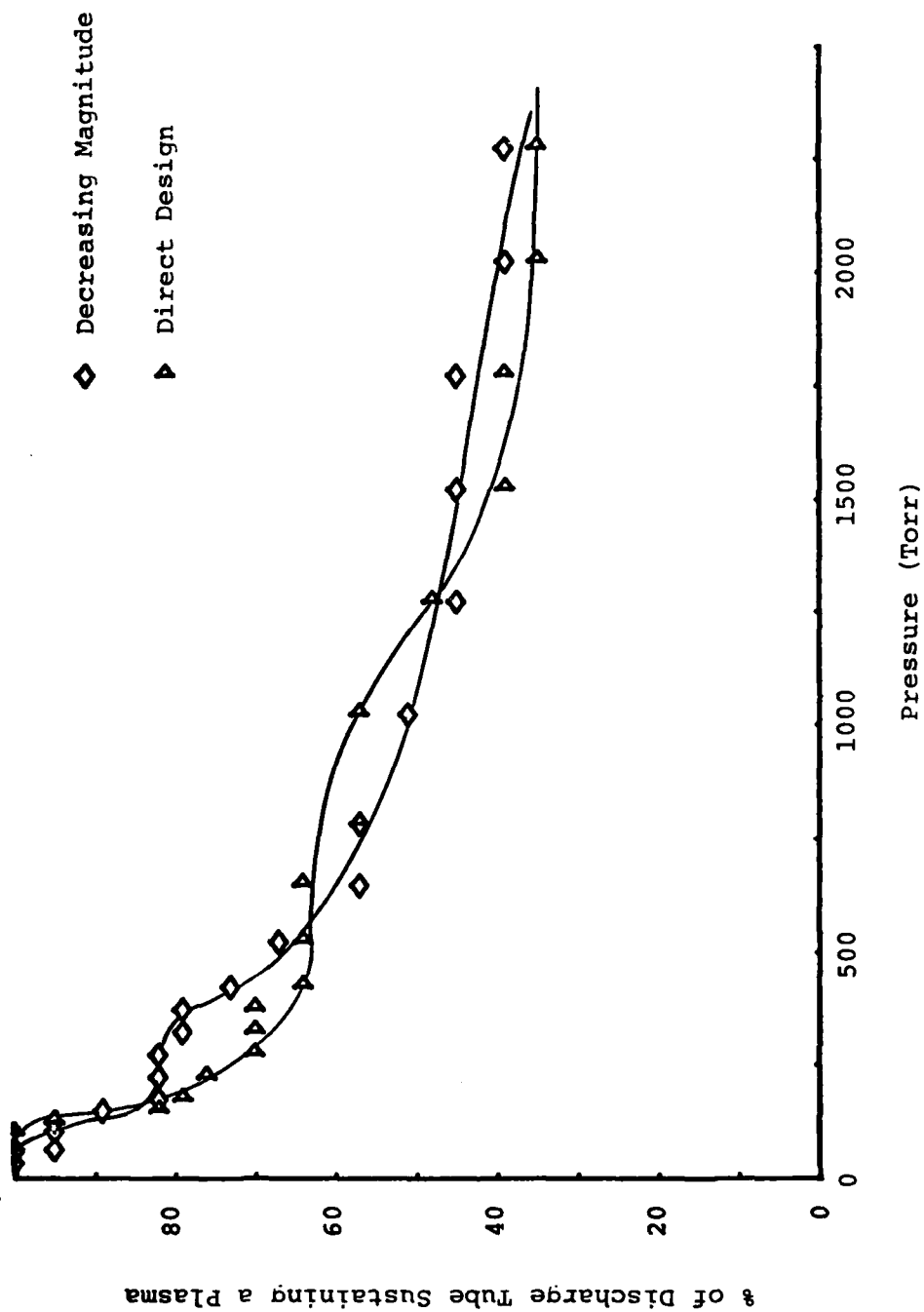


FIGURE 15 - % of 8 mm Tube Sustaining a Plasma Vs. Pressure of Ar at 600 W

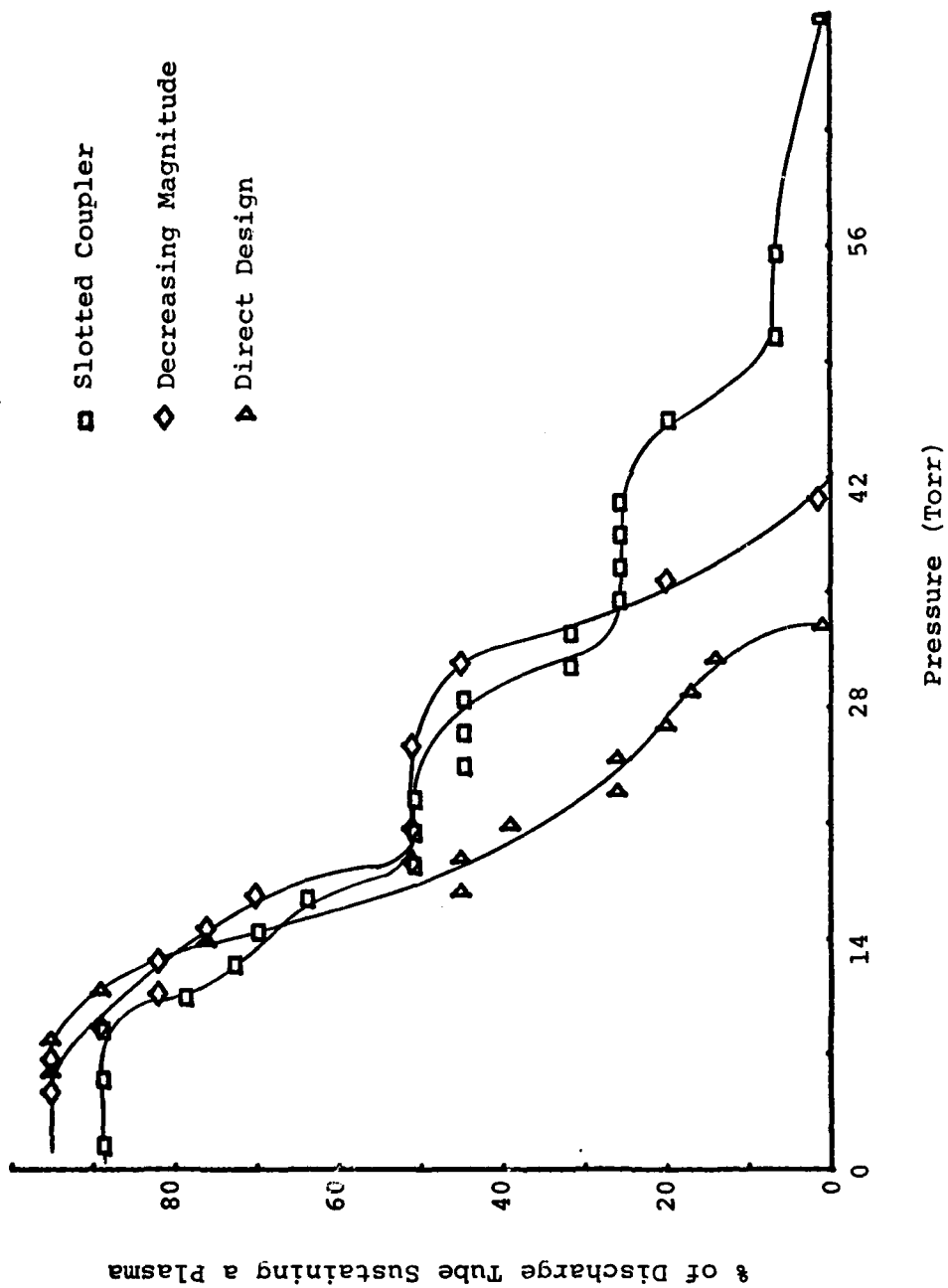


FIGURE 16 - % of 1.5 mm Tube Sustaining a Plasma Vs. Pressure of Ar at 500 W

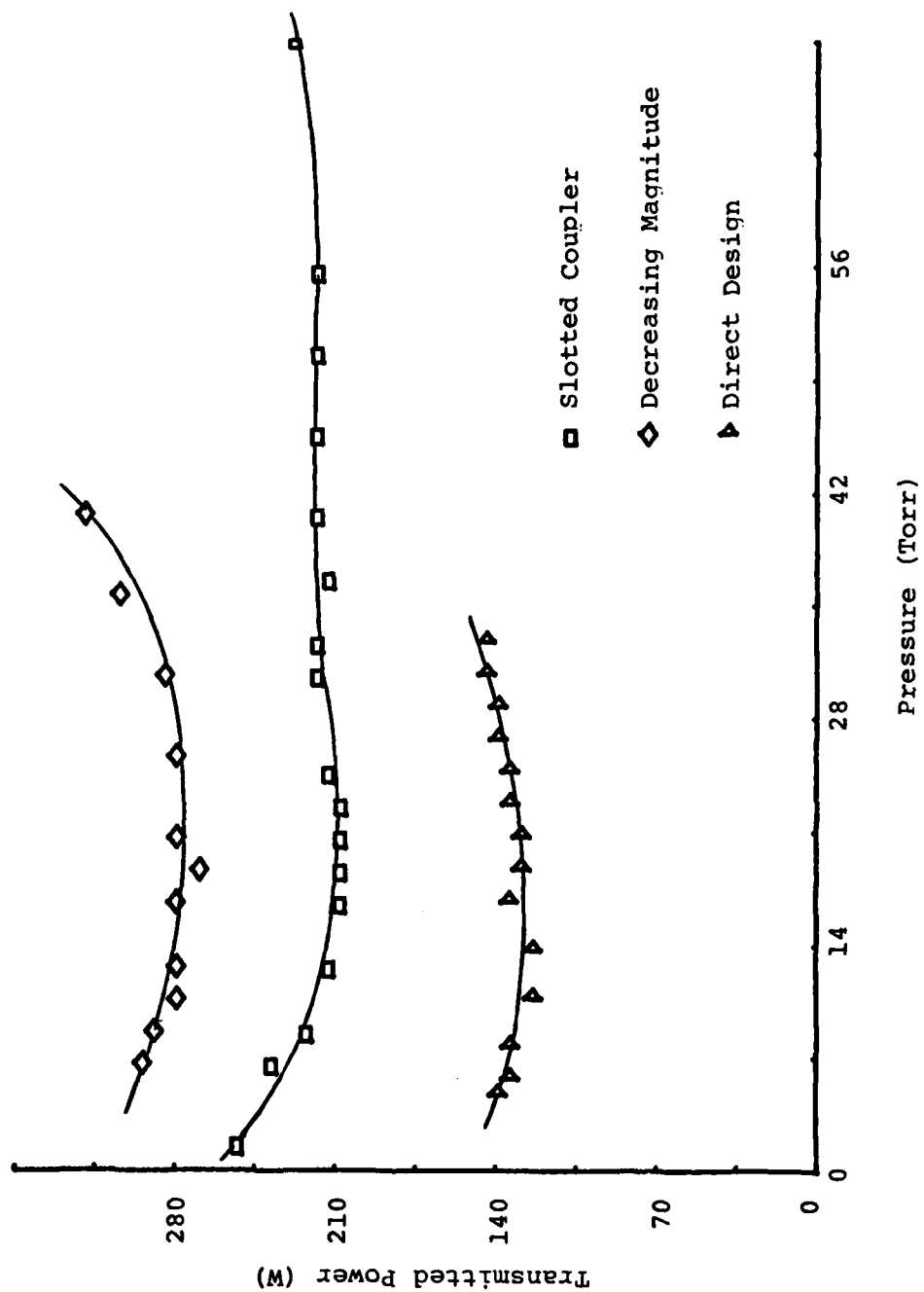


FIGURE 17 - Transmitted Power Vs. Pressure of Ar at 500 W Input in 1.5 mm Tube

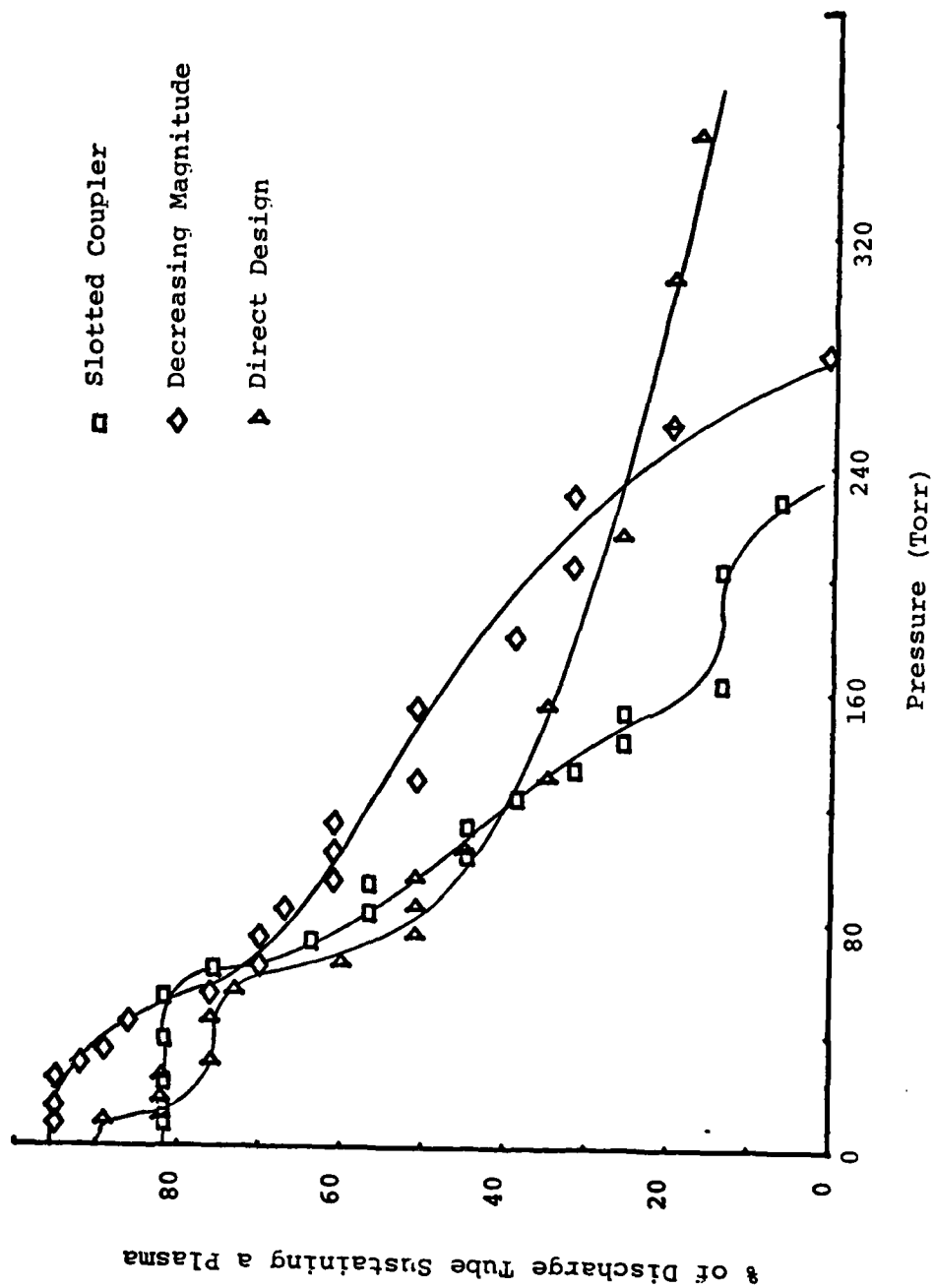


FIGURE 18 - % of 8 mm Tube Sustaining a Plasma Vs. Pressure of He at 500 W

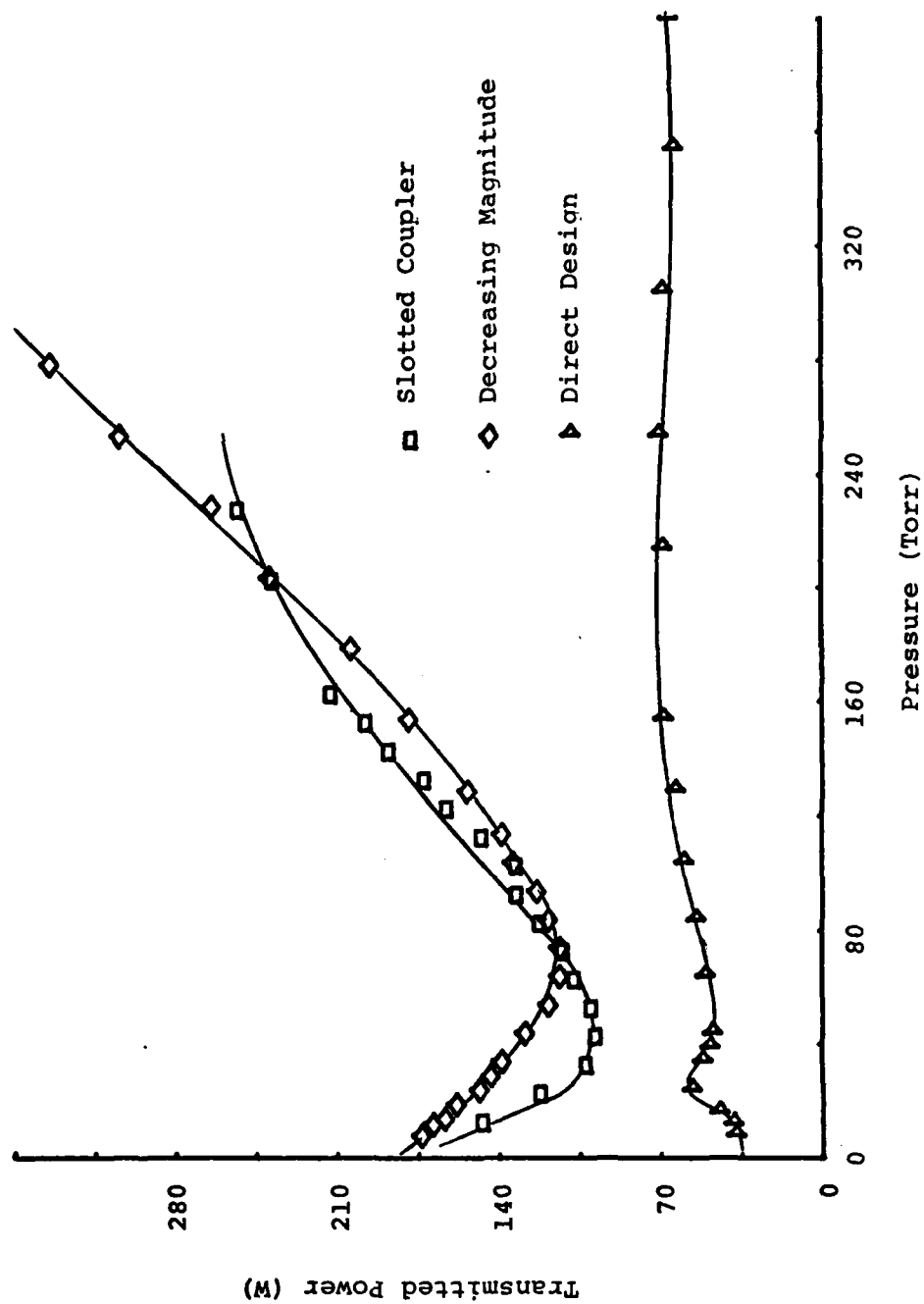


FIGURE 19 - Transmitted Power Vs. Pressure of He at 500 W Input in 8 mm Tube



## VI. CONCLUSIONS AND RECOMMENDATIONS

The most difficult task encountered in an experimental thesis is the analysis of data. The goal of this analysis is to determine which of the three coupler plates gives the most desirable performance. Once the best of these coupling plates is determined, the design procedure used to develop it can be used in other similar situations as the preferred method.

This chapter will give the conclusions reached on the three coupler plates in each of the areas being considered. Then, the design that performs best overall will be indicated. Finally, recommendations will be given for future studies along the same lines.

### Conclusions

A measure of the performance for the coupling plates involves several criteria. First, and probably most important, the plasma discharge should remain uniform over the length of the discharge tube. Second, the amount of power transmitted through the system should be as small as possible. Third, the reflected power from the system should be minimal. Fourth, the entire system should be insensitive to changes in various parameters such as frequency and gas pressure.

Uniformity of discharge. Which coupler gives the most uniform discharge depends on several conditions. As seen in Figure 12, the slotted coupler maintains the highest percentage of discharge (and hence the most uniformity) over a large pressure range. However, the coupler based on the declining amplitude model is much less sensitive to changes in the pressure of the gas. It must be noted however, that this relationship is tied closely to the type of gas in the plasma tube. Referring to Figure 17, the advantages mentioned above are attributed to different coupler plates. According to this plot, the slotted coupler is by far the worst choice. In contrast, not only is the coupler plate based on decreasing magnitude less sensitive to pressure variations, but it maintains a higher percentage of the discharge as well. Therefore, combining the fact that this plate has better characteristics in one case and less sensitivity to change in both cases, the coupler plate based on decreasing magnitude gives the most uniform excitation.

Transmitted power. Inspection of Figures 13, 17, and 19 reveals that the coupling plate based directly on the computer algorithm always couples more energy out of the primary waveguide. This is not surprising, since this design has much more of an open common wall between the waveguides. Thus, there is more coupling of energy from the primary waveguide to the secondary waveguide.

Reflected Power. Once again, it should be noted that

the reflected power measured in the CW configuration is not the actual power reflected by the system. The reflected power measured was the minimal achievable power that the system could be tuned to by using the E-H tuner. However, even this measurement gives a relative idea of the reflected power of the system without a tuner.

Based on these measurements of reflected power, the coupler plate based on the decreasing magnitude model is clearly superior. This relationship is pointed out in Figure 14 with Ar, but the relationship is still valid for other gases.

In the pulsed input configuration, direct measurement of VSWR was possible, and revealed reflected power to be on the order of 0.001 times the input power or less. This low value is primarily due to the absorbers in the secondary waveguide when used for pulsed inputs. Thus, the type of coupling plate used does not strongly affect the reflected power when these absorbers are in place.

Sensitivity to change. As noted in earlier sections, the coupling plate based on the decreasing magnitude model is the least sensitive to changes in the plasma tube. Although the variable frequency test was not run on this plate, its sensitivity to frequency variations should not be great, due to the large number of coupling elements.

Similarly, the VSWR measurements plotted in Figure 9 show that the reflected power in the pulsed configuration is

only slightly dependent on frequency. It is believed that testing of the other plates will reveal similar dependencies.

Best overall coupler plate. Of the three couplers tested, the best overall coupler plate seems to be the one modeled on the decreasing magnitude model. The only category this plate was not superior in was in the amount of power coupled out of the primary waveguide. This means that a more powerful microwave input will be necessary to get a certain level of excitation, but the other benefits of this design outweigh this handicap.

The overall conclusion of this study is that a coupling design based on the decreasing magnitude model will give improved results. The analytical model, developed in Chapters 2 through 4, can be used to design a coupler and predict its performance over a range of design parameters. With the proper modifications, the computer code listed in Appendix C can be used to design a coupling geometry for any laser gas, in any waveguide system, for any type of microwave input.

#### Recommendations

Future research in this area might include some of the following areas. First, a high-power pulsed source could be used to excite the system to evaluate its performance in a pulsed configuration. Second, put  $\text{XeCl}^*$  gas in the plasma

tube instead of the substitute gases currently used. Third, a better vacuum system is essential if closed-cycle operation is to be attempted. Finally, another means of power monitoring should be found that is more accurate than the cross-guide couplers currently being used.

The pulsed configuration of this system was not exploited because the power of the DX-453 magnetron was insufficient when pulsed. No plasma could be sustained with the pulse system regardless of pulse width or duty cycle. A higher power unit may well give good results in this area, especially since the E-H tuner can be removed for pulsed work. With the lower average powers associated with pulse work, the microwave absorbers can be placed back in the waveguide and hence minimize the reflections from the system. Thus, a high-power pulsed configuration would provide enough power to maintain a plasma, while also minimizing reflections.

The next recommendation is obvious. The coupler plates were designed for use with  $\text{XeCl}^*$ , so this gas should be used to fill the plasma tube. However, due to the high cost of these gases, this necessitates a closed system. Thus, the need arises for a good vacuum system. The system presently used can only evacuate to about 10 microns of mercury. This is good enough for a flowing-gas system, but it is unacceptable for any closed-cycle system.

One final suggestion is to replace the 30 dB cross-guide

couplers with some better type of power sampling device. Since the reflected power for the system in a pulsed configuration is on the order of 0.001 times the input power, a coupler would have to have a directivity of greater than 30 dB to obtain accurate readings. The ones used in this experiment have a directivity of about 15 or 20 dB. Therefore, all reflected power readings taken with these couplers have a certain amount of bias in them due to an undesired coupling from the input power.

Other general suggestions might include optimizing the coupler design with respect to the parameters that were varied in the experimental stages of this thesis. In this manner, the experimental results can be correlated with the design directly. One final suggestion for future research is to revert back to the broadwall coupling scheme used initially by Mendelsohn, et al., (Ref 1).

# BIBLIOGRAPHY

1. Mendelsohn, A. J. et al. "A microwave-pumped XeCl<sup>\*</sup> laser," Applied Physics Letters, 38 (8): 603-605 (15 April 1981).
2. Young, J. F. et al. "Microwave Excitation of Excimer Lasers," Laser Focus: 63-67 (April 1982).
3. Heald, M. A. and C. B. Wharton. Plasma Diagnostics with Microwaves, New York: John Wiley and Sons, Inc., 1965.
4. Golant, V. E. et al. Fundamentals of Plasma Physics, edited by Sanborn C. Brown, translated by K. Z. Vedeneyeva. New York: John Wiley and Sons, Inc., 1977.
5. Delcroix, J. L. Plasma Physics, New York: John Wiley and Sons, Ltd., 1975.
6. Allis, W. P. Electrons, Ions, and Waves, edited by Sanborn C. Brown, Cambridge Mass: Halliday Lithograph Corp., 1967.
7. Schuebel, W. K. Electro-optical Technology Branch, Electronic Technology Division. Personal interview. Air Force Wright Aeronautical Laboratories, Wright-Patterson AFB, Ohio. 1982.
8. Altman, J. L. Microwave Circuits, Princeton, New Jersey: D. Van Nostrand Company, Inc., 1964.
9. Harrington, R. F. Time-Harmonic Electromagnetic Fields, New York: McGraw-Hill Book Company, Inc., 1961.
10. Shelton, W. L. "S-Band Sidewall Directional Coupler" in The Microwave Engineers' Handbook and Buyers' Guide - 1966, editor in chief Theodore S. Saad. New York: Horizon House - Microwave, Inc., 1966.
11. Sporleder, F. and H. G. Unger. Waveguide Tapers Transitions and Couplers, New York: The Institute of Electrical Engineers, London and New York, 1979.

APPENDIX A  
UNSUCCESSFUL APPROXIMATIONS  
TO THE COUPLED WAVE EQUATIONS

This appendix is included solely for the interest of others who may try to solve this system of equations. The following methods were initial attempts at formulating an approximation to Eq 43.

1. Breaking the system into a summation of eigenmodes. If there were a known functional form for the coupling coefficients, the method of eigenmode analysis would work. However, for a totally unknown functional form there is no closed form solution.

2. Ignoring the (1,2) element of the matrix in Eq 43. If the upper right hand element of the matrix in Eq 43 is assumed to have a negligible effect, there is a closed form solution to the system. However, this type of system does not allow the magnitude of the field in the primary waveguide to decline as it must.

3. Assuming  $K=c(\beta_2-\beta_1)$ . If the coupling coefficient  $K$  is assumed to be of the form  $K=c(\beta_2-\beta_1)$  where  $c$  is an arbitrary complex constant, the system has a closed-form solution. However, this assumption proves too restrictive to achieve a uniform energy distribution.

4. All attempts at transforming the present  $z$  varying system to a  $z$  invariant system failed completely.



5. Assuming an exponential form for  $A_1$  and  $A_2$  and utilizing the conservation of power. If  $A_1$  and  $A_2$  are assumed to have a complex exponential form, applying the restriction of conservation of power should allow the unknowns to be evaluated. Unfortunately, more unknowns are introduced in this method than are solved.

Any attempt to use any of these methods will not, in general, produce the desired solution. Therefore, they were listed to prevent further effort from being spent on them.

APPENDIX B  
SOLVING FOR THE ELEMENTS OF THE T MATRIX

The following derivation is a direct application of the approach developed by Sporleder (Ref 11:32-52). Some simplifications are allowed in the present case of using holes centered in the narrow wall of the waveguide. There is also a slight change of notation presented.

To evaluate the elements of the T matrix given in Eq 43, the following approach is taken. Each element is evaluated by solving the following

$$T_{mn} = j \omega \epsilon / 2 P_I E_{hn} \cdot E_{h-m} + j \omega \mu / 2 P_M H_{hn} \cdot H_{h-m} \quad ( 72 )$$

where

- $\epsilon$  = the complex permittivity of the structure
- $P_I$  = the electric polarization current
- $P_M$  = the magnetic polarization current
- $E_{hn}$  = the equivalent magnetic field for the mode n  
that would exist in the absence of a hole
- $H_{hn}$  = the equivalent electric field for mode n  
that would exist in the absence of a hole

For small holes centered in the narrow common wall between

AD-A124 686 DESIGNING WAVEGUIDE COUPLERS FOR MICROWAVE EXCITATION OF LASER GASES(U) AIR FORCE INST OF TECH WRIGHT-PATTERSON AFB OH SCHOOL OF ENGINEERING

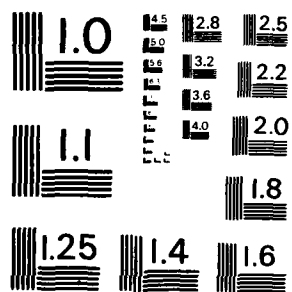
22

UNCLASSIFIED L C SHELTON 1982 AFIT/OEO/PM/820-13 P/G 20/5

**F/G 20/5**

NL

END  
DATE  
FILMED  
3 83  
DTIC



MICROCOPY RESOLUTION TEST CHART  
NATIONAL BUREAU OF STANDARDS - 1963 - A

two waveguides, the first term of Eq 72 becomes zero.

Therefore, in the present case, Eq 72 can be simplified to

$$T_{mn} = j\omega\mu/2 P_M H_{hn} \cdot H_{h-m} \quad (73)$$

The evaluation of Eq 73 depends on evaluation of  $H_{hn}$ . Sporleder gives the following equation for this evaluation.

$$H_{hn} = H_{h-n} = T_i k_{ci}^2 / [\gamma_i(z_i)]^{1/2} \quad (74)$$

The parameters embedded in this equation are evaluated for a  $TE_{10}$  mode by using the following equations.

$$T_i = 1/\pi [(2ab\epsilon_n \epsilon_m) / (m^2 b^2 + 4n^2 a^2)]^{1/2} \cos(n\pi y/b) F(x) \quad (75)$$

where

$a$  = one half the waveguide's broad dimension

$b$  = the narrow dimension of the waveguide

$y$  = the distance along the narrow dimension

(see Figure 4)

$x$  = the distance along the broad dimension

$F(x) = (-1)^{(m-1)/2} \sin(m\pi x/2a)$  if  $m$  is odd

$F(x) = (-1)^{m/2} \cos(m\pi x/2a)$  if  $m$  is even

$\epsilon_n = 1$  for  $n=0$ , and  $\epsilon_n=2$  for  $n>0$

For the fundamental  $TE_{10}$  mode of the primary waveguide ( $i=1$ ), Eq 75 can be simplified by substituting the known variables. For  $x=a$ ,  $m=1$ , and  $n=0$ ; the equation becomes

$$T_1 = 1/\pi [4ab/b^2]^{1/2} \sin(\pi/2) \quad (76)$$

For the secondary waveguide ( $i=2$ ), this term is evaluated in the same manner; however, in order to use the same reference system the value for  $x$  is now  $x=-a$ . In this case, Eq 75 evaluates to

$$T_2 = 1/\pi [4ab/b^2]^{1/2} \sin(-\pi/2) \quad (77)$$

Thus, Eqs 76 and 77 are negatives of each other.

The equation describing  $k_{ci}^2$  for the  $TE_{10}$  mode is given by

$$K_{ci}^2 = (m\pi/2a)^2 + (n\pi/b)^2 \quad (78)$$

This equation evaluates to the same value for both waveguides. For the  $TE_{10}$  mode  $k_{ci}^2$  evaluates to

$$k_{ci}^2 = (\pi/2a)^2 \quad (79)$$

Another undefined parameter in Eq 74 is  $Z_1$ . This

parameter is evaluated according to the following equation.

$$Z_i = j\omega\mu/\gamma_i \quad (80)$$

A more useful form of this equation is given below

$$\gamma_i (Z_i)^{1/2} = (j\omega\mu\gamma_i)^{1/2} \quad (81)$$

Combining Eqs 76, 79, and 81 and substituting into Eq 72 gives

$$T_{mn} = P_M \pi^2 / [8(a/2)^3 b (\gamma_m \gamma_n)^{1/2}] \quad (45)$$

where the value for a is now the waveguide broad dimension. Notice that this equation does not incorporate the negative sign presented in Eq 77. The reason for this is that this sign is incorporated into Eq 47.

$$P_M = 4/3 r^3 R_{M MO} \quad (47)$$

This equation is the negative of the definition given by Sporleder. Since this equation is only used when n and m are not equal, (the conditions under which Eq 45 should be negative) the two minus signs always cancel each other.

The equation for n and m equal is always the same, since in one case both terms of Eq 45 are positive and in the

other case both terms are negative. The value for  $P_M$  as given by Eq 46 is then as defined by Sporleder.

$$P_M = 4/3 r^3 R_M K_{ME} \quad ( 46 )$$

The values for  $R_M$  and  $K_{MO}$  are as listed in the text, and correspond directly to the equations of Sporleder. At this point, the derivation as listed in the text takes over and is complete.



APPENDIX C  
COMPUTER ALGORITHM FOR SOLVING  
THE COUPLED WAVE EQUATIONS

The following algorithm utilizes the approximations made in Chapter IV to solve the coupled wave equations. The code is written in BASIC and is simple enough to run on a microcomputer. Run times should be on the order of one minute.

To use the algorithm, the user must first enter a distribution for hole radius versus distance on program line 1110. During program execution, the user must input a value for hole separation in centimeters. Although this value remains constant in the algorithm as it stands, it would be a simple matter to allow the hole separation to vary in a manner similar to the varying hole size.

Listing 3 gives the algorithm as it was first developed. This is the form used to produce listing 1. The additional program lines of listing 4 were inserted in listing 3 to get the declining magnitude results of listing 2.

No explanation of the code will be given, since the code is well documented and self explanatory.

# LISTING 3 - Computer Algorithm

```

0  CADD=30050:CSUB=30000:POLAR=30100:CMULT=30150
1  CDIV=30200:CPOWER=30250:CEXP=30300:CSINH=30350:CCOSH=30400:DEG
2  DIM A(2,2),KR(2,2),KI(2,2),AO(2,2),GAMMA(2,2),LAMBDA(2,2),E2(2),B1(2),B2(2)
3  DIM C(4,2):REM -----
4  REM ----- A(I,J) = AMPLITUDE OF EXCITED MODES -----
5  REM ----- J=1 IS REAL PART, AND J=2 IS IMAGINARY PART OF A(I,J) --
6  REM ----- GAMMA(I,J) = PROPAGATION CONSTANTS OF MODES IN BOTH GUIDES -----
7  REM ----- J=1 IS REAL PART, AND J=2 IS IMAG PART OF GAMMA(I,J) --
8  REM ----- KR(I,J) = REAL PART OF KAPPA MATRIX POSITION (I,J) -----
9  REM ----- KI(I,J) = IMAGINARY PART OF KAPPA MATRIX POSITION (I,J) -----
10 REM ----- AO(I,J) = AMPLITUDE OF INCIDENT MODES-----
11 REM ----- J=1 IS REAL PART, AND J=2 IS IMAGINARY PART OF AO(I,J)-
12 REM ----- PME = POSITIVE REAL FUNCTION OF "Z" RELATED TO HOLE SIZE ----
13 REM ----- PMO = NEGATIVE REAL FUNCTION OF "Z" RELATED TO HOLE SIZE ----
14 REM ----- S = HOLE SPACING -----
15 REM ----- C1 = CONSTANT FOR REAL PART OF "T" MATRIX (1,1) POSITION ---
16 REM ----- C2 = CONSTANT FOR IMAG PART OF "T" MATRIX (1,1) POSITION ---
17 REM ----- C3 = CONSTANT FOR REAL PART OF "T" MATRIX (1,2) POSITION ---
18 REM ----- C4 = CONSTANT FOR IMAG PART OF "T" MATRIX (1,2) POSITION ---
19 REM ----- C5 = CONSTANT FOR REAL PART OF "T" MATRIX (2,2) POSITION ---
20 REM ----- C6 = CONSTANT FOR IMAG PART OF "T" MATRIX (2,2) POSITION ---
21 REM ----- K0 = WAVE NUMBER OF LOSSLESS GUIDE AT CUTOFF -----
22 REM ----- T = THICKNESS OF COMMON WALL BETWEEN WAVEGUIDES -----
23 REM ----- Z = DISTANCE ALONG AXIS OF WAVEGUIDE W/RES TO INPUT -----
24 REM ----- L = LENGTH OF COUPLER SECTION ( 6 GUIDE WAVELENGTHS ) -----
25 REM ----- E(I,J) = EXP[ LAMBDA(I,1) + j LAMBDA(I,2) ] -----
26 REM ----- J=1 IS REAL PART, AND J=2 IS IMAG PART OF GAMMA(I,J) --
27 REM ----- J=1 IS REAL PART, AND J=2 IS IMAG PART OF GAMMA(I,J) --
28 REM ----- J=1 IS REAL PART, AND J=2 IS IMAG PART OF LAMBDA(I,J)--
29 REM ----- B1(I) = -GAMMA(1) + KAPPA(1,1) -----
30 REM ----- B2(I) = -GAMMA(2) + KAPPA(2,2) -----
31 REM ----- I=1 IS REAL PART, AND I=2 IS IMAG PART OF B1(I)/B2(I)--
32 REM ----- C(I,J) = NORMALIZATION CONSTANTS MULTIPLYING THE EXPONENTIALS --
33 REM ----- J=1 IS REAL PART, AND J=2 IS IMAG PART OF C(I,J) -----
34 REM ----- A = TEMPORARY STORAGE REGISTER A -----
35 REM ----- B = TEMPORARY STORAGE REGISTER B -----
50 REM -----
51 REM ----- THIS PROGRAM GIVES THE SOLUTION TO DIFFERENTIAL EQUATIONS
52 REM ----- OF THE FOLLOWING FORM -----
53 REM -----
54 REM ----- d/dz(A1) = B1*A1 + KAPPA*A2 -----
55 REM ----- d/dz(A2) = KAPPA*A1 + B2*A2 -----
56 REM ----- where -----
57 REM ----- B1 = -GAMMA1 + KAPPA(1,1) -----
58 REM ----- B2 = -GAMMA2 + KAPPA(2,2) -----
59 REM ----- PROVIDED THAT B1 AND B2 ARE CONSTANT OVER THE REGION --
60 REM ----- BEING INTEGRATED -----

```

```

61 REM -----
62 REM ----- USING THE EIGENVALUE APPROACH, GIVES EIGENVALUES OF -----
63 REM ----- LAMBDA(1)= .5*(B1+B2)+[.25*(B1+B2)^2 - B1*B2 + KAPPA^2]^-.5--
64 REM ----- LAMBDA(2)= .5*(B1+B2)-[.25*(B1+B2)^2 - B1*B2 + KAPPA^2]^-.5--
65 REM -----
66 REM ----- THUS, A SOLUTION TO THE EQUATIONS IS -----
67 REM ----- A1 = C(1)*EXP[LAMBDA(1)*S] + C(2)*EXP[LAMBDA(2)*S] -----
68 REM ----- A2 = C(3)*EXP[LAMBDA(1)*S] + C(4)*EXP[LAMBDA(2)*S] -----
69 REM -----
70 REM ----- DIFFERENTIATING THESE EQUATIONS REVEALS THAT -----
71 REM ----- C(3) = C(1)*[(LAMBDA(1) - B1)/KAPPA] -----
72 REM ----- C(4) = C(2)*[(LAMBDA(2) - B1)/KAPPA] -----
73 REM -----
74 REM ----- THUS, ALL THAT REMAINS IS TO NORMALIZE C(1),C(2),C(3),C(4)-
75 REM ----- SO THAT AT THE BEGINNING OF EACH SECTION BEING INTEGRATED -
76 REM ----- AO(1) = C(1) + C(2) -----
77 REM ----- and -----
78 REM ----- AO(2) = C(3) + C(4) -----
79 REM -----
80 REM ----- SET THE VALUES FOR THE CONSTANTS -----
91 GAMMA(1,1)=0:GAMMA(1,2)=0.3362:GAMMA(2,1)=0.46:GAMMA(2,2)=0.3214
92 L=112.2448:T=0.2032:K0=0.55016383:GOTO 1000
100 REM ----- SUBROUTINE TO COMPUTE "PME" AND "PMO"
110 REM ----- EQUATIONS FROM TABLE 2.3 PG. 53 SPORLEDER
120 RM=1/(1-0.4*(K0*K0*R*R))
130 GAMH=SQR(3.3856/R/R-K0*K0)
140 A=0.35+0.15*K0*K0*R*R:B=1-EXP(-2*GAMH*T):KME=1-A*B
150 A=A-0.05:A=A*A:KMO=EXP(-GAMH*T)*(1-(0.1+A)*B)
160 PME=4/3*R*R*R*RM*KME:PMO=-4/3*R*R*R*RM*KMO
170 RETURN
200 REM ----- SUBROUTINE TO NORMALIZE CONSTANTS -----
201 REM --- C(1) = [KAPPA*AO(2)-AO(1)*(LAMBDA(2)-B1)]/[LAMBDA(1) - LAMBDA(2)]
202 REM --- C(2) = AO(1) - C(1) -----
203 REM --- C(3) = C(1)*[(LAMBDA(1)-B1)/KAPPA] -----
204 REM --- C(4) = C(2)*[(LAMBDA(2)-B1)/KAPPA] -----
205 REAL1=LAMBDA(2,1)-B1(1)
206 IMAG1=LAMBDA(2,2)-B1(2)
207 REAL2=AO(1,1):IMAG2=AO(1,2)
208 GOSUB CMULT:REM ----- COMPUTE SECOND TERM OF EQUATION -----
210 C(1,1)=REAL:C(1,2)=IMAG:REM ----- STORE THIS TERM TEMPORARILY -----
212 REAL1=KR(1,2):IMAG1=KI(1,2)
214 REAL2=AO(2,1):IMAG2=AO(2,2)
216 GOSUB CMULT:REM ----- COMPUTE FIRST TERM OF EQUATION -----
218 REAL1=REAL-C(1,1):IMAG1=IMAG-C(1,2)
220 REAL2=LAMBDA(1,1)-LAMBDA(2,1)
222 IMAG2=LAMBDA(1,2)-LAMBDA(2,2)
224 GOSUB CDIV:REM ----- COMPUTE C(1) -----
226 C(1,1)=REAL:C(1,2)=IMAG:REM ----- SET VALUE FOR C(1) -----
228 C(2,1)=AO(1,1)-C(1,1)
230 C(2,2)=AO(1,2)-C(1,2):REM ----- SET VALUE FOR C(2) -----
232 REAL1=LAMBDA(1,1)-B1(1)
234 IMAG1=LAMBDA(1,2)-B1(2)

```

```

236 REAL2=KR(1,2):IMAG2=KI(1,2)
238 GOSUB CDIV:REM ----- FIRST STEP TO EVALUATE C(3) -----
240 REAL1=REAL:IMAG1=IMAG
242 REAL2=C(1,1):IMAG2=C(1,2)
244 GOSUB CMULT:REM ----- FINISH COMPUTING C(3) -----
246 C(3,1)=REAL:C(3,2)=IMAG:REM ----- SET VALUES FOR C(3) -----
248 REAL1=LAMBDA(2,1)-B1(1)
250 IMAG1=LAMBDA(2,2)-B1(2)
252 REAL2=KR(1,2):IMAG2=KI(1,2)
254 GOSUB CDIV:REM ----- FIRST STEP TO EVALUATE C(4) -----
256 REAL1=REAL:IMAG1=IMAG
258 REAL2=C(2,1):IMAG2=C(2,2)
260 GOSUB CMULT:REM ----- FINISH COMPUTING C(4) -----
262 C(4,1)=REAL:C(4,2)=IMAG:REM ----- SET VALUES FOR C(4) -----
264 RETURN
300 REM ----- SUBROUTINE TO COMPUTE THE SINC FUNCTN -
310 REM ----- COMPUTES THE NUMBER FOR THE EQUATION --
320 REM ----- [ (GAMMA1 - GAMMA2( *S/2 )
330 REM ----- / SINH [ (GAMMA1 - GAMMA2( * S/2 )
340 REAL=GAMMA(1,1)-GAMMA(2,1):REAL=REAL*S/2
350 IMAG=GAMMA(1,2)-GAMMA(2,2):IMAG=IMAG*S/2
360 A=REAL:B=IMAG:REM ----- TEMP STORAGE FOR THE SINH'S ARGUMENT --
365 IF A=0 AND B=0 THEN SINCR=1:SINCI=0:GOTO 410
370 GOSUB CSINH:REM ----- SINH [ (GAMMA1 - GAMMA2) * S/2 ] -----
380 REAL2=REAL:IMAG2=IMAG:REAL1=A:IMAG1=B
390 GOSUB CDIV:REM ----- X / SINH[ X ] -----
400 SINCR=REAL:SINCI=IMAG:REM ----- REAL AND IMAG PARTS OF SINC FUNCTION --
410 RETURN
500 REM ----- NOW COMPUTE THE CONSTANTS OF THE "T" --
501 REM ----- MATRIX AS DEFINED BY SPORLEDER -----
502 REM ----- FOR CIRCULAR HOLES CENTERED IN THE ----
503 REM ----- NARROW WALL BETWEEN TWO WAVEGUIDES, ---
504 REM ----- THE EQUATION FOR THE "T(M,N)" MATRIX --
505 REM ----- SIMPLIFIES TO -----
506 REM -----  $T(M,N) = P_{me} * \pi^2 / [8 * A^3 * B * \text{GAMMA}(M)]$  -----
507 REM ----- FOR M=N, i e. FOR MODES IN THE SAME WAVEGUIDE
508 REM ----- OR, FOR MODES IN SEPARATE WAVEGUIDES, -----
509 REM -----  $T(M,N) = -P_{mo} * \pi^2 / (8 * A^3 * B * [\text{GAMMA}(1) * \text{GAMMA}(2)]^{0.5})$ 
510 REM ----- WHERE, -----
511 REM ----- A = ONE HALF THE WAVEGUIDE'S BROAD DIMENSION -----
512 REM ----- B = THE WAVEGUIDE'S NARROW DIMENSION -----
513 REM -----  $\pi = \text{ARCTAN}(1) * 4 = 3.14159267$  -----
514 REM ----- THE CONSTANTS, C1 TO C6, COMPUTED BY --
515 REM ----- THIS SUBROUTINE INCLUDES ALL PARTS OF -
516 REM ----- THE ABOVE EQUATIONS EXCEPT FOR Pmo Pme
517 REM -----
520 A=3.14159267*3.14159267/8/3.607/3.607/3.607/3.404
530 REAL1=1:IMAG1=0:REAL2=GAMMA(1,1):IMAG2=GAMMA(1,2)
540 GOSUB CDIV:REM ----- FIND  $1/([\text{GAMMA}(1)*\text{GAMMA}(1)]^{0.5})$  -----
550 C1=REAL*A:C2=IMAG*A:REM ----- SET CONSTANTS C1 and C2 -----

```

```

560 REAL2=GAMMA(2,1):IMAG2=GAMMA(2,2)
570 GOSUB CDIV:REM ----- FIND 1/([GAMMA(2)*GAMMA(2)]^0.5) -----
580 C5=REAL*A:C6=IMAG*A:REM ----- SET CONSTANTS C5 AND C6 -----
590 REAL1=GAMMA(1,1):IMAG1=GAMMA(1,2)
600 REAL2=GAMMA(2,1):IMAG2=GAMMA(2,2)
610 GOSUB CMULT:REM ----- FIND GAMMA(1)*GAMMA(2) -----
620 POWER=0.5:GOSUB CPOWER:REM ----- FIND SQUARE ROOT OF THE PRODUCT -----
630 REAL1=1:IMAG1=0:REAL2=REAL:IMAG2=IMAG
640 GOSUB CDIV:REM ----- FIND 1/SQUARE ROOT -----
650 C3=REAL*-A:C4=IMAG*-A:REM ----- SET CONSTANTS C3 AND C4 -----
660 RETURN
1000 REM ----- BEGIN MAIN PROGRAM -----
1010 PRINT "ENTER THE HOLE SEPARATION";:INPUT S
1020 GOSUB 300:REM ----- COMPUTE [ X/SINH(X) ] -----
1025 GOSUB 500:REM ----- COMPUTE THE "T" MATRIX'S CONSTANTS -----
1030 REM ----- INITIALIZE INCIDENT AMPLITUDES -----
1040 AO(1,1)=100:AO(1,2)=0:AO(2,1)=0:AO(2,2)=0
1050 POKE 201,15:REM ----- SET COLUMN SPACING AT 15 SPACES -----
1060 LPRINT "THE HOLE SPACING IS ";S;" cm.":LPRINT
1070 LIST "P:",1110:REM ----- LIST THE FUNCTIONAL FORM FOR HOLE -----
1080 REM ----- RADIUS USED IN THIS RUN -----
1090 LPRINT :LPRINT "Z","R","|A(1)|","|A(2)|":PRINT
1100 FOR Z=0 TO L STEP 5
1110 R=0.87*EXP(-3.8E-03*Z)+0.47*EXP(7.65E-03*Z):REM -- HOLE SIZE Vs. DISTANCE
1114 IF Z=0 THEN R=1.42
1115 IF Z>104 THEN R=1.638
1116 IF Z>107 THEN R=1.665
1117 IF Z>110 THEN R=1.702
1120 GOSUB 100:REM ----- FIND PMO AND PME -----
1130 REM ----- FIND KAPPA(I,J) = T(I,J)/S*X/SINH(X) -----
1140 KR(1,1)=PME/S*C1:KI(1,1)=PME/S*C2
1150 KR(2,2)=PME/S*C5:KI(2,2)=PME/S*C6
1160 REAL1=PMO/S*C3:IMAG1=PMO/S*C4
1170 REAL2=SINCR:IMAG2=SINCI
1175 GOSUB CMULT:REM ----- COMPUTE KAPPA(1,2) -----
1180 KR(1,2)=REAL:KI(1,2)=IMAG:REM --- KAPPA(1,2) INVOLVES THE SINH FUNCTION -
1190 IR(2,1)=REAL:KI(2,1)=IMAG:REM --- KAPPA(2,1) = KAPPA(1,2) -----
1200 REAL1=KR(1,2):IMAG1=KI(1,2)
1210 REAL2=KR(1,2):IMAG2=KI(1,2)
1220 GOSUB CMULT:REM ----- COMPUTE KAPPA(1,2)^2 -----
1230 A=REAL:B=IMAG:REM ----- TEMP STORAGE OF REAL AND IMAG PARTS ---
1235 REM ----- DEFINE B1(1),B1(2),B2(1),AND B2(2) -----
1240 B1(1)=-GAMMA(1,1)+KR(1,1):REM --- REAL PART OF B1 -----
1245 B1(2)=-GAMMA(1,2)+KI(1,1):REM --- IMAGINARY PART OF B1 -----
1250 B2(1)=-GAMMA(2,1)+KR(2,2):REM --- REAL PART OF B2 -----
1255 B2(2)=-GAMMA(2,2)+KI(2,2):REM --- IMAGINARY PART OF B2 -----
1260 REAL1=B1(1):IMAG1=B1(2)
1265 REAL2=B2(1):IMAG2=B2(2)
1270 GOSUB CMULT:REM ----- COMPUTE B1*B2 -----
1275 A=A-REAL:B=B-IMAG:REM ----- SUBTRACT FROM PREVIOUS VALUES -----
1280 REAL1=0.5*(B1(1)+B2(1))
1285 IMAG1=0.5*(B1(2)+B2(2))

```

```

1290 REAL2=0.5*(B1(1)+B2(1))
1295 IMAG2=0.5*(B1(2)+B2(2))
1300 GOSUB CMULT:REM ----- COMPUTE [0.5*(B1 + B2)]^2 -----
1310 A=A+REAL:B=B+IMAG:REM ----- ADD TO PREVIOUS VALUES -----
1320 REAL=A:IMAG=B:POWER=0.5
1330 GOSUB CPOWER:REM ----- COMPUTE THE SQUARE ROOT OF A + jB -----
1340 LAMBDA(1,1)=0.5*(B1(1)+B2(1))+REAL
1350 LAMBDA(1,2)=0.5*(B1(2)+B2(2))+IMAG
1360 LAMBDA(2,1)=0.5*(B1(1)+B2(1))-REAL
1370 LAMBDA(2,2)=0.5*(B1(2)+B2(2))-IMAG
1380 REAL=LAMBDA(1,1)*S
1390 IMAG=LAMBDA(1,2)*S
1400 GOSUB CEXP:REM ----- COMPUTE EXP [ LAMBDA(1)*S ] -----
1410 E(1,1)=REAL:E(1,2)=IMAG:REM --- SET THE VALUES FOR E(1) -----
1420 REAL=LAMBDA(2,1)*S
1430 IMAG=LAMBDA(2,2)*S
1440 GOSUB CEXP:REM ----- COMPUTE EXP [ LAMBDA(2)*S ] -----
1450 E(2,1)=REAL:E(2,2)=IMAG:REM --- SET THE VALUES FOR E(2) -----
1460 GOSUB 200:REM ----- NORMALIZE THE CONSTANTS FOR THIS SECTION -----
1470 REAL1=C(1,1):IMAG1=C(1,2)
1480 REAL2=E(1,1):IMAG2=E(1,2)
1490 GOSUB CMULT:REM ----- COMPUTE THE FIRST TERM OF A(1) -----
1500 A(1,1)=REAL:A(1,2)=IMAG:REM --- STORE THESE VALUES TEMPORARILY -----
1510 REAL1=C(2,1):IMAG1=C(2,2)
1520 REAL2=E(2,1):IMAG2=E(2,2)
1530 GOSUB CMULT:REM ----- COMPUTE THE SECOND TERM OF A(1) -----
1540 A(1,1)=REAL+A(1,1)
1550 A(1,2)=IMAG+A(1,2):REM ----- SET THE VALUES FOR A(1) -----
1560 REAL=A(1,1):IMAG=A(1,2)
1570 GOSUB POLAR:REM ----- FIND THE MAGNITUDE OF A(1) -----
1580 AIMAG=MAGN:REM ----- SET THE VALUE FOR AIMAG -----
1590 REAL1=C(3,1):IMAG1=C(3,2)
1600 REAL2=E(1,1):IMAG2=E(1,2)
1610 GOSUB CMULT:REM ----- COMPUTE THE FIRST TERM OF A(2) -----
1620 A(2,1)=REAL:A(2,2)=IMAG:REM --- STORE THESE VALUES TEMPORARILY -----
1630 REAL1=C(4,1):IMAG1=C(4,2)
1640 REAL2=E(2,1):IMAG2=E(2,2)
1650 GOSUB CMULT:REM ----- COMPUTE THE SECOND TERM OF A(2) -----
1660 A(2,1)=REAL+A(2,1)
1670 A(2,2)=IMAG+A(2,2):REM ----- SET THE VALUES FOR A(2) -----
1680 REAL=A(2,1):IMAG=A(2,2)
1690 GOSUB POLAR:REM ----- FIND THE MAGNITUDE OF A(2) -----
1700 A2MAG=MAGN:REM ----- SET THE VALUE FOR A2MAG -----
1710 REM ----- NOW REPLACE THE A0(I,J) VALUES WITH -----
1720 REM ----- THOSE OF A(I,J) FOR THE NEXT SECTION -----
1730 A0(1,1)=A(1,1):A0(1,2)=A(1,2)
1740 A0(2,1)=A(2,1):A0(2,2)=A(2,2)
1750 R=INT(R*1000+0.5)/1000:REM ---- ROUND OFF THE HOLE RADIUS FOR PRINTOUT -
1760 AIMAG=INT(AIMAG*L)+0.5/100:REM -ROUND OFF THE MAGNITUDE OF A(1) -----
1770 A2MAG=INT(A2MAG*100+0.5)/100:REM -ROUND OFF THE MAGNITUDE OF A(2) -----
1800 REM ----- PRINTOUT OF Z,R,AIMAG, AND A2MAG -----
1810 LPRINT INT(Z*100+0.5)/100,R,AIMAG,A2MAG
1900 NEXT Z:REM ----- LOOP UNTIL DONE -----
2000 LPR ' ' CHR$(12)

```

```

20000 REM ----- COMPLEX ARITHMETIC SUBROUTINES -----
30000 REM ----- CSUB -----
30010 REAL2=-REAL2:IMAG2=-IMAG2
30050 REM ----- CADD -----
30060 REAL=REAL1+REAL2:IMAG=IMAG1+IMAG2:RETURN
30100 REM ----- POLAR -----
30110 MAGN=SQR(REAL*REAL+IMAG*IMAG)
30113 IF REAL=0 AND IMAG<0 THEN THETA=-90:GOTO 30140
30115 IF REAL=0 AND IMAG=0 THEN THETA=0:GOTO 30140
30117 IF REAL=0 AND IMAG>0 THEN THETA=90:GOTO 30140
30119 IF REAL<0 AND IMAG=0 THEN THETA=180:GOTO 30140
30120 THETA=ATN(IMAG/REAL):IF IMAG<0 AND REAL<0 THEN THETA=THETA-180
30130 IF REAL<0 AND IMAG>0 THEN THETA=THETA+180
30140 RETURN
30150 REM ----- CMULT -----
30160 REAL=REAL1*REAL2-IMAG1*IMAG2
30170 IMAG=REAL1*IMAG2+IMAG1*REAL2
30180 RETURN
30200 REM ----- CDIV -----
30210 REAL=REAL1*REAL2+IMAG1*IMAG2
30220 IMAG=IMAG1*REAL2-REAL1*IMAG2
30230 REAL=REAL/(REAL2*REAL2+IMAG2*IMAG2)
30235 IMAG=IMAG/(REAL2*REAL2+IMAG2*IMAG2)
30240 RETURN
30250 REM ----- CPOWER -----
30260 GOSUB POLAR:REAL=MAGN^POWER*COS(POWER*THETA)
30270 IMAG=MAGN^POWER*SIN(POWER*THETA)
30280 RETURN
30300 REM ----- CEXP -----
30310 RAD:REALZ=EXP(REAL)*COS(IMAG)
30320 IMAG=EXP(REAL)*SIN(IMAG):REAL=REALZ
30330 DEG:RETURN
30350 REM ----- CSINH -----
30355 REAL2=REAL:IMAG2=IMAG:GOSUB CEXP
30360 REAL1=REAL:IMAG1=IMAG:REAL=-REAL2:IMAG=-IMAG2:GOSUB CEXP
30370 REAL2=-REAL:IMAG2=-IMAG:GOSUB CADD
30380 REAL=REAL/2:IMAG=IMAG/2:RETURN
30400 REM ----- CCOSH -----
30405 REAL2=REAL:IMAG2=IMAG:GOSUB CEXP
30410 REAL1=REAL:IMAG1=IMAG:REAL=-REAL2:IMAG=-IMAG2:GOSUB CEXP
30420 REAL2=REAL:IMAG2=IMAG:GOSUB CADD
30430 REAL=REAL/2:IMAG=IMAG/2:RETURN

```

LISTING 4 - ALTERATIONS TO COMPUTER ALGORITHM TO  
FORCE THE MAGNITUDE OF  $A_1$  TO DECLINE

```
1585 GOSUB 700:REM ----- ARTIFICIALLY FORCE |A(1)| TO DECLINE --  
700 REM ----- SUBROUTINE TO FORCE THE MAGNITUDE OF --  
701 REM ----- A(1) TO DECLINE LINERALLY -----  
710 MAG=SQR(1-8.0E-03*Z)*100  
720 A(1,1)=MAG*COS(THETA)  
730 A(1,2)=MAG*SIN(THETA)  
740 RETURN
```



APPENDIX D  
DISCRETE COUPLER DESIGN

The "slotted coupler" referred to throughout the text is actually an ad hoc design which uses standard coupling elements in cascade. The basic assumption used in designing this coupler is that any energy coupled into the secondary waveguide is immediately dissipated. Under this assumption, only the amount of coupling caused by each coupling element need be known. Using this remaining power as the input power for the next coupling element, the power it couples out can be found. By repeating this procedure, the entire length of the coupler can be included. The object, of course, is to maintain a nearly constant power along the length of the secondary waveguide by varying the amount of coupling at each element. This must take into account the reduced power reaching the element caused by the power coupled out at the previous element. An eight slot section was chosen as the coupling element used for the coupler (see Figure 20.) Since this design is one waveguide wavelength long, only six elements could fit in the space allotted and thus, the coupler consists of 48 slots (see Figure 21.)

The coupling per section was obtained from a microwave

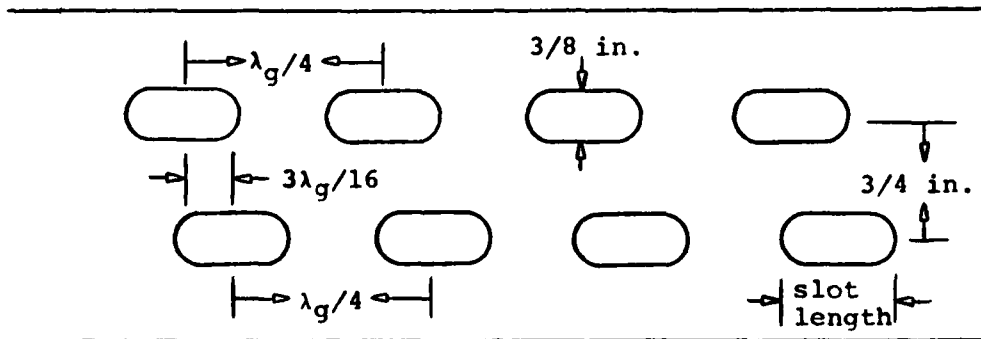


Figure 20 - 8-slot Sidewall Coupler Section

handbook (Ref 10:165) for the case of "lossless waveguides." If there is no significant difference from this system and the lossless system, then the values for coupling given in the handbook should be valid. The following is a list of the coupling for each element necessary to maintain nearly constant power in the secondary waveguide. It also gives the percentages of the power input at one end of the coupler that is coupled into the secondary waveguide by each element (section). This table was used to construct the coupler that was used in the testing.

coupler section	1	2	3	4	5	6
coupling/sectn	8.7	8.1	7.4	6.5	5.4	4.0
slot length (in)	1.245	1.273	1.311	1.370	1.460	1.680
% of $P_{IN}$ coupled	13.49	13.40	13.31	13.39	13.39	13.15

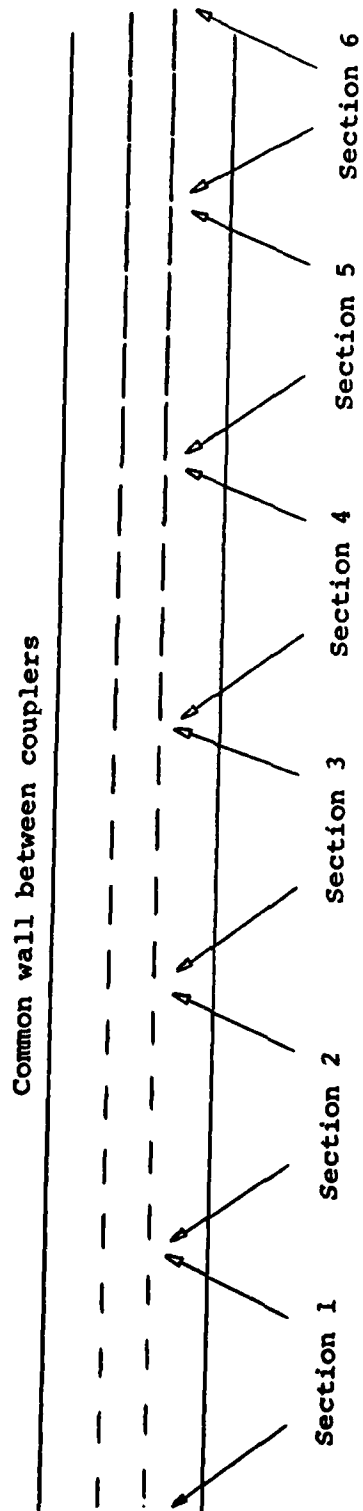


Figure 21 - Coupler made from 6 Cascaded 8-slot Sections

APPENDIX E  
SEPARABLE COUPLER DESIGN

This appendix gives the design used in making a separable coupler. As stated in the text, this type of design is motivated to reduce the "down time" when different coupling geometries are to be used. Thus, the following is the basis for the separable coupler design.

The basic idea in this design is to modify the standard radial choke design to run along the length of the coupler. Thus, instead of a flange with a choke slot in it meeting another flange, one waveguide with a choke slot along its length meets another waveguide. Figure 22 gives the overall view of the entire system as it was built. The shaded areas on both waveguides are 2.5 X 1.5 inch brass bars soldered to the sides of the waveguides that contain the choke slots. The coupler plate is just a flat brass or aluminum plate with the desired coupling holes in it that is "sandwiched" between the two waveguides.

Before going further, the design method for the choke slots will be given. Referring to a nomograph for standard choke designs (Ref 10:67) the following equations for a radial choke are presented.

$$\lambda_c = 2\pi b$$

( 82 )

$$\lambda_g = \lambda_o / [1 - (\lambda_o / \lambda_c)^2]^{1/2} \quad (83)$$

$$C = \lambda_g / 4 \quad (84)$$

where

$\lambda_c$  = the cutoff wavelength of the choke

$\lambda_g$  = the waveguide wavelength of the choke

C = the depth of the choke slot

b = the total distance from the center of the  
waveguide to the center of the slot

The nomograph gives the desired value of b, given the distance from the center of the waveguide to the inner edge of the waveguide (a corner in this case.) Thus, for WR-284 waveguide where this distance is 3.988 cm, the value from the nomograph is  $b = 6.716$  cm. Using this value in Eqs 82, 83, and 84 gives  $C = 2.966$  cm. Thus, the choke slot should be 2.966 cm deep and  $6.716 \text{ cm} - 3.988 \text{ cm} = 3.75 \text{ cm}$  from the edge of the waveguide.

Figure 23 shows the location of these slots on the primary waveguide. Figure 24 gives a similar view of the slots on the secondary waveguide. In both cases, the cross-hatched areas signify the open wall of the waveguide. Figure 25 shows the location of the coupling holes in a typical coupling plate for this "coupler sandwich."

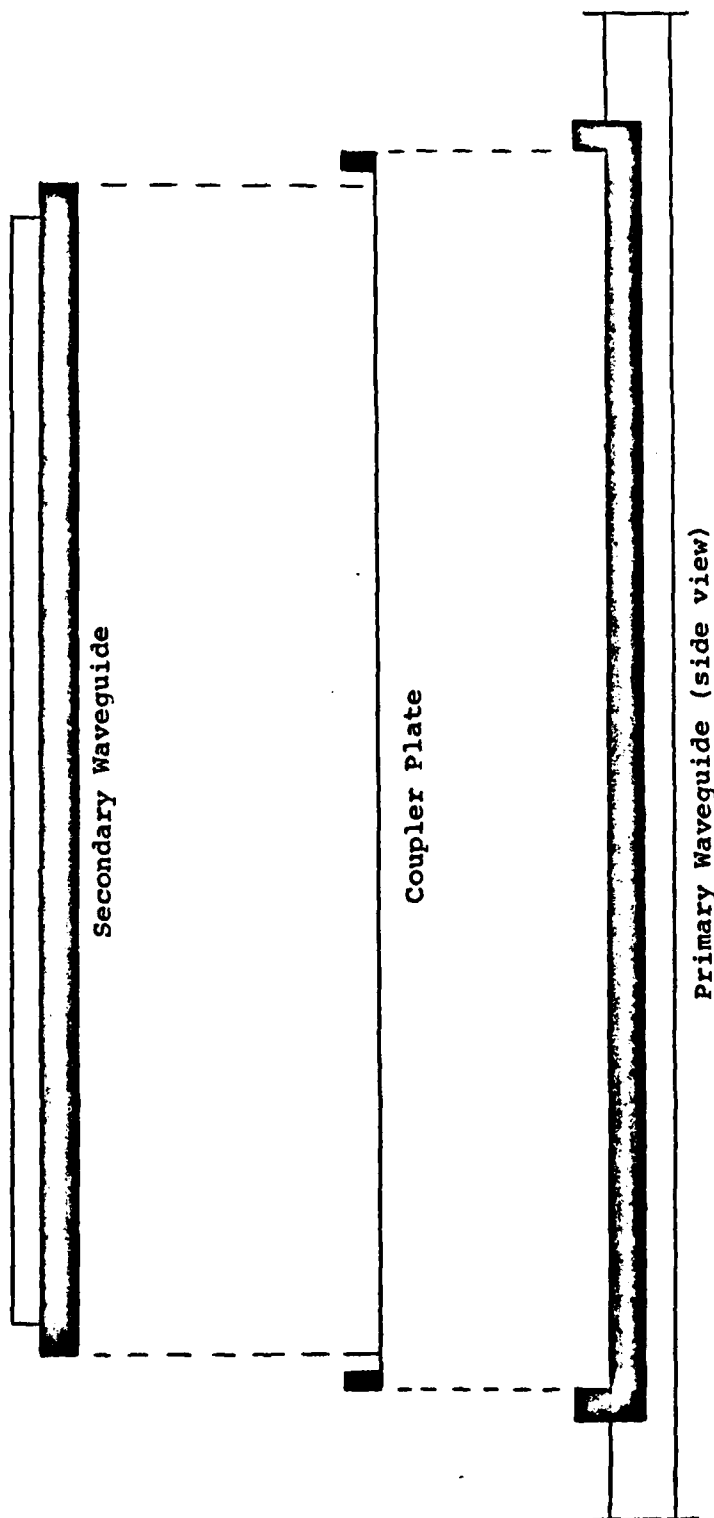


Figure 22 - Overall View of Separable Coupler

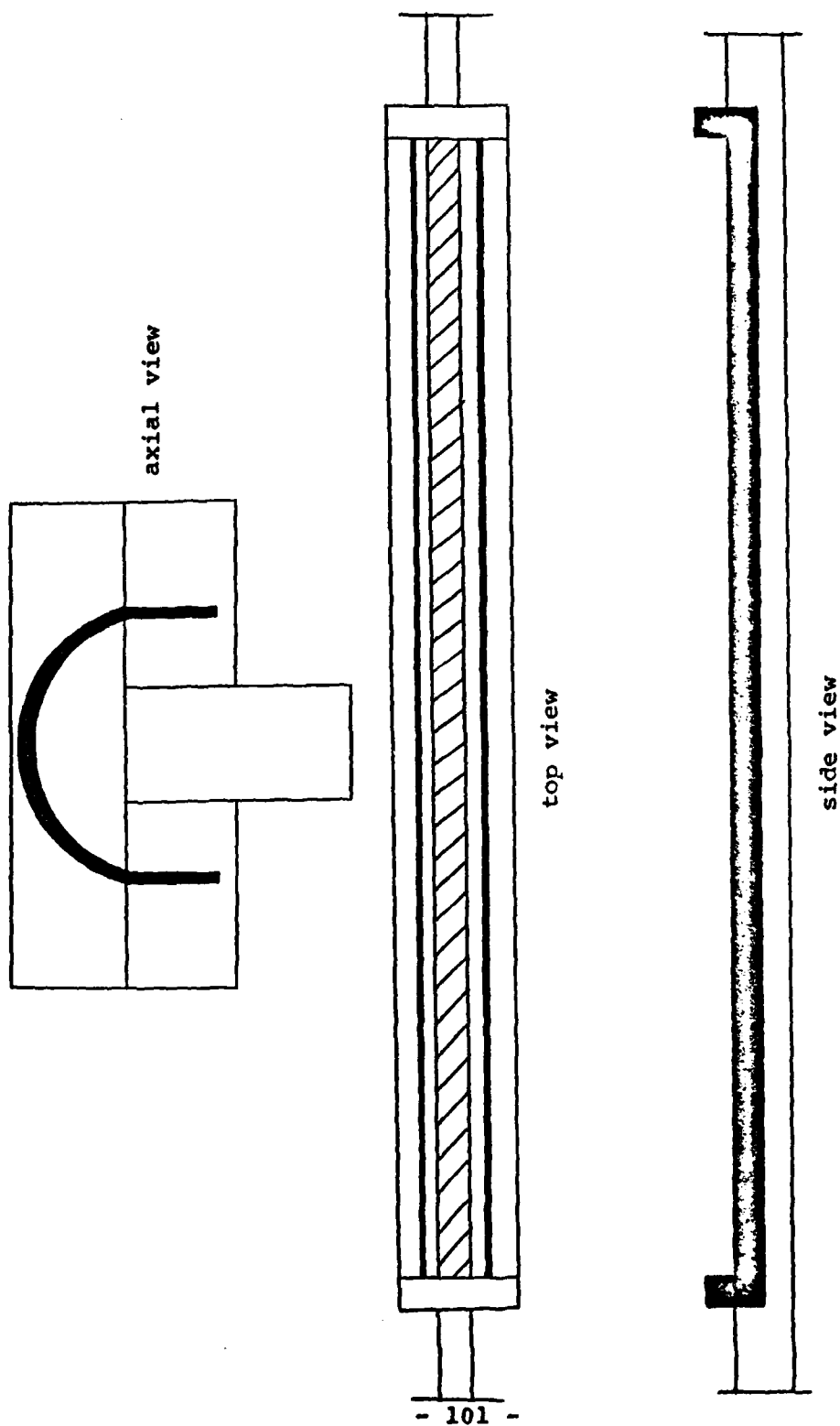


Figure 23 - Separable Coupler (Primary Waveguide Part)

5

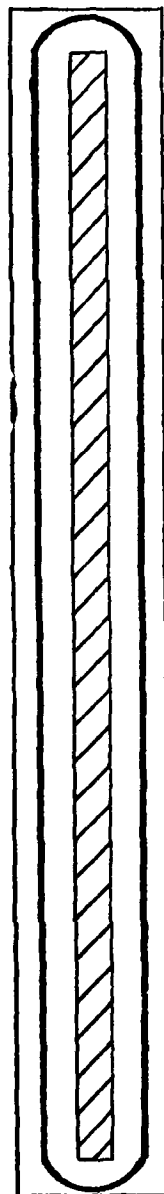
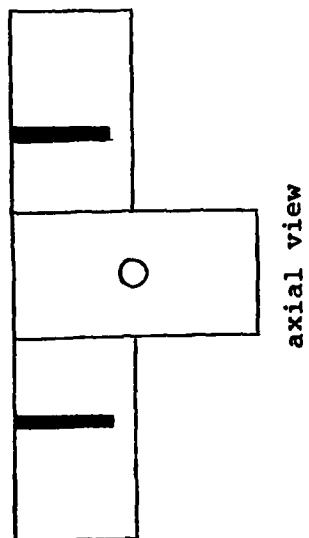
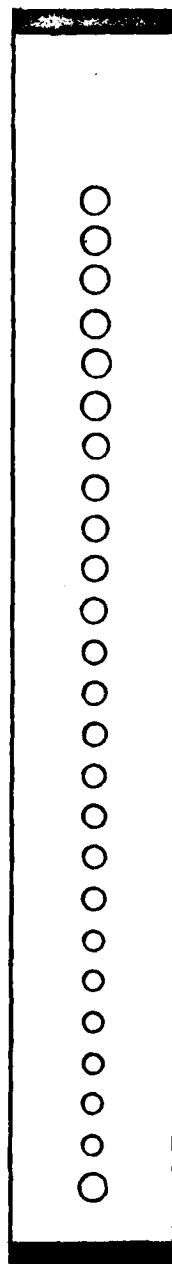


Figure 24 - Separable Coupler (Secondary Waveguide Part)





top view



side view

Figure 25 - Separable Coupler (Plate With Coupling Holes)

APPENDIX F  
SUPPLEMENTARY DATA

The following figures are a graphical representation of additional data taken during the experimental stages of the thesis. The graphical form is presented because it allows direct visual comparison of the three coupler designs being tested.

These additional plots are meant to give added proof of the merits of the "decreasing magnitude" design which was chosen to be superior. The plots are also included for completeness.

The titles for each figure are self explanatory, and give the pertinent test conditions.

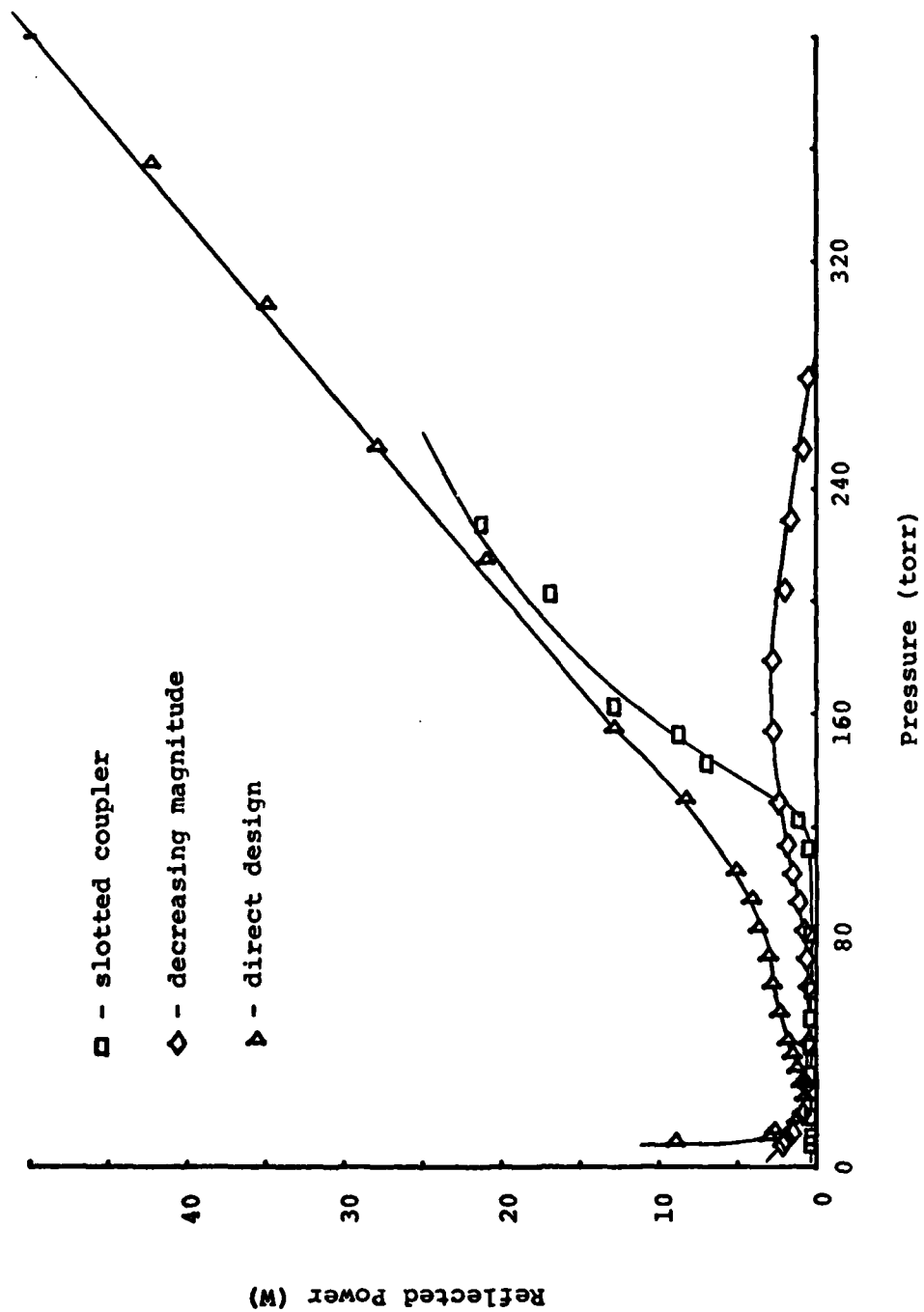


Figure 26 - Reflected Power Vs. Pressure of He at 500 W Input and 8 mm Tube

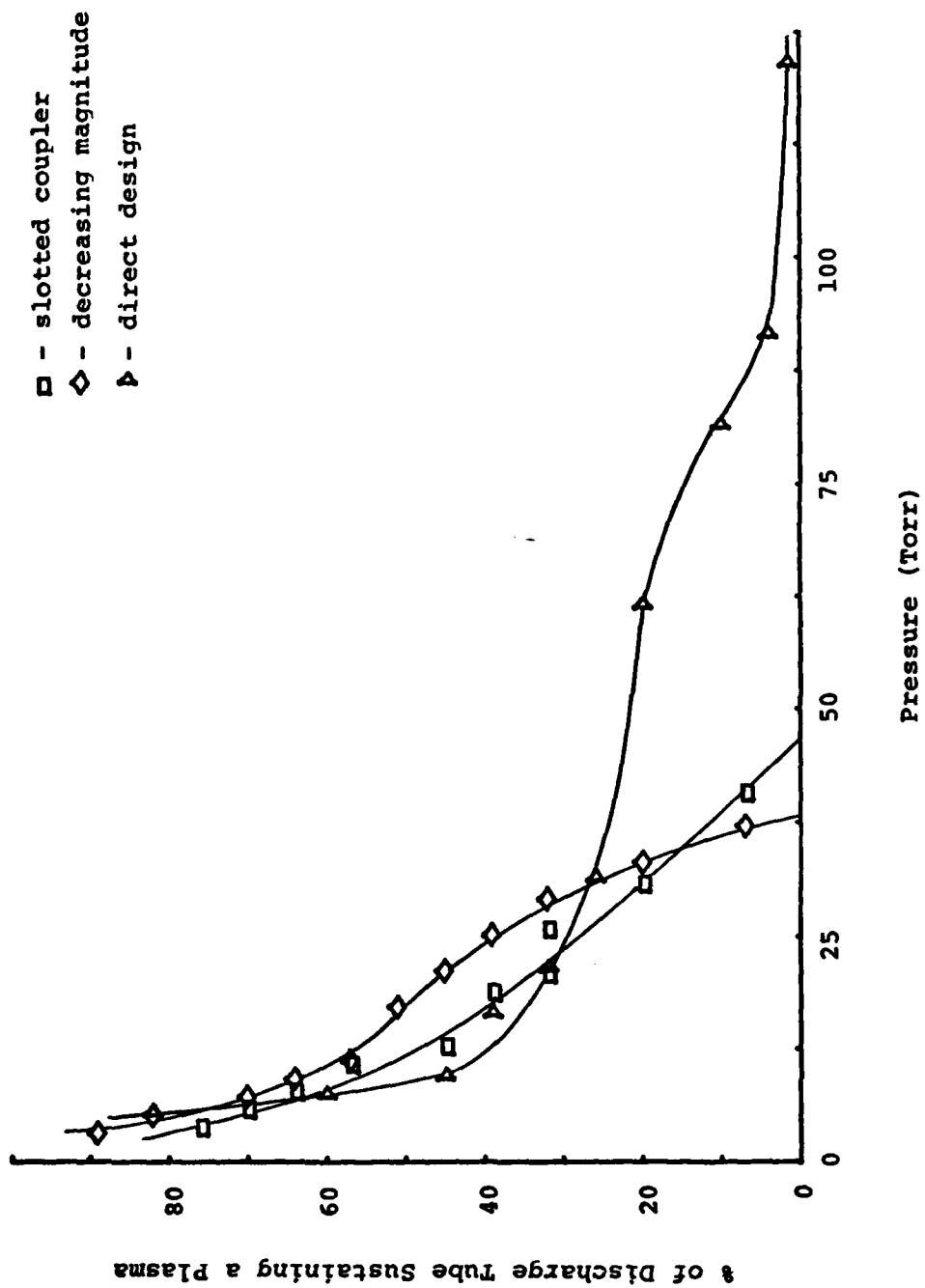


Figure 27 - % of 8 mm Tube Sustaining a Plasma Vs. Pressure of  $N_2$  at 500 W

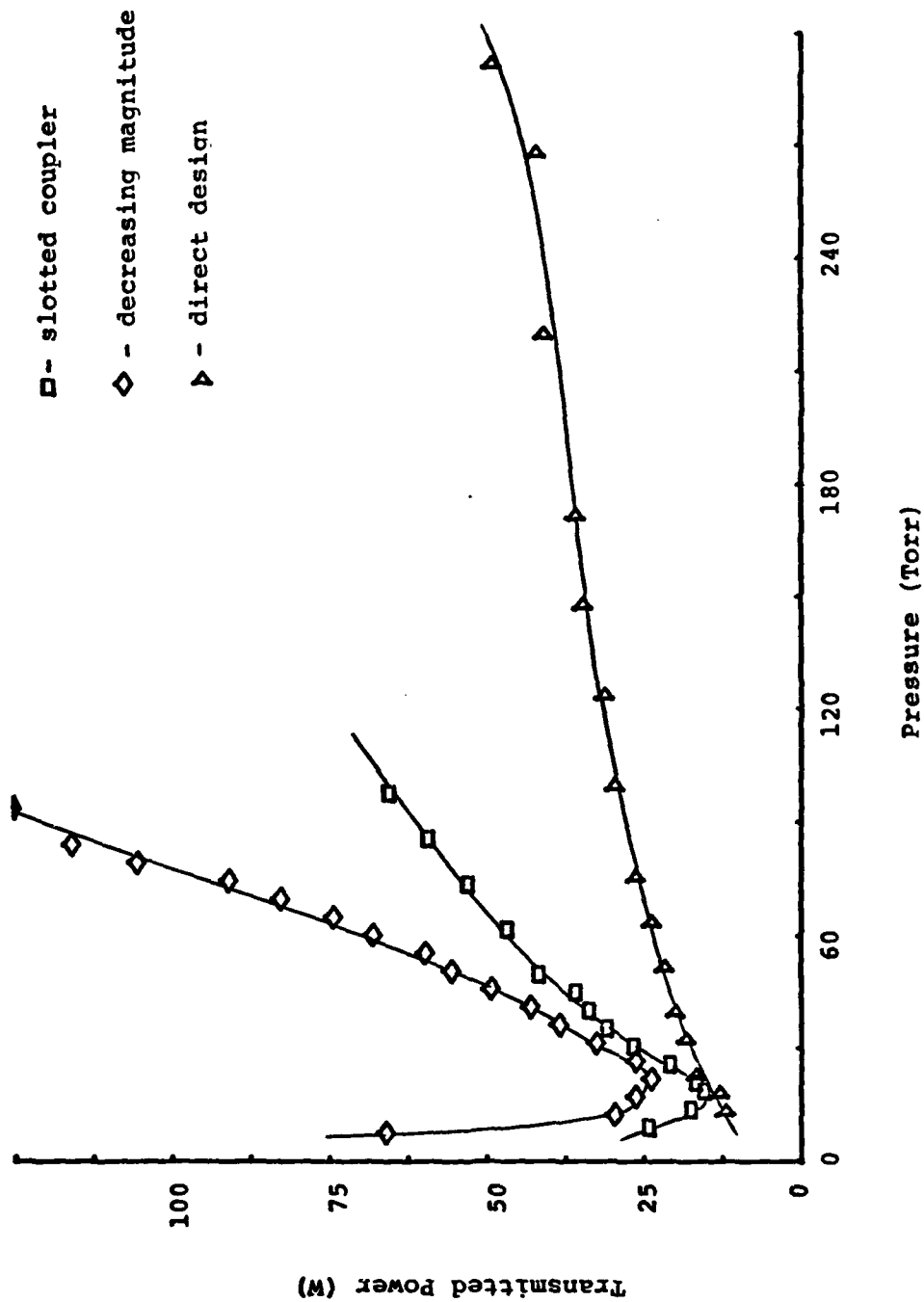


Figure 28 - Transmitted Power Vs. Pressure of  $N_2$  at 500 W Input and 8 mm Tube

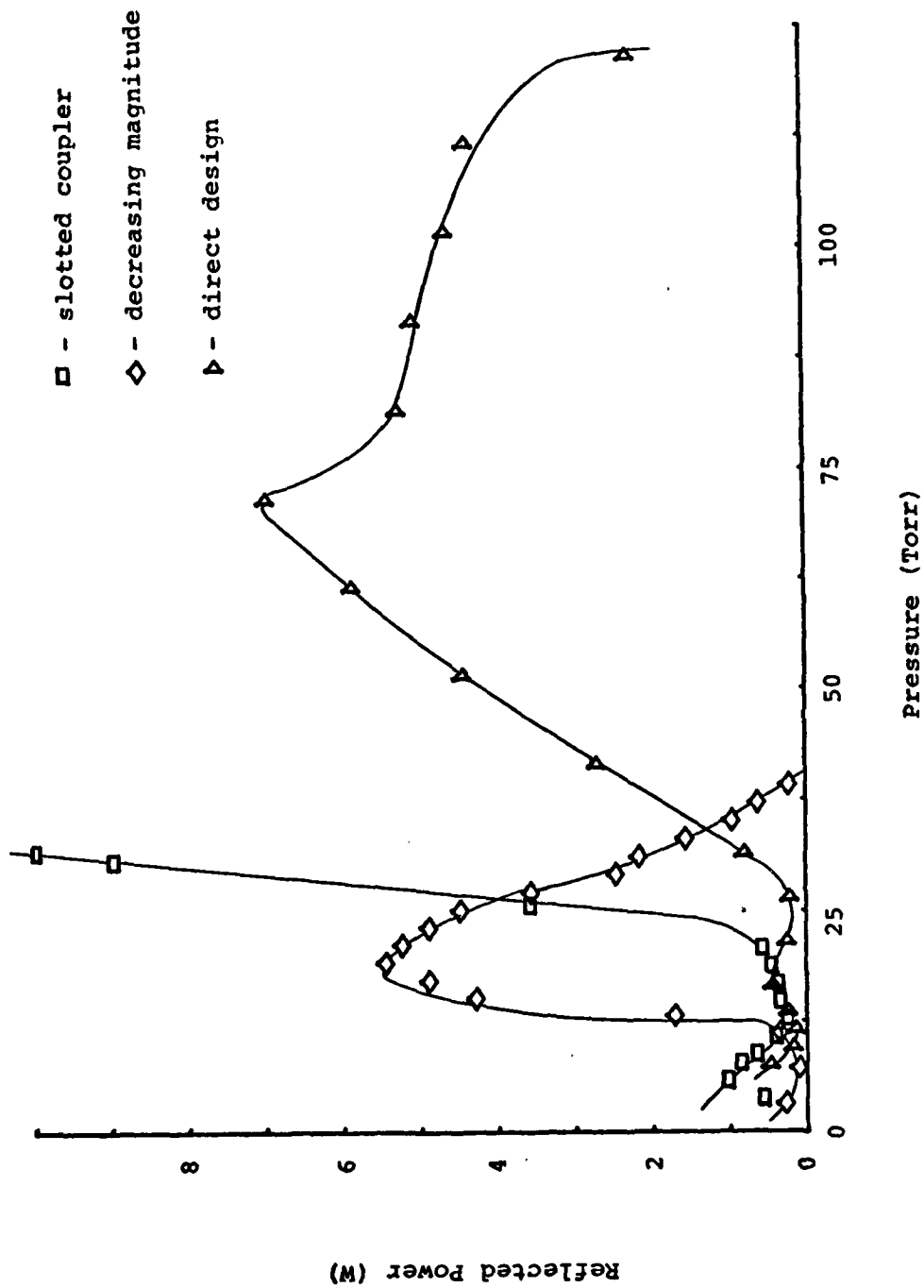


Figure 29 - Reflected Power Vs. Pressure of N at 500 W Input and 8 mm Tube

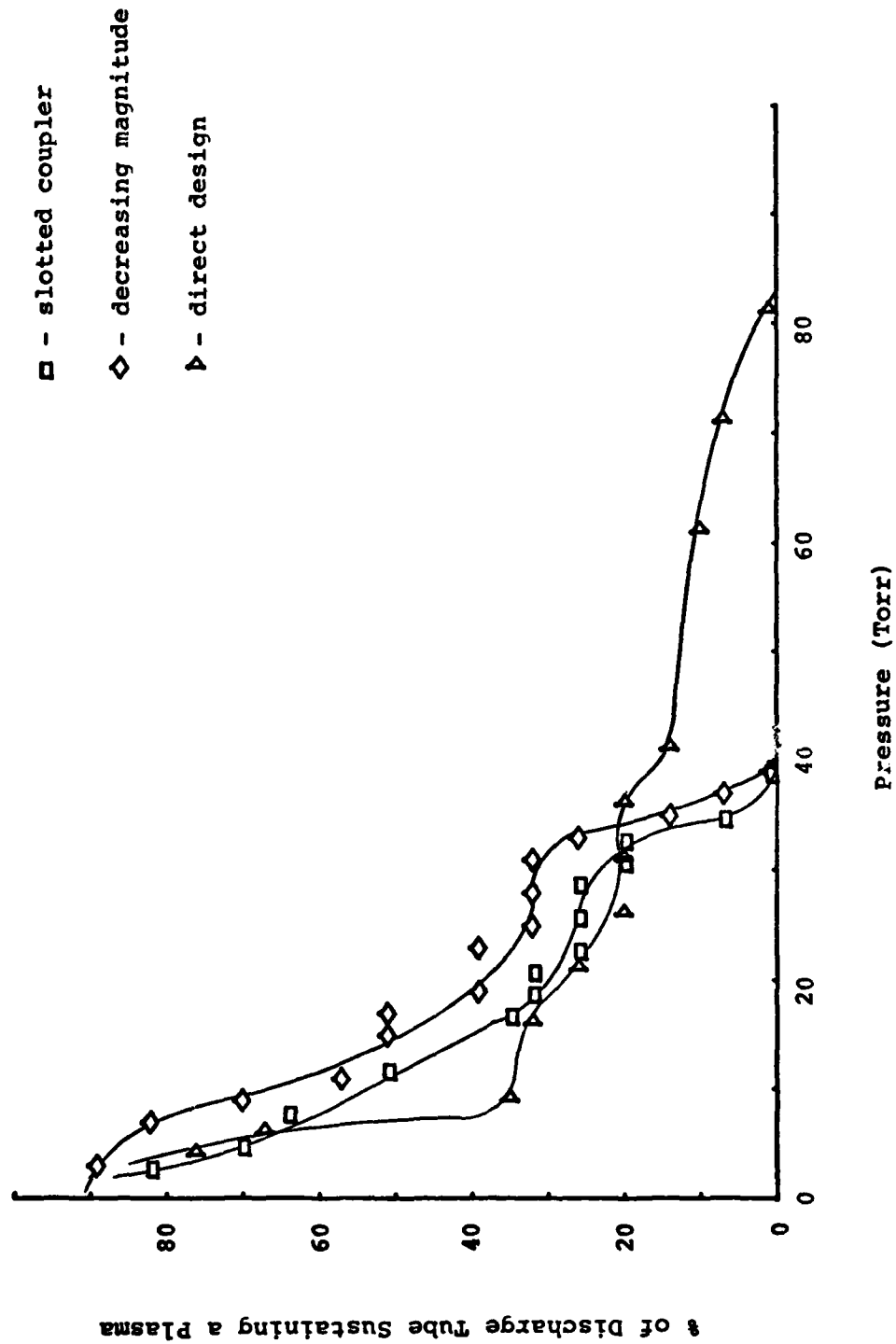


Figure 30 - % of 8 mm Tube Sustaining a Plasma Vs. Pressure of CO<sub>2</sub> at 500 W

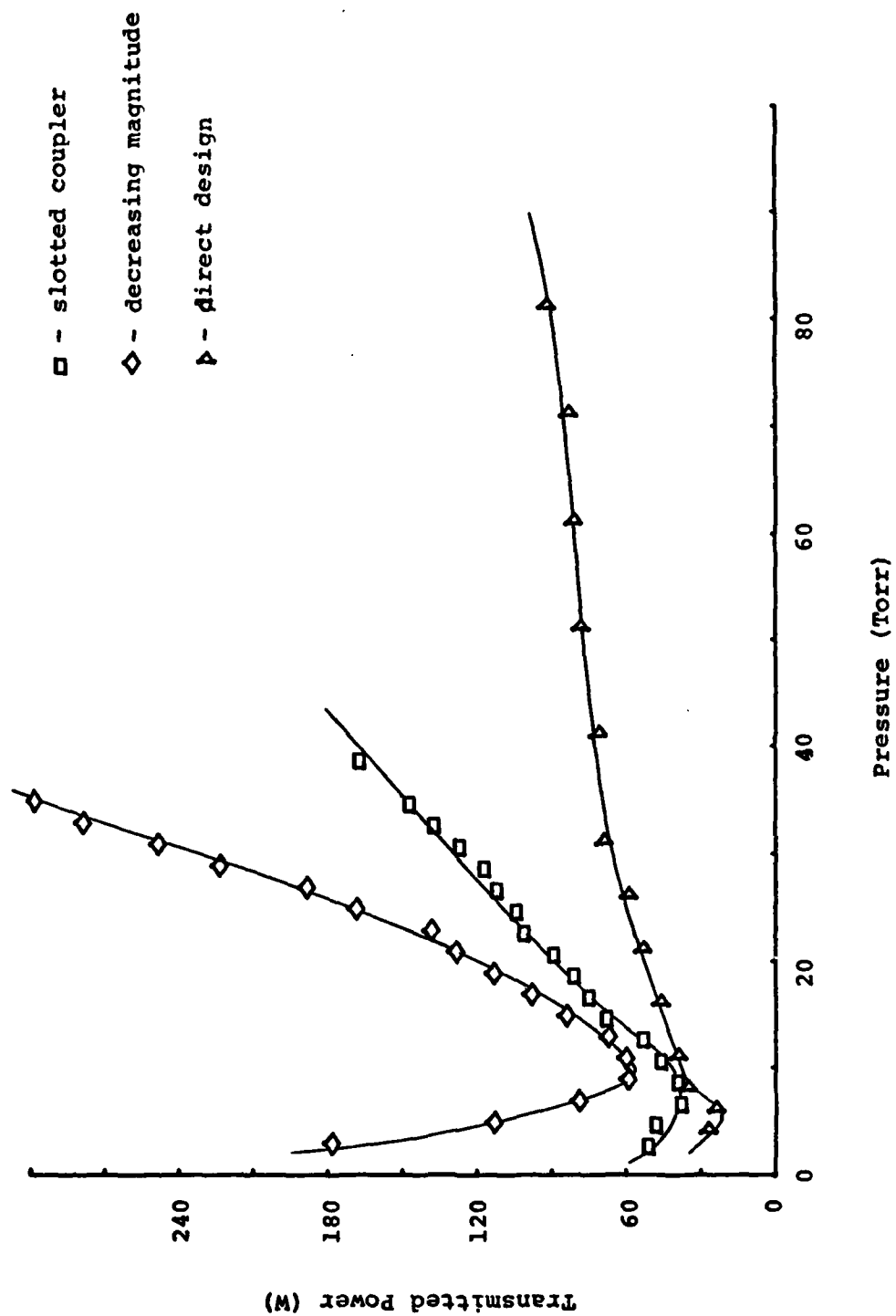


Figure 31 - Transmitted Power vs. Pressure of CO<sub>2</sub> at 500 W Input and 8 mm Tube



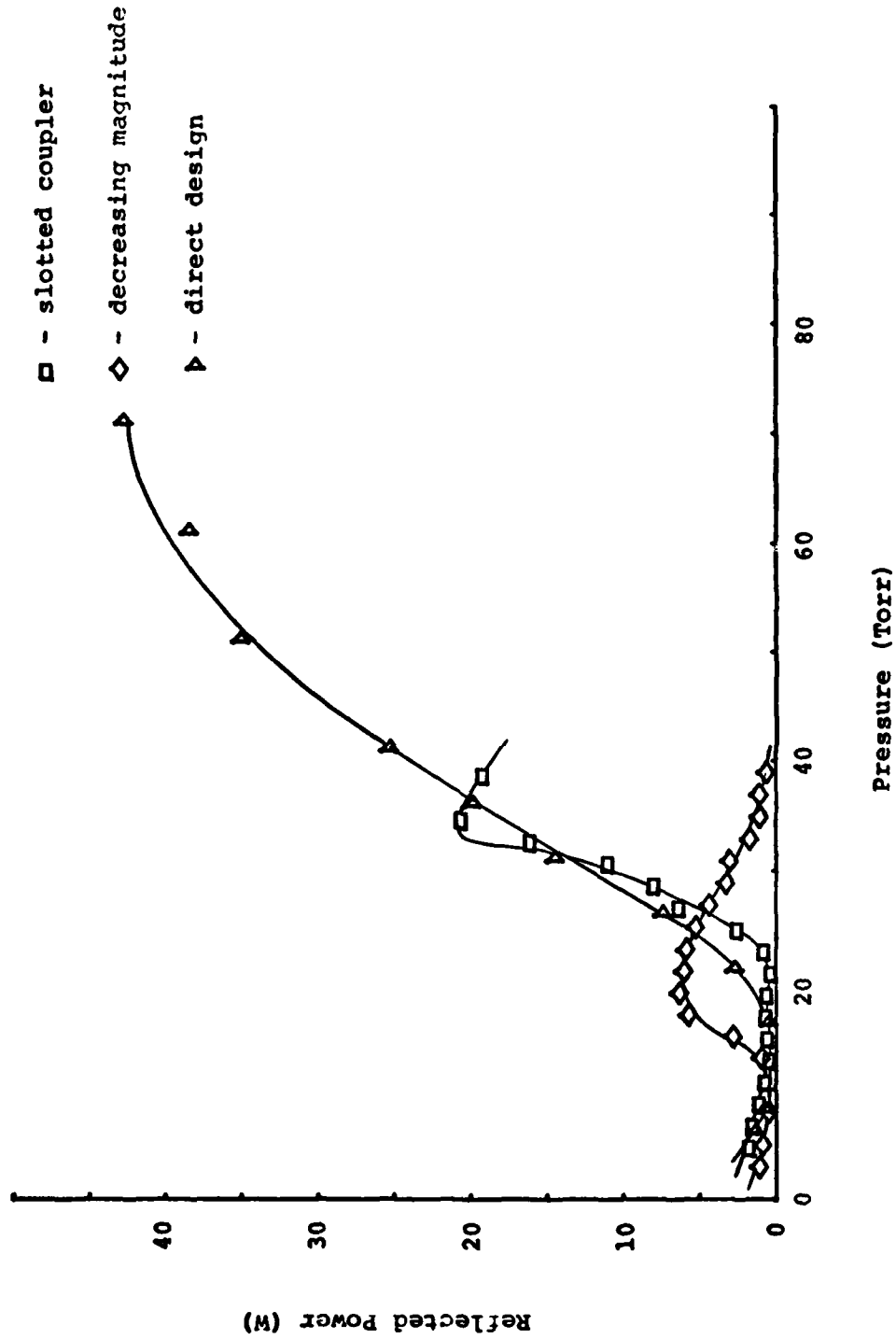


Figure 32 - Reflected Power Vs. Pressure of CO<sub>2</sub> at 500 W Input and 8 mm Tube

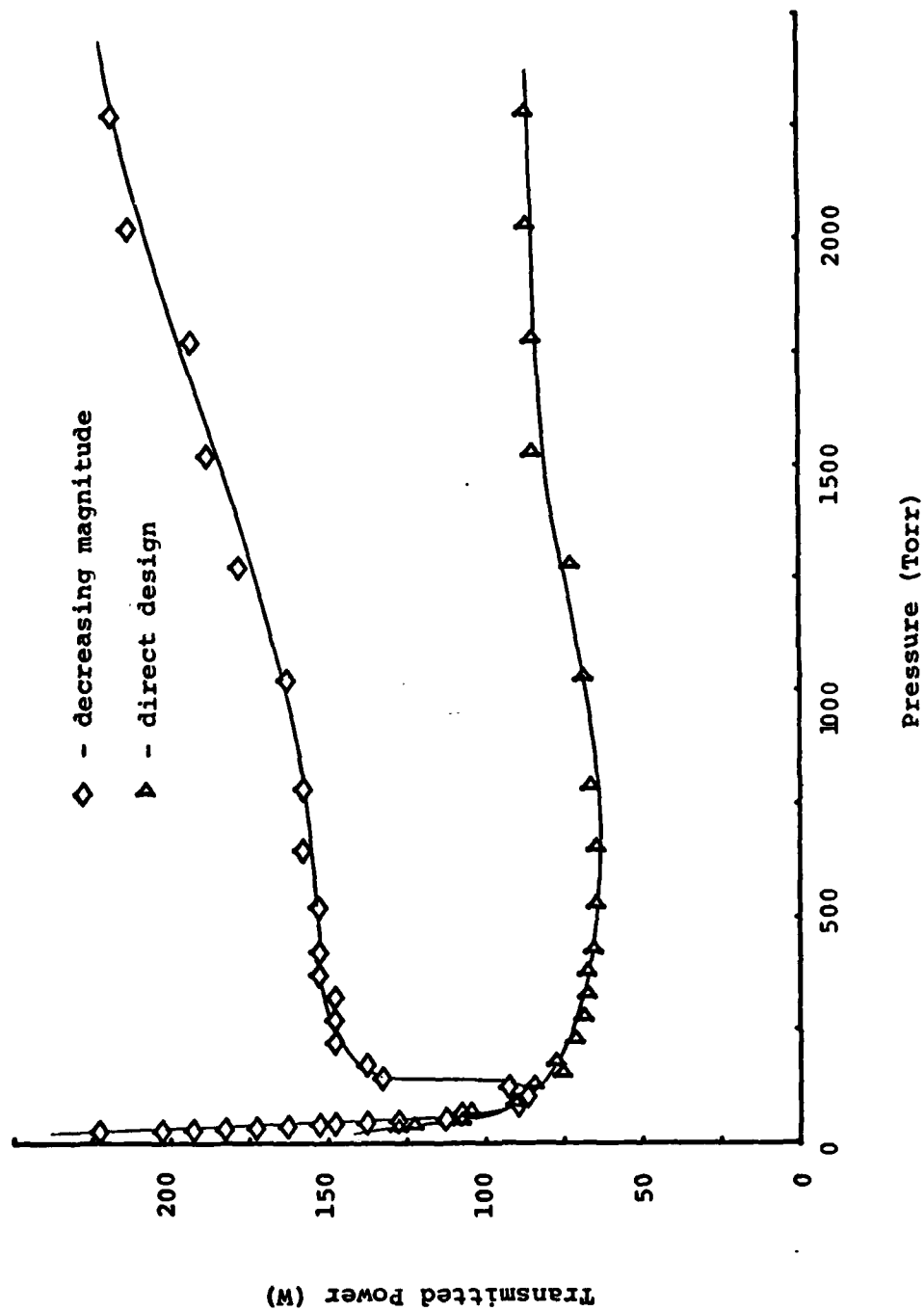


Figure 33 - Transmitted Power Vs. Pressure of Ar at 600 W Input and 8 mm Tube

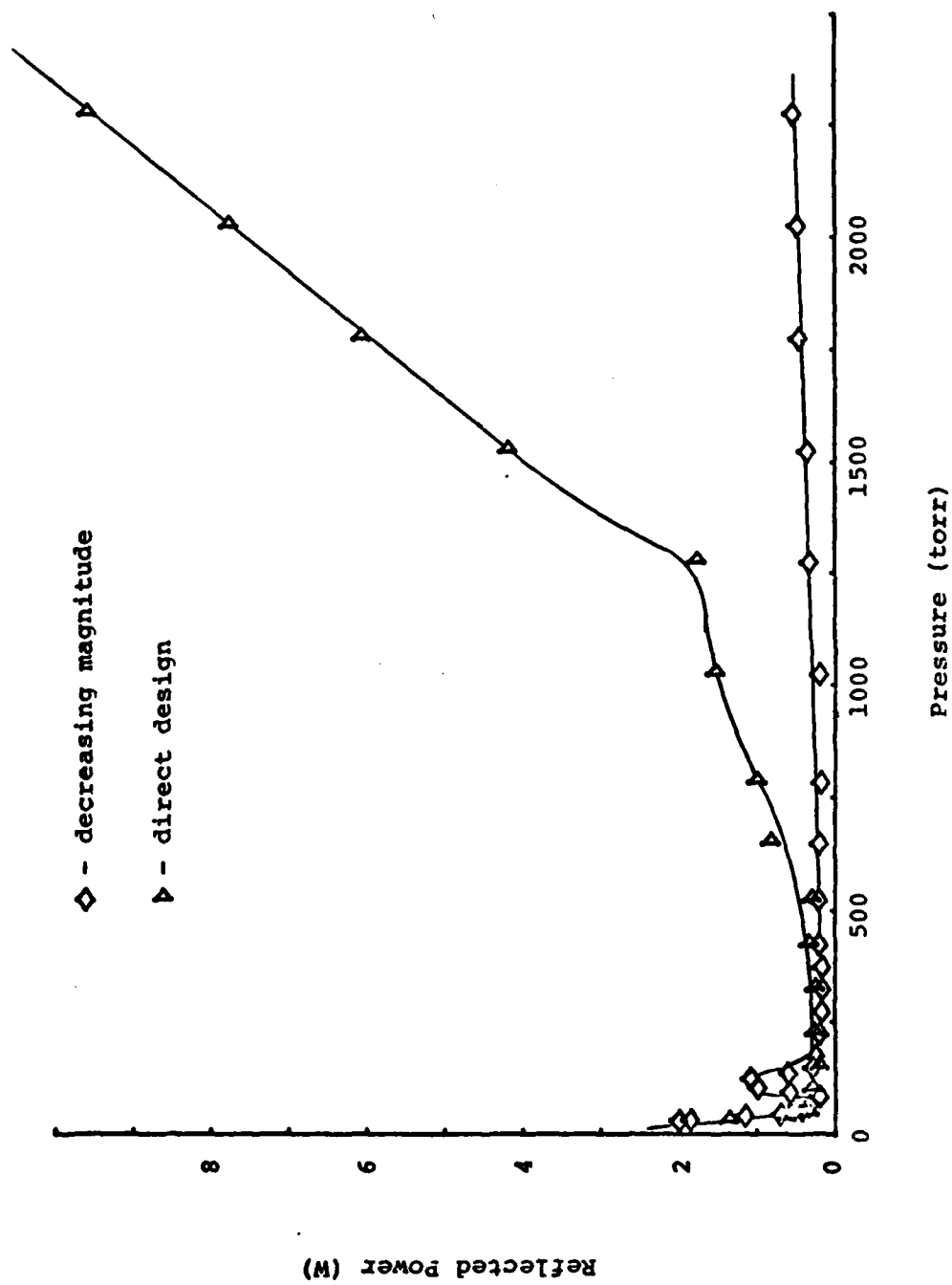


Figure 34 - Reflected Power Vs. Pressure of Ar at 600 W Input and 8 mm Tube

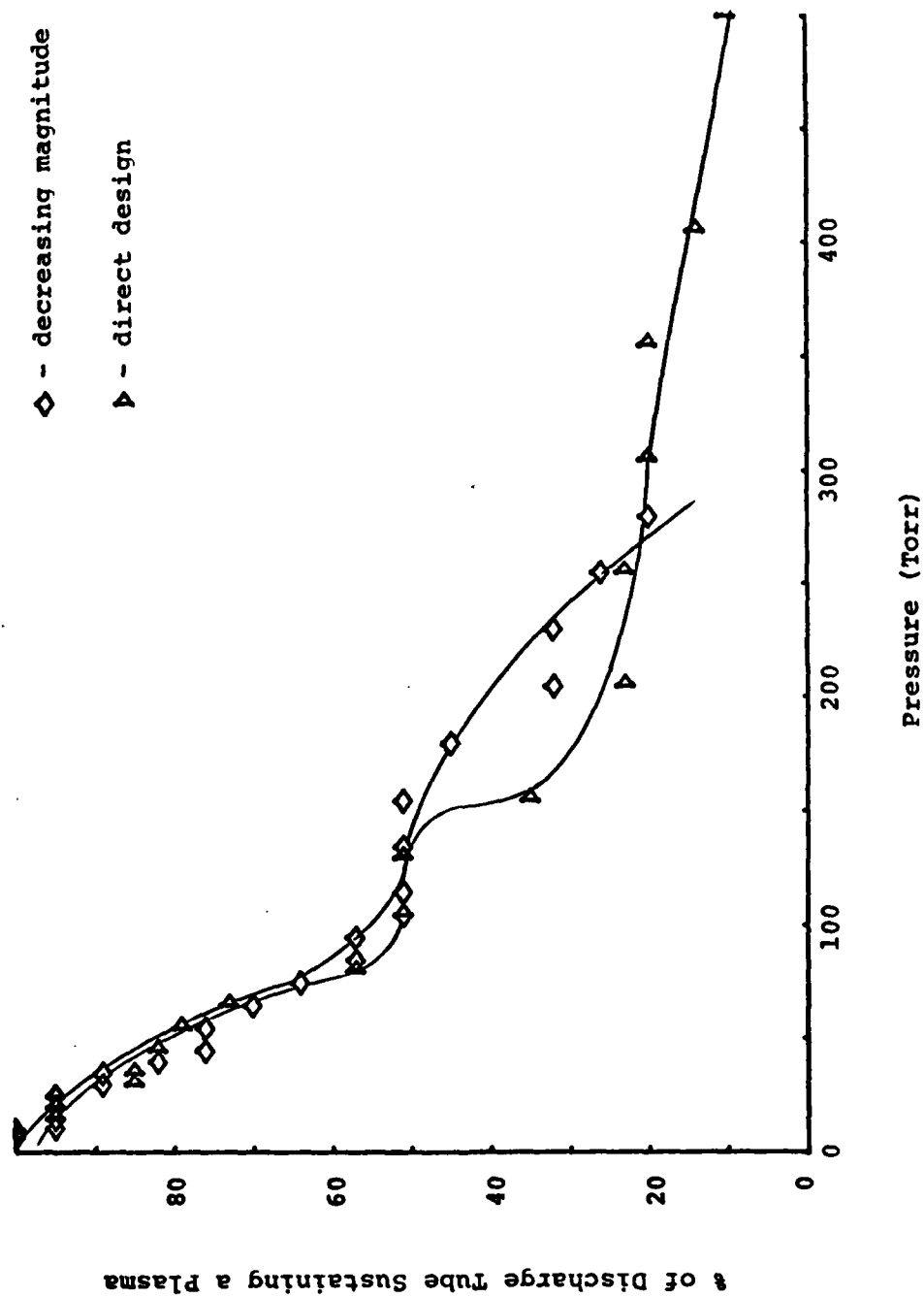


Figure 35 - % of 8 mm Tube Sustaining a Plasma Vs. Pressure of He at 600 W

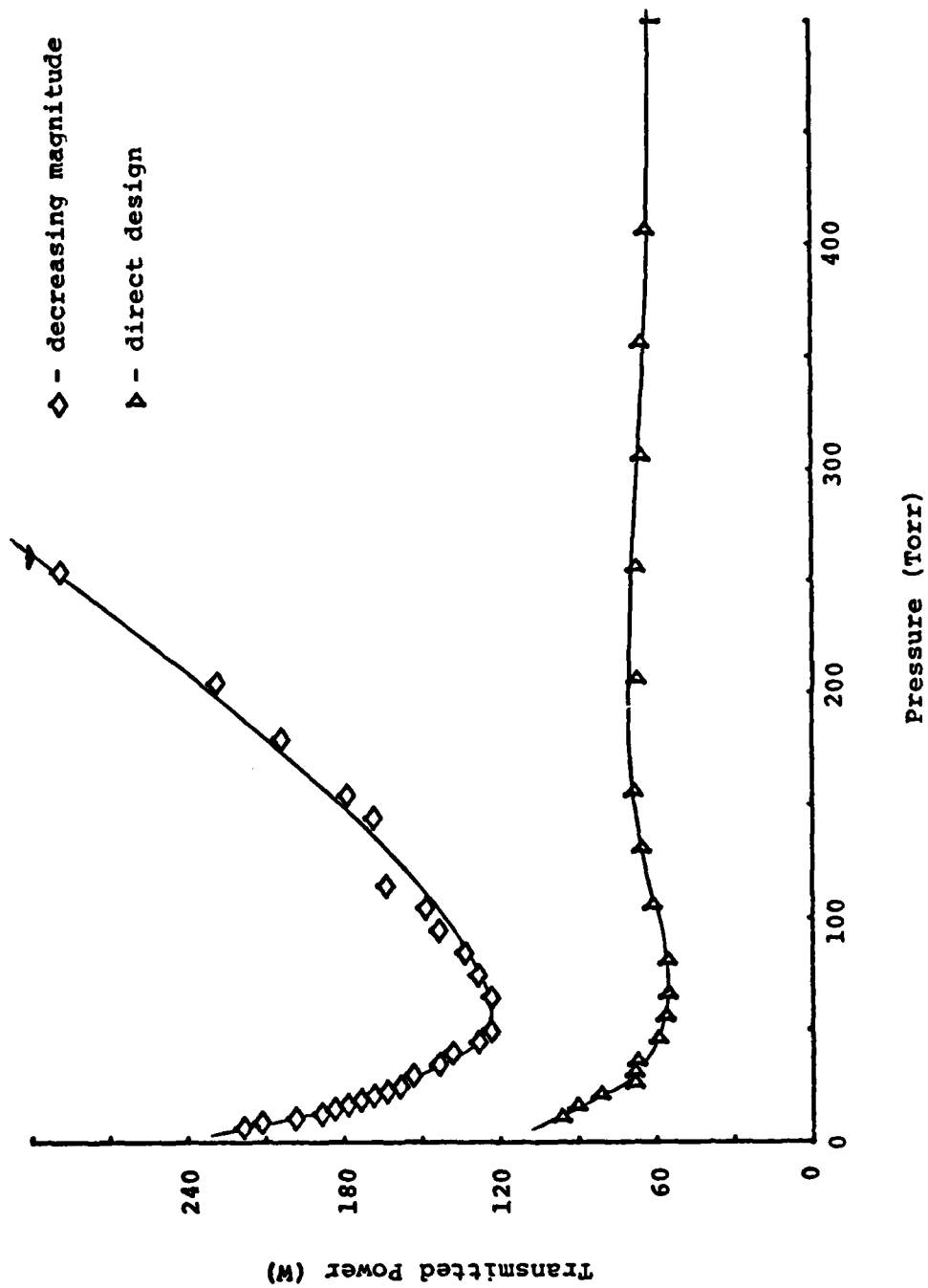


Figure 36 - Transmitted Power Vs. Pressure of He at 600 W Input and 8 mm Tube

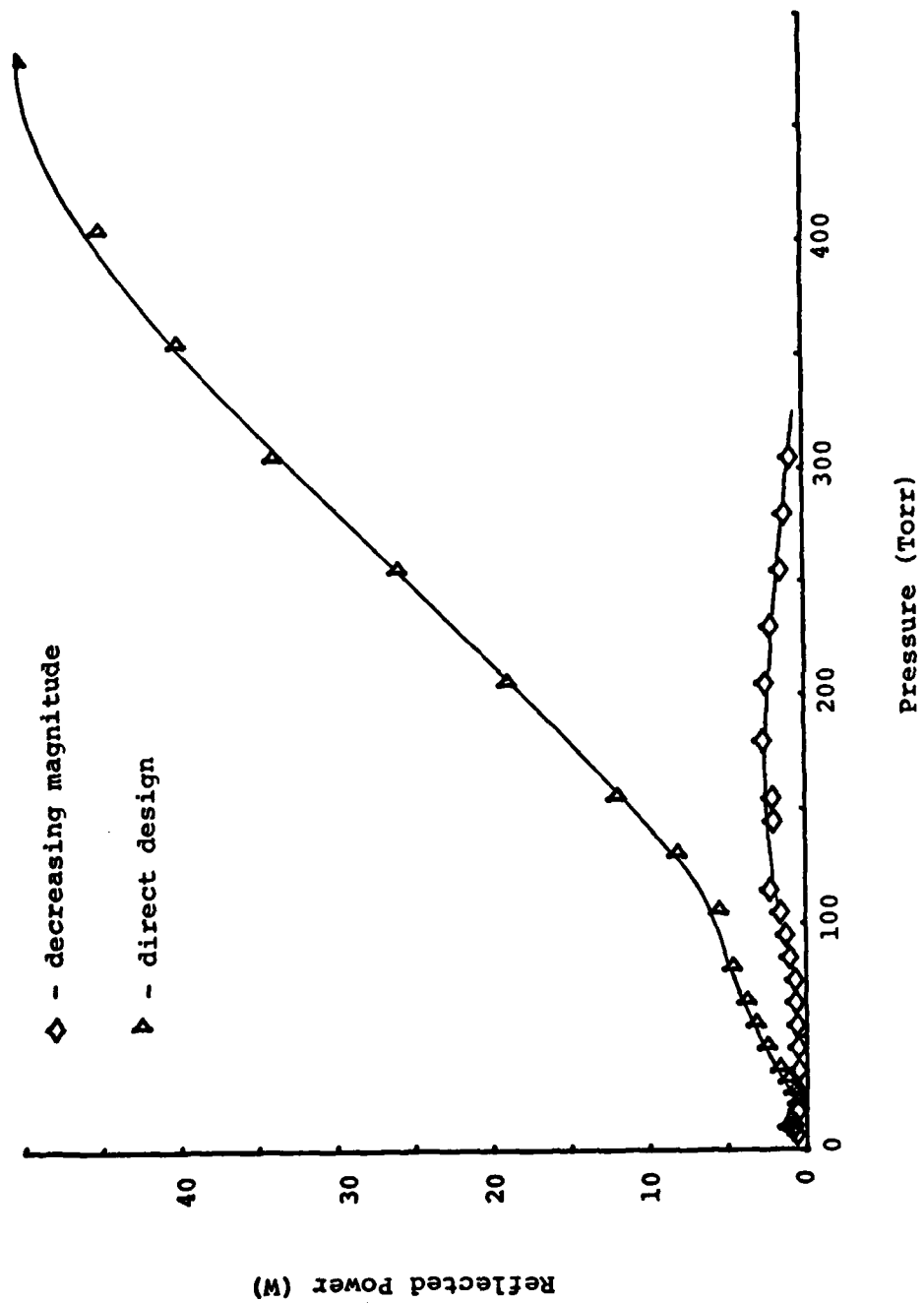


Figure 37 - Reflected Power Vs. Pressure of He at 600 W Input and 8 mm Tube

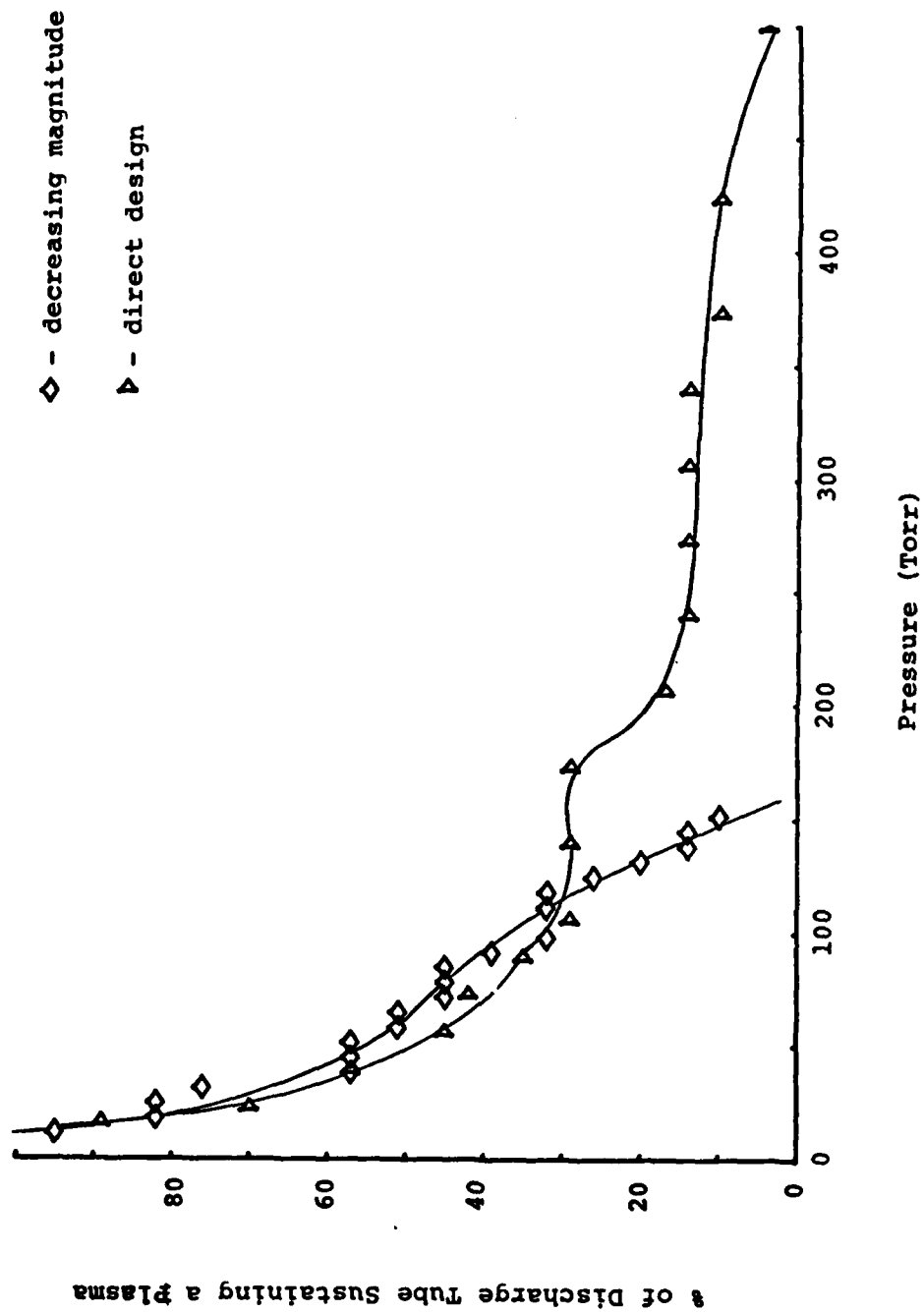


Figure 38 - % of 8 mm Tube Sustaining a Discharge Vs. Pressure of  $N_2$  at 600 W

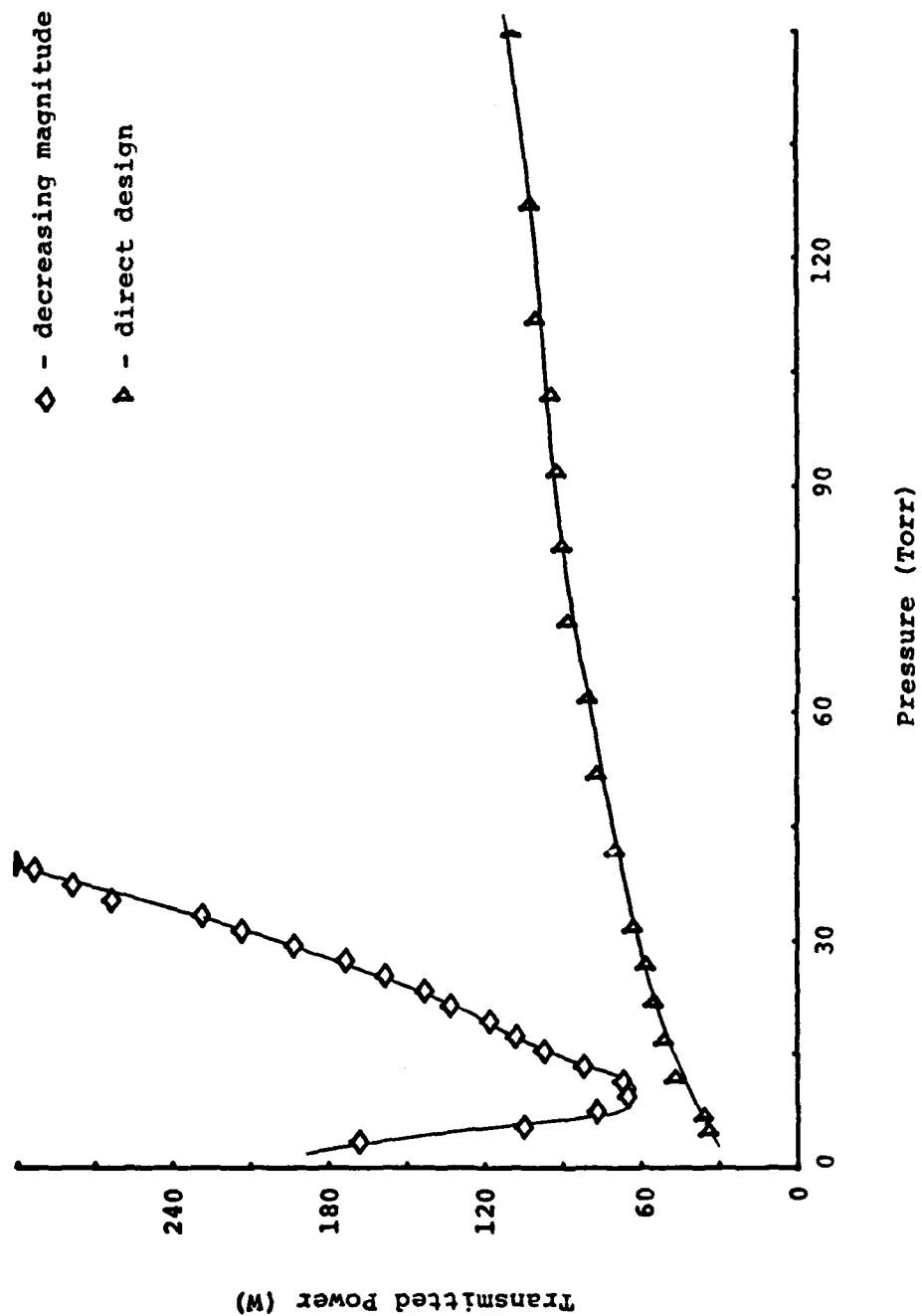


Figure 39 - Transmitted Power Vs. Pressure of  $N_2$  at 600 W Input and 8 mm Tube



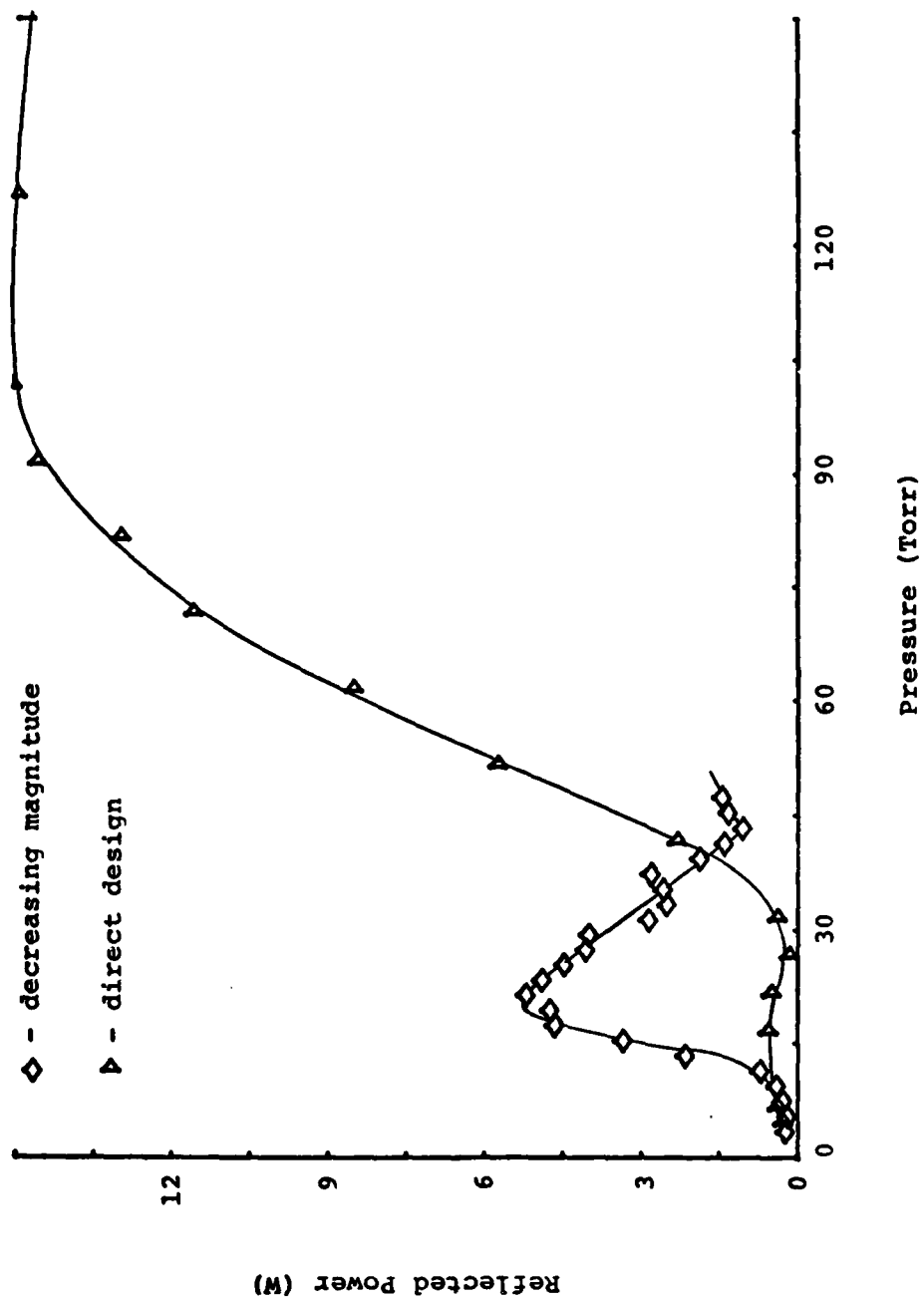


Figure 40 - Reflected Power Vs. Pressure of N<sub>2</sub> at 600 W Input and 8 mm Tube

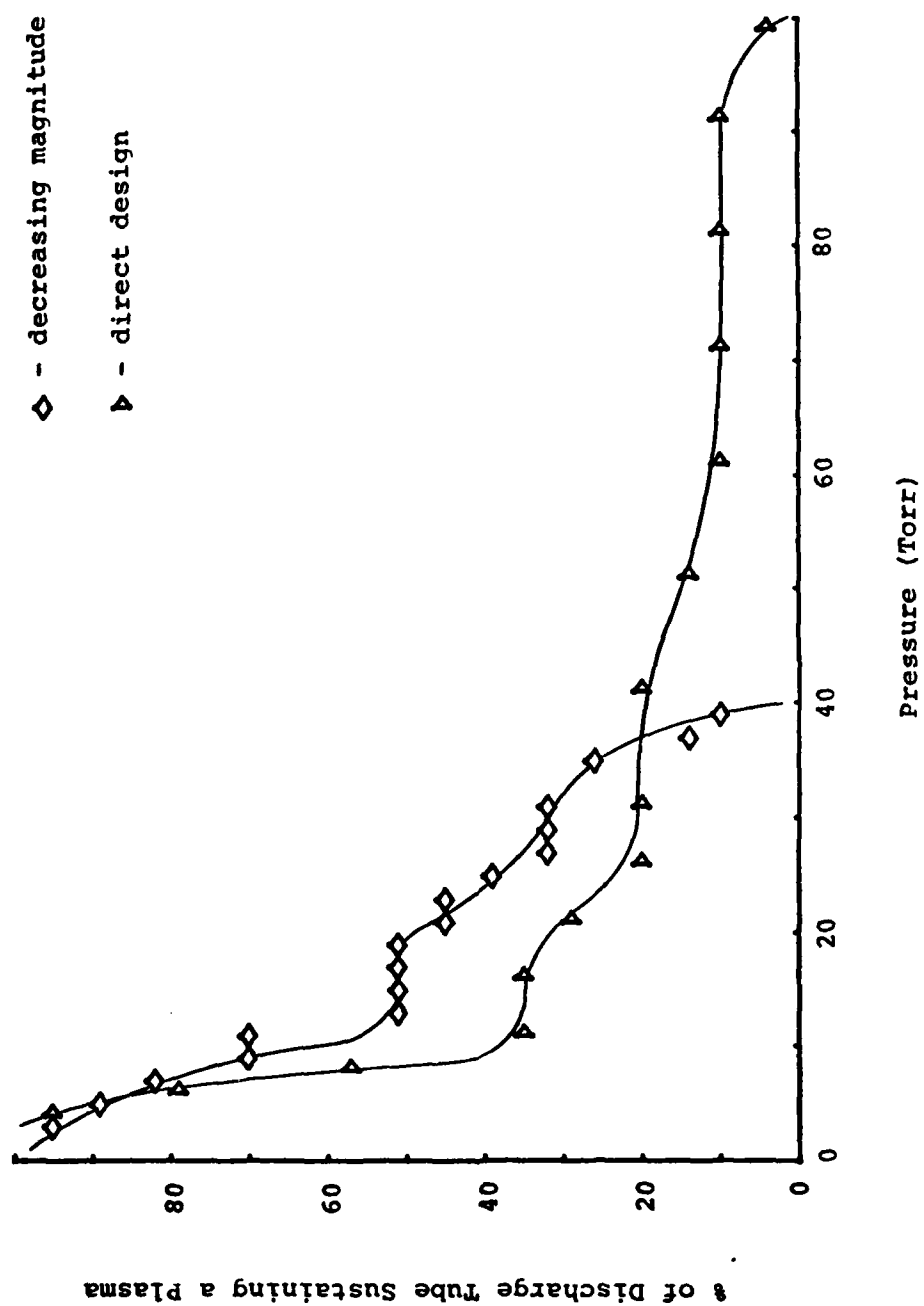


Figure 41 - % of 8 mm Tube Sustaining a Plasma Vs. Pressure of CO<sub>2</sub> at 600 W

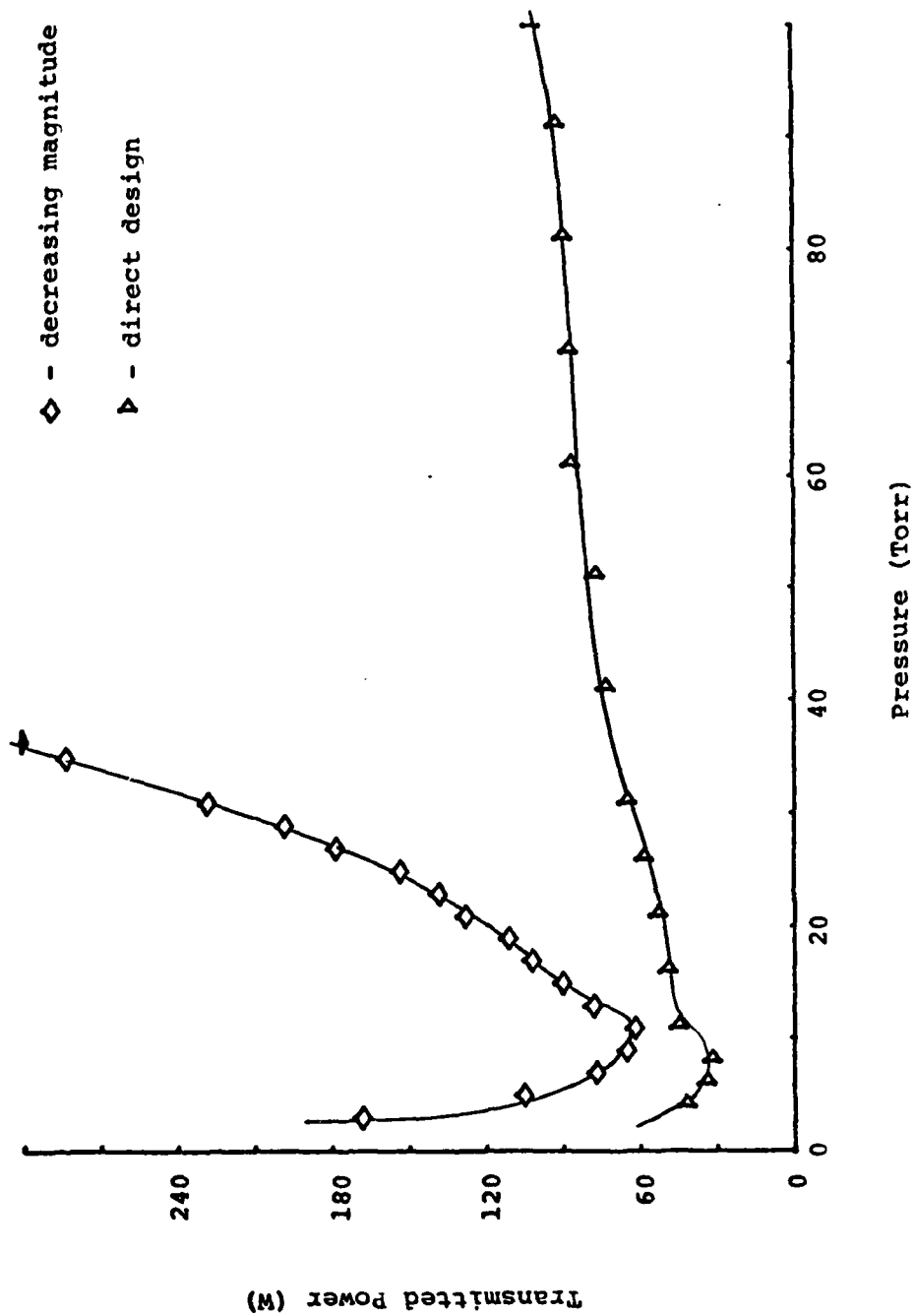


Figure 42 - Transmitted Power Vs. Pressure of CO<sub>2</sub> at 600 W Input and 8 mm Tube

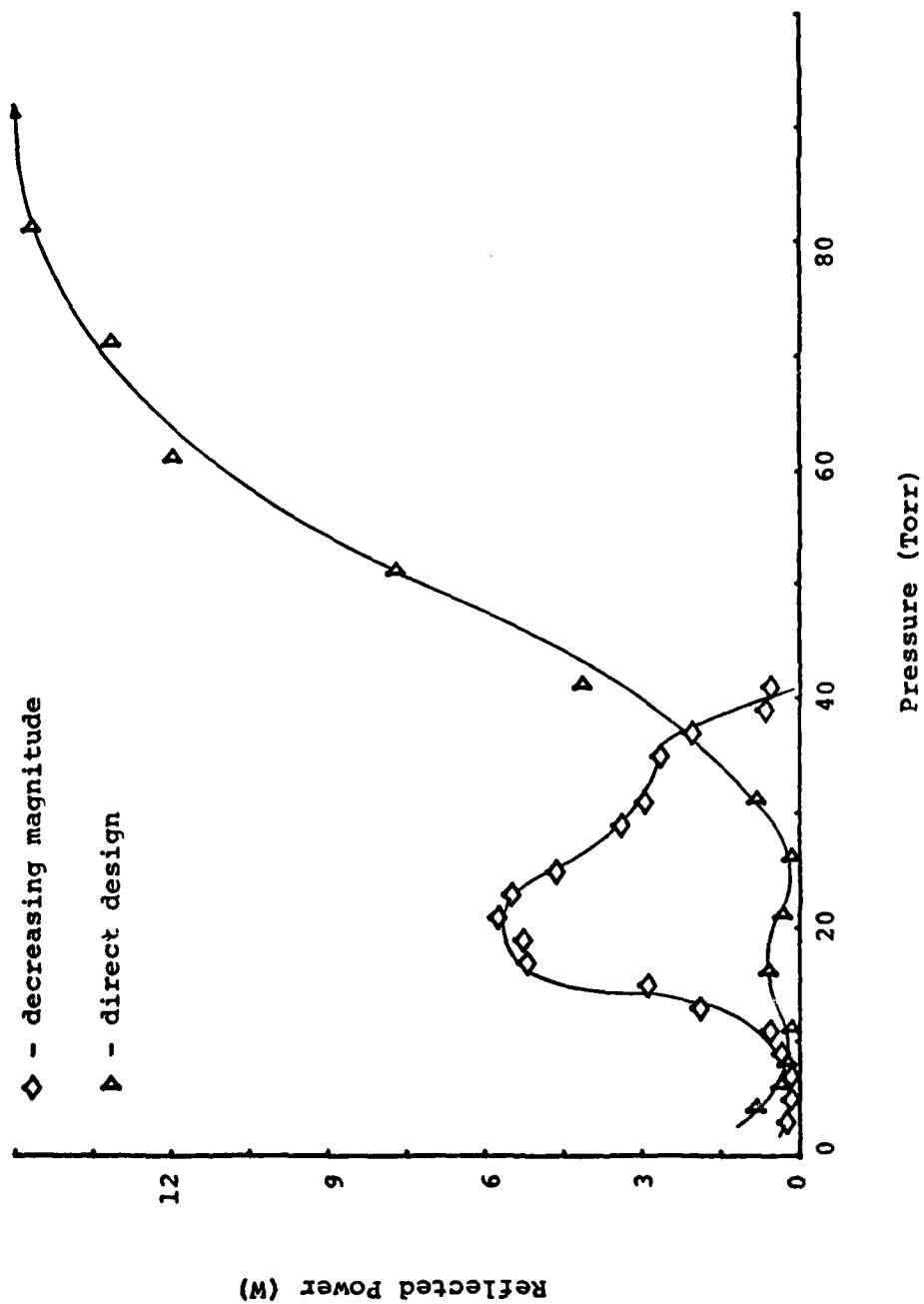


Figure 43 - Reflected Power Vs. Pressure of CO<sub>2</sub> at 600 W Input and 8 mm Tube

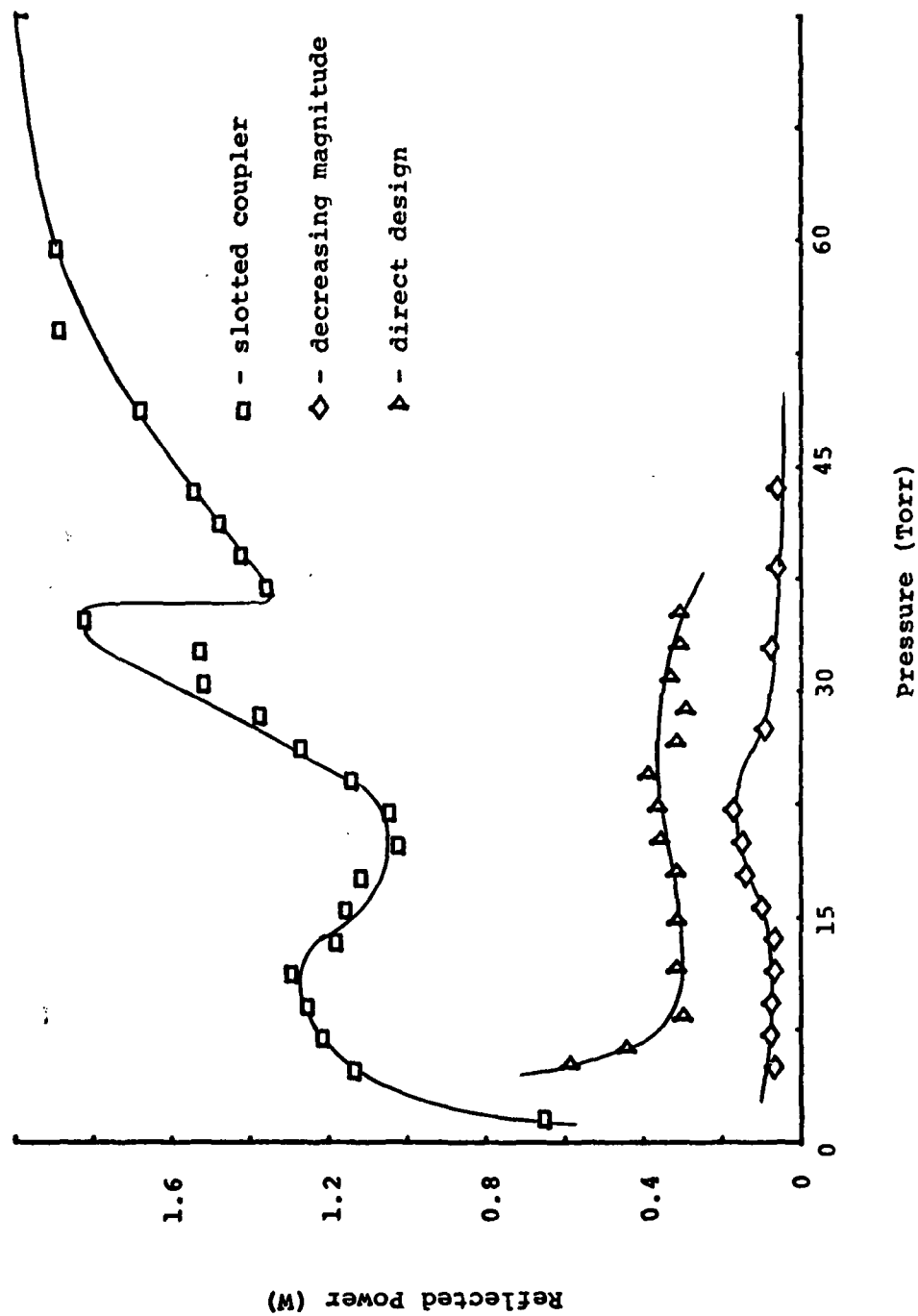


Figure 44 - Reflected Power Vs. Pressure of Ar at 500 W Input and 1.5 mm Tube

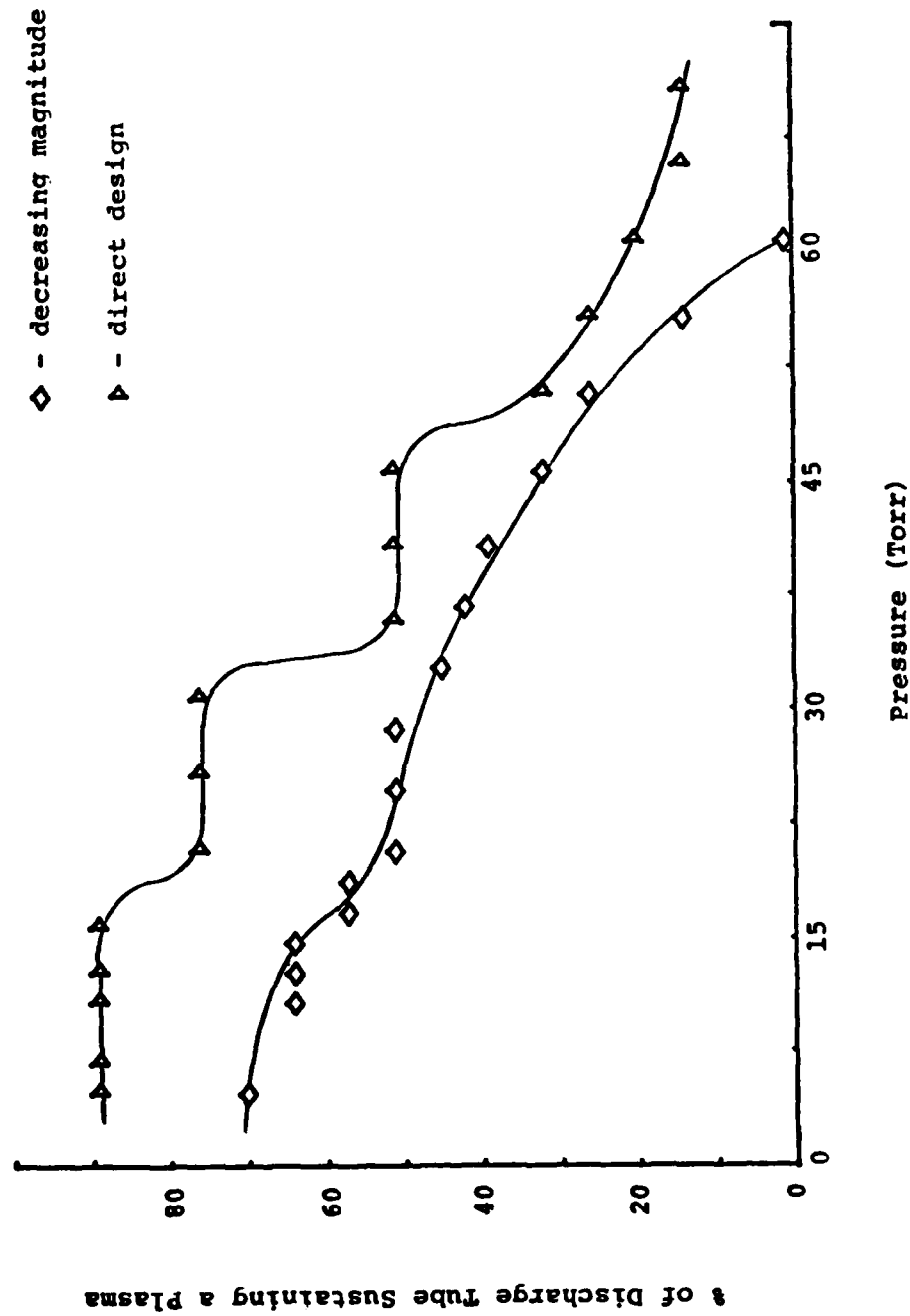


Figure 45 - % of 1.5 mm Tube Sustaining a Plasma Vs. Pressure of He at 500 W

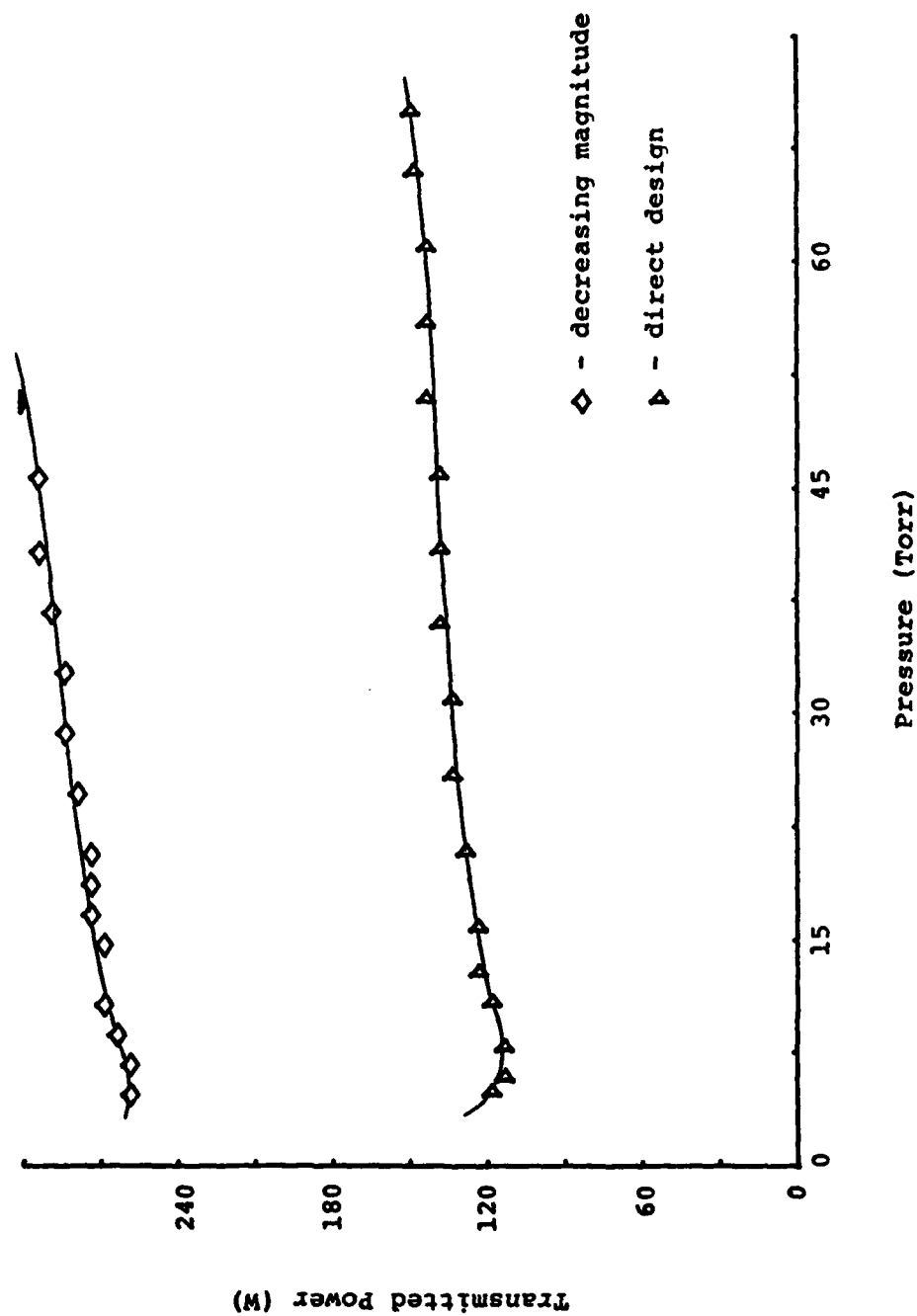


Figure 46 - Transmitted Power Vs. Pressure of He at 500 W Input and 1.5 mm Tube

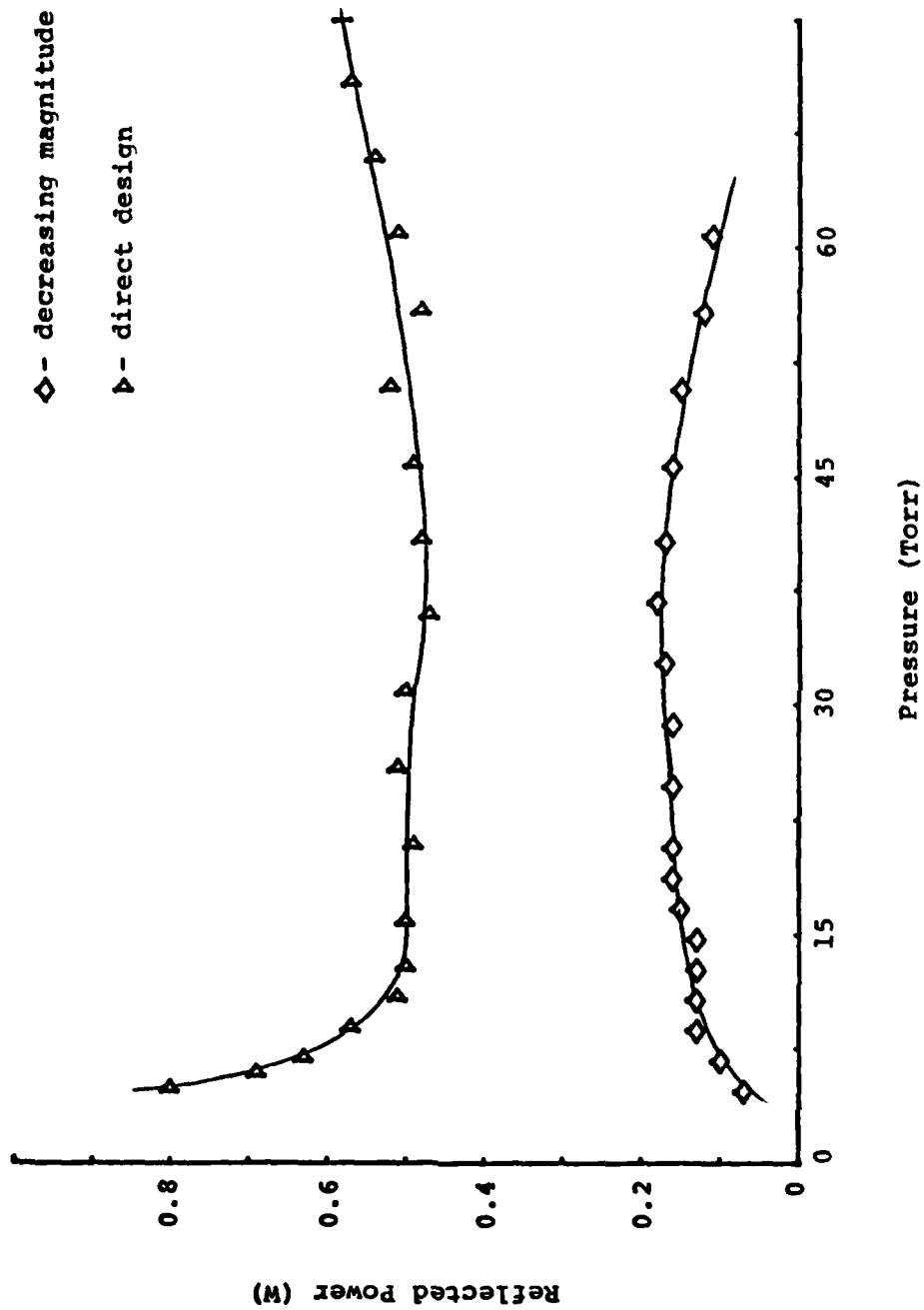


Figure 47 - Reflected Power Vs. Pressure of He at 500 W Input and 1.5 mm Tube



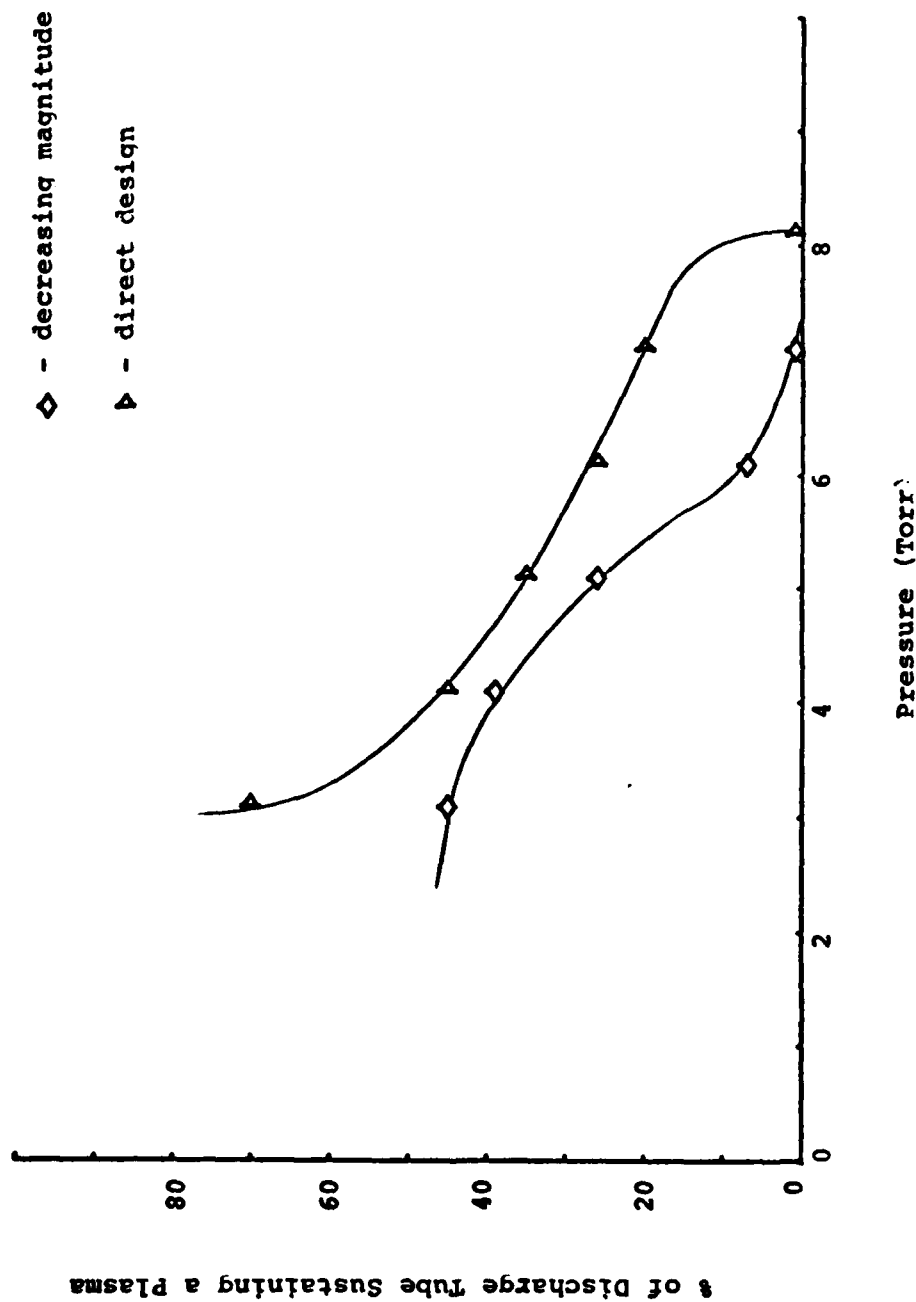


Figure 48 - % of 1.5 mm Tube Sustaining a Plasma Vs. Pressure of  $N_2$  at 500 W

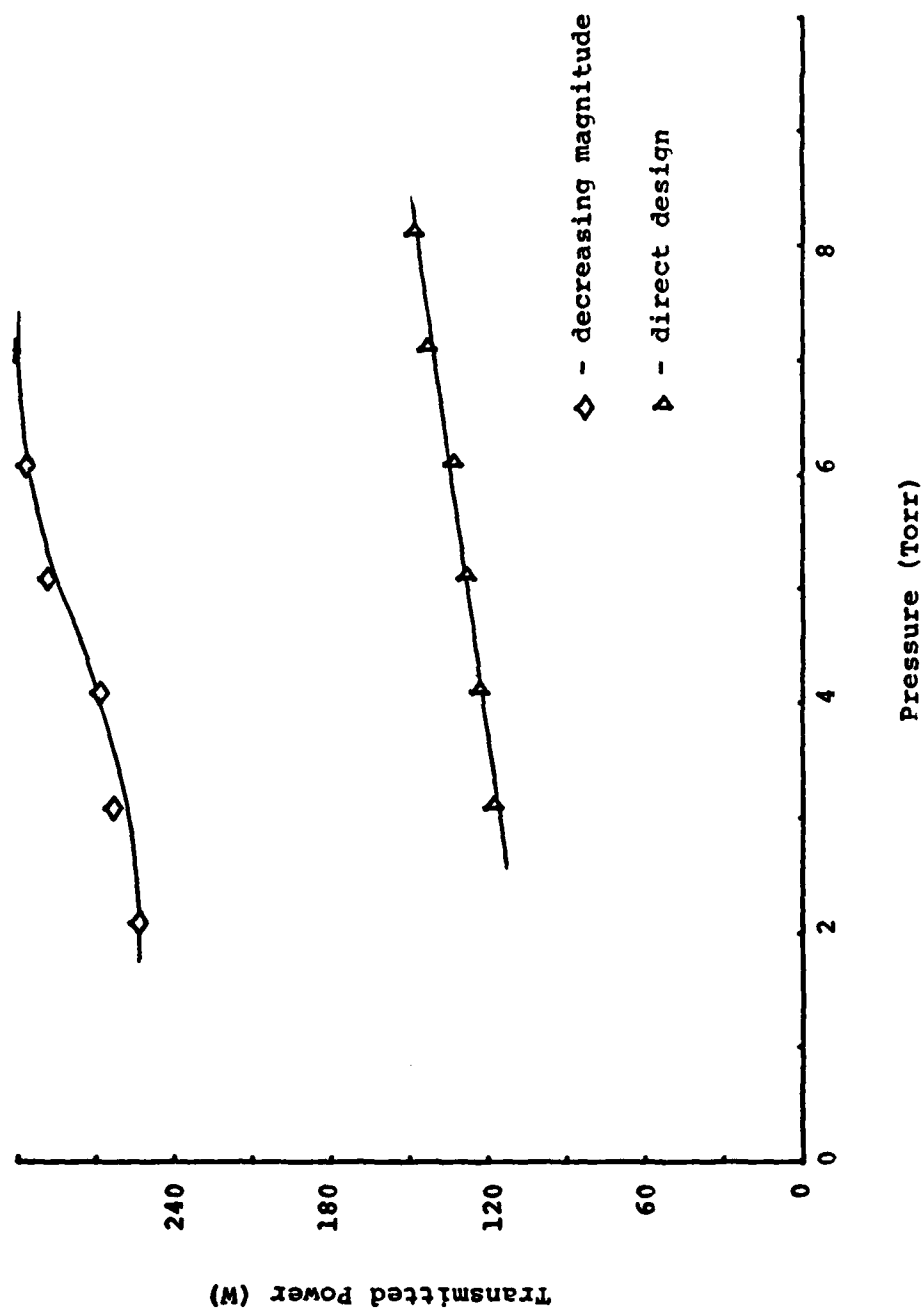


Figure 49 - Transmitted Power Vs. Pressure of N<sub>2</sub> at 500 W Input and 1.5 mm Tube

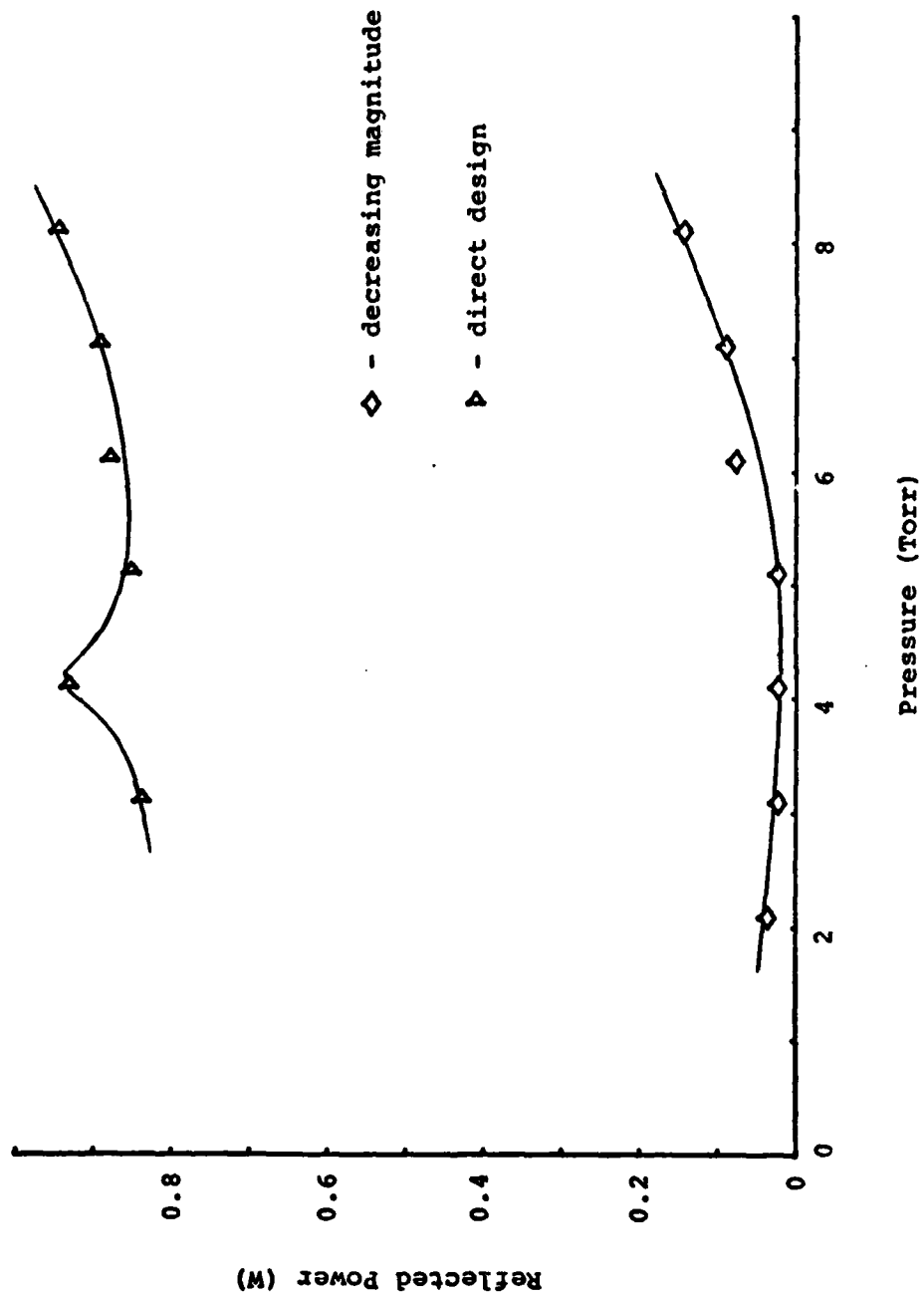


Figure 50 - Reflected Power Vs. Pressure of  $N_2$  at 500 W Input and 1.5 mm Tube

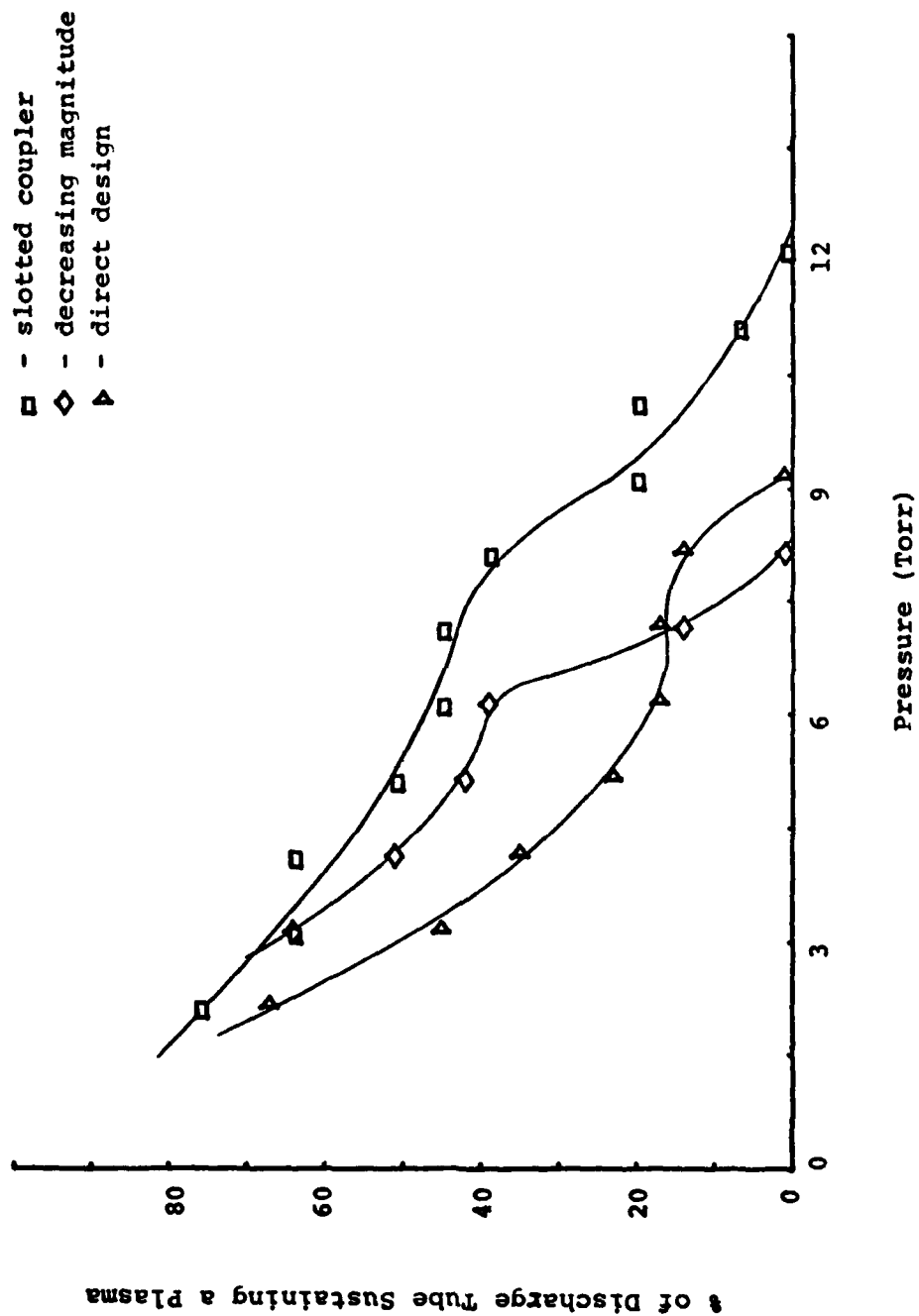


Figure 51 - % of 1.5 mm Tube Sustaining a Plasma Vs. Pressure of  $\text{CO}_2$  at 500 W

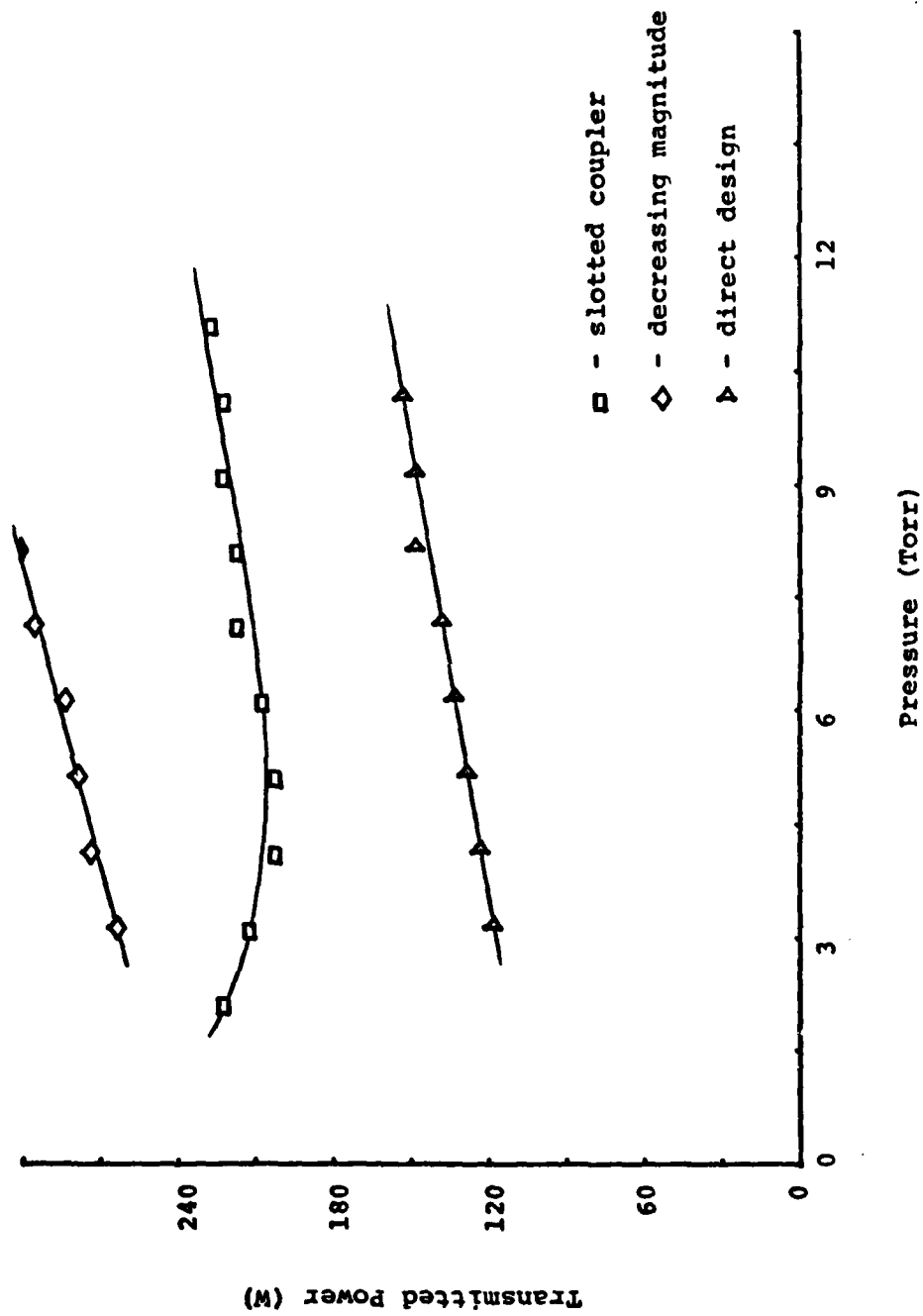


Figure 52 - Transmitted Power Vs. Pressure of CO<sub>2</sub> at 500 W Input and 1.5 mm Tube

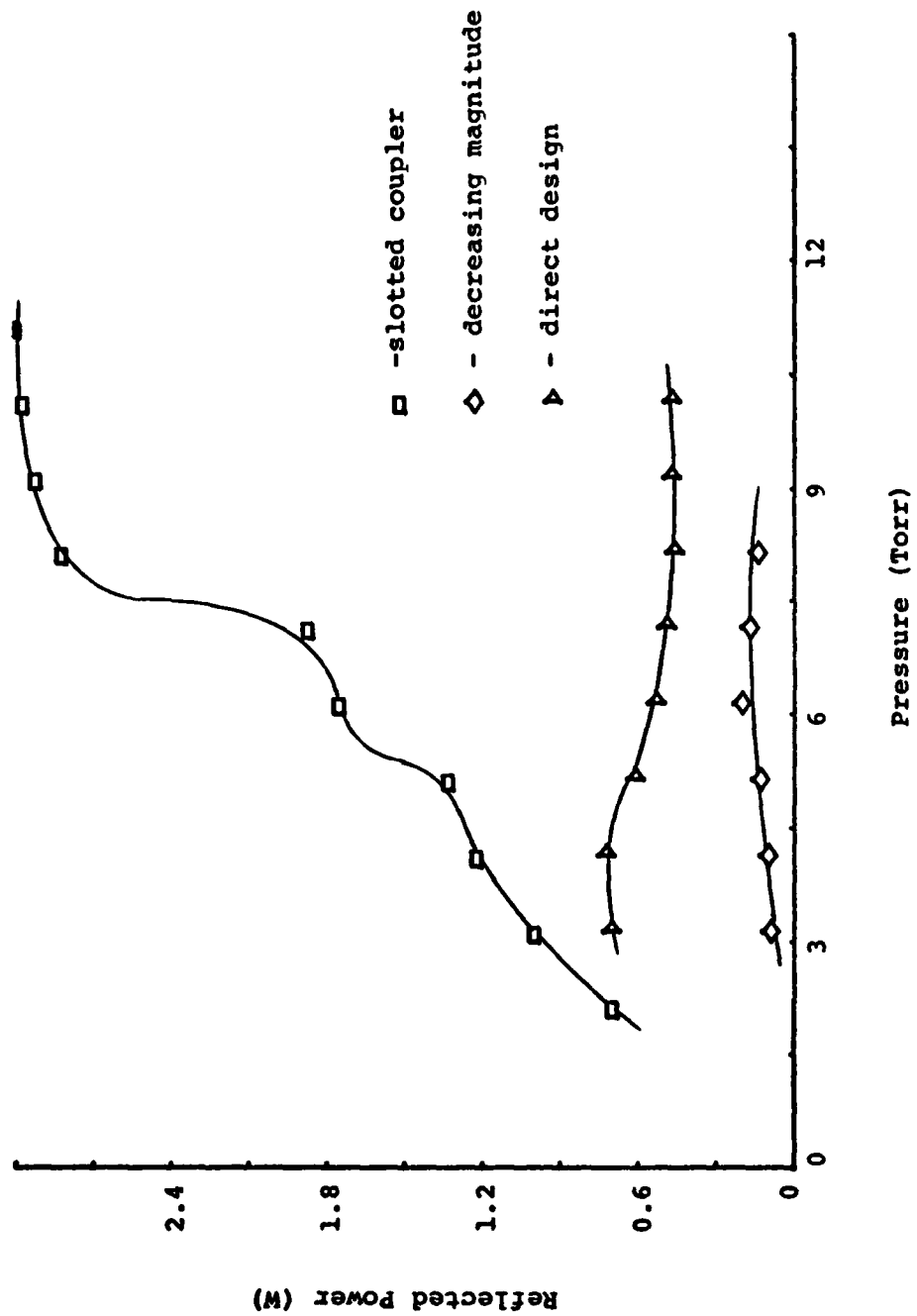


Figure 53 - Reflected Power Vs. Pressure of CO<sub>2</sub> at 500 W Input and 1.5 mm Tube

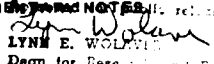
VITA

Leonard Carl Shelton Jr. was born on 17 January 1959 in Prince Edward County of Virginia. He graduated from high school in Farmville, Virginia in 1977 and entered the Virginia Military Institute on a four year Air Force Reserve Officer Training Corps scholarship. He received the Bachelor of Science Degree in Electrical Engineering in May 1981. He was commissioned on 15 May 1981 and entered the School of Engineering, Air Force Institute of Technology in June 1981. He is a member of Sigma Pi Sigma.

Permanent address: Rt. 2 Box 85  
Pamplin, Virginia  
23958

## UNCLASSIFIED

SECURITY CLASSIFICATION OF THIS PAGE (When Data Entered)

REPORT DOCUMENTATION PAGE		READ INSTRUCTIONS BEFORE COMPLETING FORM
1. REPORT NUMBER AFIT/GEO/PH/82D-13	2. GOVT ACCESSION NO.	3. RECIPIENT'S CATALOG NUMBER
4. TITLE (and Subtitle) DESIGNING WAVEGUIDE COUPLERS FOR MICROWAVE EXCITATION OF LASER GASES		5. TYPE OF REPORT & PERIOD COVERED MS Thesis
7. AUTHOR(s) Leonard Carl Shelton Jr. 2 Lt. USAF		6. PERFORMING ORG. REPORT NUMBER
9. PERFORMING ORGANIZATION NAME AND ADDRESS Air Force Institute of Technology (AFIT-EN) Wright-Patterson AFB, Ohio 45433		8. CONTRACT OR GRANT NUMBER(s)
11. CONTROLLING OFFICE NAME AND ADDRESS Electro-optical Technology Branch (AADO-1) Electronic Technology Division Wright-Patterson AFB, Ohio 45433		10. PROGRAM ELEMENT, PROJECT, TASK AREA & WORK UNIT NUMBERS Task 4-2001
14. MONITORING AGENCY NAME & ADDRESS (if different from Controlling Office)		12. REPORT DATE December 1982
		13. NUMBER OF PAGES 147
		15. SECURITY CLASS. (of this report) Unclassified
		15a. DECLASSIFICATION/DOWNGRADING SCHEDULE
16. DISTRIBUTION STATEMENT (of this Report)  Approved for public release; distribution unlimited		
17. DISTRIBUTION STATEMENT (of the abstract entered in Block 20, if different from Report)		
18. SUPPLEMENTARY NOTES  LYNN E. WOLANIN Dean for Research and Technological Development Air Force Institute of Technology (AFIT) Wright-Patterson AFB OH 45433 Approved for public release; IAW AFR 190-17 4 JAN 1983		
19. KEY WORDS (Continue on reverse side if necessary and identify by block number) Waveguide Coupler                      Plasma in Waveguide Analytic Design Model                  Uniform Power Transfer Sidewall Coupling                      Microwave Excited Plasma Separable Coupler		
20. ABSTRACT (Continue on reverse side if necessary and identify by block number) <p>The goal of this thesis is to develop an analytical model from which a waveguide coupler can be designed. The specific application considered here is to use a waveguide coupler to excite a plasma tube inside a waveguide. This application is desirable in laser systems.</p> <p>The approach taken is to model the plasma as an equivalent dielectric centered in the secondary waveguide.</p> <p>(over)</p>		

DD FORM 1 JAN 73 1473 EDITION OF 1 NOV 65 IS OBSOLETE

Unclassified  
SECURITY CLASSIFICATION OF THIS PAGE (When Data Entered)



UNCLASSIFIED

SECURITY CLASSIFICATION OF THIS PAGE(When Data Entered)

Standard waveguide analysis techniques are used to find a perturbed propagation constant in that waveguide. Successive approximations are made to the coupled wave equations until a piece-wise linear solution is obtained. This solution gives the field distribution resulting from any arbitrarily chosen coupling geometry. Thus, the distribution for any desired coupling characteristics can be determined in an iterative manner, essentially by trial and error.

Preliminary tests were made on couplers designed using the model; initial results are promising but inconclusive. It is believed that this design method will provide the tool for designing couplers to obtain a desired field distribution in the secondary waveguide.

UNCLASSIFIED

SECURITY CLASSIFICATION OF THIS PAGE(When Data Entered)

END

DATE  
FILMED

3-83

DTI